

# UNIVERSITY OF CATANIA

FACULTY OF MATHEMATICAL, PHYSICAL AND NATURAL SCIENCES

DEPARTMENT OF CHEMICAL SCIENCES

INTERNATIONAL Ph.D. IN CHEMICAL SCIENCES -XXIV cycle

---

SALVATORE BATTIATO

## STUDIES OF NEW POLYMERIC MATERIALS PRODUCED BY REACTIVE BLENDING

Ph.D. THESIS

**Coordinator:**

**Prof. CORRADO TRINGALI**

**Tutors:**

**Prof. ALBERTO BALLISTRERI**

**Prof. FILIPPO SAMPERI**

---

ACADEMIC YEARS 2008-2011

# TABLE OF CONTENTS

<b><u>1.- INTRODUCTION</u></b>	1
1.1 – Preface	1
1.2 – Reactive melt blending	4
1.3 - Aim of the work	7
1.4 - References	8
<b><u>2. – CHARACTERIZATION TECHNIQUES</u></b>	9
2.1 – Nuclear Magnetic Resonance ( $^1\text{H}$ and $^{13}\text{C}$ - NMR)	9
2.2 – Differential Scanning Calorimetry (DSC)	14
2.3 – Thermogravimetry (TGA)	17
2.4 – MALDI-TOF mass spectrometry	19
2.5 – FTIR spectroscopy	24
2.6 – Viscosimetry	26
2.7 – Gel Permeation Chromatography (GPC)	29
2.8 – Rereferences	32

## PART I

### **CHARACTERIZATION OF COPOLYESTERAMIDES FROM REACTIVE BLENDING OF PET AND MXD6 IN THE MOLTEN STATE**

3.1 – Introduction	34
3.2 – Materials	38
3.3 – Poly(ethylene terephthalate) - PET	39
3.4 – Poly( <i>m</i> -xylene adipamide) - MXD6	41
3.5 – Reactive blending procedure	42
3.6 – Synthesis of poly( <i>m</i> -xylene terephthalamide) - MXDT	43
3.7 – Characterization of Samples	44
3.8 – Results and discussion	45
3.9 – Studies on PET and MXD6 Samples	48
3.10 – Characterization of PET-MXD6 melt-mixed blends	57
3.11 – MALDI-TOF ms characterization	72
3.12 – DSC analysis	75
3.13 – Thermogravimetric analysis (TGA)	80
3.14 – Conclusions	81

**PART II****REACTIVE MELT MIXING OF PC-PEN BLENDS:  
STRUCTURAL CHARACTERIZATION OF REACTION  
PRODUCTS**

4.1 – Introduction	86
4.2 – Poly (bisphenolA carbonate) - PC	89
4.3 – Poly(ethylene naphthalate) - PEN	91
4.4 – Reactive blending procedure	93
4.5 – Synthesis of polymer models	94
4.6 – Synthesis of poly(bisphenolA naphthalate)	96
4.7 – Synthesis of copoly(bisphenolA carbonate)-alt-(ethylene carbonate)	98
4.8 – Synthesis of poly(ethoxy-bisphenolA naphthalate)-co-(diethoxy-bisphenolA naphthalate)	100
4.9 – Synthesis o poly(diethoxy bisphenolA naphthalate)	102
4.10 – Characterization of models polymers	104
4.11 – Characterization of PC and PEN	110
4.12 – Characterization of poly(bisphenolA naphthalate)	118
4.13 – Characterization of copoly(bisphenolA carbonate)-alt-(ethylene carbonate)	121
4.14 – Characterization of poly(ethoxy-bisphenolA naphthalate)-co-(diethoxy-bisphenolA naphthalate)	123
4.15 – Characterization of poly(diethoxy-bisphenolA naphthalate)	127
4.16 – Characterizations of PC-PEN melt blended materials	129
4.17 - Solvent Extractions	130
4.18 – <sup>1</sup> H and <sup>13</sup> C NMR analysis of PC-PEN melt blended materials	132
4.19 – Thermogravimetric analysis of PC-PEN melt blended materials	143
4.20 – DSC analysis of melt mixed PC-PEN materials	146
4.21 – FTIR analysis of PC-PEN Blends	151
4.22 – Viscosimetric analysis of PC-PEN Blends	153
4.23 – GPC analysis of melt mixed PC-PEN materials	154
4.24 - MALDI-TOF measurements of PC-PEN Blends	157
4.25 – Conclusions	163
4.26 – References	164

## List of figures

**Figure 1.1.** Copolymer action as compatibilizer.

**Figure 1.2.** Schematic representation of the exchange reactions which can occur in polymer blends containing reactive functional groups as a function of temperature.

**Figure 2.1.** The spin states of a proton both in the absence and in the presence of applied magnetic field.

**Figure 2.2.** Schematic representation of a typical DSC sample cell showing the sample (S) and reference (R) pans, as well as the heating and temperature sensing elements.

**Figure 2.3.** Typical DSC curve, using convention that endothermic peak goes down.  $\Delta$  indicates the differential signal of temperature between reference and sample.

**Figure 2.4.** A schematic thermobalance.

**Figure 2.5.** Schematic of a MALDI-TOF Mass Spectrometer.

**Figure 2.6.** MALDI-TOF MS Sample Ionization.

**Figure 2.7.** Conversion from TOF spectra to Conventional Spectra.

**Figure 2.8.** Schematic plots of  $\eta_{sp}/c$  and  $\eta_{inh}$  vs. concentrations of polymer solution.

**Figure 2.9.** Schematic of a Gel Permeation Chromatography column.

**Figure 3.1.** MALDI-TOF mass spectra of PET heated at 285 °C for (a) 0 min, (b) 5 min, and (c) 5 min in the presence of TA (1 wt%).

**Figure 3.2.** MALDI-TOF mass spectra of MXD6 heated at 285 °C for (a) 0 min, (b) 5 min, and (c) 5 min in the presence of TA (1 wt%).

**Figure 3.3.** Sections of the  $^1\text{H-NMR}$  spectra of (a) an equimolar mixture (with respect of the repeat units) of the polymer models (PET, MXD6, MXDT, and PEA) and of PET-MEXD6-(1 wt%)TA melt-mixed blends at 285 °C for: (b) 30 min, (c) 45 min, (d) 75 min, and (e) 120 min.

**Figure 3.4.** Sections of the  $^{13}\text{C}$ -NMR spectra of (a) an equimolar mixture (with respect of the repeat units) of the polymer models (PET, MXD6, MXDT, and PEA) and of PET-MEXD6-(1 wt%)TA melt-mixed blends at 285 °C for: (b) 20 min, (c) 30 min, (d) 60 min, (e) 75 min, (f) 90 min, and (g) 120 min.

**Figure 3.5.** (a) Theoretical and (b) experimental MALDI-TOF mass spectra of PET-MXD6 (120 min) random copolymer, in the mass range 1100–2200 Da.

**Figure 4.1.**  $^1\text{H}$  NMR spectra of polymer models: (a) PC, (b) PEN, (c) pBAN, (d) p(BPAC)-alt-(EtC), (e) p(BPAEtN)-co-(EtBPAEtN), and (f) pEtBPAEtN.

**Figure 4.2.**  $^{13}\text{C}$ -NMR spectra of polymer models: (a) PC, (b) PEN, (c) pBAN, (d) p(BPAC)-alt-(EtC), (e) p(BPAEtN)-co-(EtBPAEtN), and (f) pEtBPAEtN.

**Figure 4.3.** FTIR Spectra of polymer models (a) PC, (b) PEN, (c) pBAN, (d) p(BPAC)-alt-(EtC), (e) p(BPAEtN)-co-(EtBPAEtN), and (f) pEtBPAEtN.

**Figure 4.4.** DSC thermograms of polymer models (a) PC, (b) PEN, (c) pBAN, (d) p(BPAC)-alt-(EtC), (e) p(BPAEtN)-co-(EtBPAEtN), and (f) pEtBPAEtN.

**Figure 4.5.** MALDI TOF spectrum (in positive mode) of the homopolymer PC.

**Figure 4.6a.** MALDI TOF spectrum (in positive mode) of the homopolymer PEN.

**Figure 4.6b.** MALDI TOF spectrum (in positive mode) of the homopolymer PEN.

**Figure 4.7.** MALDI TOF spectrum of poly(bisphenolA- naphthalate) - pBPAN.

**Figure 4.8.** MALDI-TOF spectrum of copoly(bisphenolA carbonate)-alt-(ethylene carbonate) – p(BPAC)-alt-(EtC).

**Figure 4.9.** MALDI-TOF mass spectrum (in positive mode) of poly(ethoxy-bisphenolA naphthlate)-co-(diethoxy-bisphenolA naphthlate) - p(BPAEtN)-co-(EtBPAEtN).

**Figure 4.10.** MALDI TOF mass spectrum (in positive mode) of poly(diethoxy-bisphenolA naphthlate) pEtBPAEtN.

**Figure 4.11.** block diagram of solvent extractions.

**Figure 4.12.**  $^1\text{H}$  NMR spectra of equimolar PC-PEN mixture melt-mixed at  $280^\circ\text{C}$  for 0, 2, 5, 20, 45, and 60 min in the presence of  $\text{Ti}(\text{OBut})_4$  as catalyst. (EtC = adsorbed molecules of ethylene carbonate; \* = solvent signal –  $\text{CDCl}_3/\text{d-TFA} - 80/20 \text{ v:v}$ ).

**Figure 4.13.**  $^{13}\text{C}$  NMR spectra of equimolar PC-PEN mixture melt-mixed at  $280^\circ\text{C}$  for 0, 2, 5, 20, 45, and 60 min in the presence of  $\text{Ti}(\text{OBut})_4$  as catalyst. The carbon assignments are given in Table 1. (EtC = adsorbed molecules of Ethylene Carbonate).

**Figure 4.14.** Evolution of the molar composition of the sequences A, B, C, D, E and F into PC-PEN copolymers as a functions of reactions time: (A) bisphenolA-carbonate, (B) ethylene-naphthalate, (C) bisphenolA-naphthalate, (D) ethylene-carbonate, (E) ethoxy-bisphenolA-naphthalate, (F) diethoxy-bisphenolA-naphthalate.

**Figure 4.15.** Thermogravimetric curves obtained by TGA of the PC-PEN copolymers produced by reactive blending of PC and PEN in the molten state.

**Figure 4.16.** Loss weight derivative curves (DTGA) obtained by TGA of the PC-PEN copolymers produced by reactive blending of PC and PEN in the molten state.

**Figure 4.17.** DSC thermograms of PC-PEN equimolar mixtures (50/50 in mole) melt blended at  $280^\circ\text{C}$  in nitrogen flow at different mixing times.

**Figure 4.18.** FTIR spectra in the range  $1630 - 1870 \text{ cm}^{-1}$  of the materials obtained by reactive melt mixing of PC and PEN to 0, 10, 20, 30, 45 and 60 min.

**Figure 4.19.** Comparison of GPC curves of the initial PC homopolymer with that of THF soluble PC-PEN copolymers (20, 30, 45 and 60 min).

**Figure 4.20.** MALDI-TOF spectra of PC-PEN copolymers obtained after 60 min of reactive melt blending at 280°C of equimolar PC-PEN blend.

**Figure 4.21.** MALDI-TOF spectra of THF soluble PC-PEN copolymers (20, 30, 45 and 60 min) obtained by reactive melt blending at 280 °C of equimolar mixture PC-PEN (respect to the repeat unit) in the presence of Ti(OBut)<sub>4</sub> (0,2% w) as catalyst.

## List of tables

**Table 2.1.** Nuclei used in Polymer NMR.

**Table 3.1.** Some properties of polymer models and of heated PET and MXD6 samples with and without TA at 285 °C.

**Table 3.2.** Mass Assignments of peak present in the MALDI spectra of unprocessed and processed PET and MXD6 samples, reported in Figures 3.1 and 3.2.

**Table 3.3.** Assignments of Chemical Shift due to the Protons and Carbons belonging to sequences centered in the Ethylene Glycol, Terephthalate, Adipate structural units along the PET-MXD6 copolymer chains, as observed in their NMR spectra portrayed in figures 3.3, and 3.4.

**Table 3.4.** Material Balance, Molar fraction of Dyads, Average Sequences Lengths, Degree of Exchange (DE) and Degree of Randomness (DR) calculated from <sup>1</sup>H-NMR spectra of equimolar PET-MXD6-(1 wt%)TA blends Melt Mixed at 285 °C for different time.

**Table 3.5.** Molar fraction of Dyads and Triads, Average Sequences Lengths, Degree of Exchange (DE) and Degree of Randomness (DR) calculated from <sup>13</sup>C NMR spectra of equimolar PET-MXD6-(1 wt%)TA blends Melt Mixed at 285 °C for different time.

**Table 3.6.** Mass Assignments of peaks present in the experimental and calculated MALDI Mass Spectra of the PET-MXD6 (120 min) Random Copolymers reported in Figure 3.5.

**Table 3.7.** Viscosity ( $\eta_{inh}$ ), thermal properties (T<sub>g</sub>, T<sub>cc</sub>, T<sub>c</sub> and T<sub>m</sub>) and TGA data (PDT) of PET-MXD6-(1%w)TA blend melt mixed at 285 °C for different times. Thermal properties were determined by DSC analysis.

**Table 4.1.** Thermal and viscosimetric characteristic of polymer models.

**Table 4.2.** m/z values of the chemical species detected on the MALDI-TOF spectrum of the PC.



**Table 4.3.** m/z values of the chemical species detected on the MALDI-TOF spectrum of the PEN.

**Table 4.4.** Assignments of oligomers families observed in the MALDI TOF spectrum of pBPAN in the region 1660-2300 Da.

**Table 4.5.** m/z values of the chemical species detected on the MALDI-TOF mass spectrum of the p(BPAEtN)-co-(EtBPAEtN).

**Table 4.6.** Carbon signal assignments of structural units in the PC-PEN copolymers as observed in their  $^{13}\text{C}$ -NMR spectra.

**Table 4.7.** Molar ratio of ethylenic to naphthalate units (Et/N) and normalized molar composition (%mol) of the sequences A, B, C, D, E and F in the PC-PEN copolymers calculated by  $^1\text{H}$  and  $^{13}\text{C}$  NMR analysis.

**Table 4.8.** Average sequence lengths ( $L_A$ ,  $L_B$ ,  $L_C$ ,  $L_D$ ,  $L_E$  and  $L_F$ ), Degree of Exchange (DE), and Degree of Randomness (DR) in the PC-PEN copolymers calculated by  $^1\text{H}$  and  $^{13}\text{C}$  NMR analysis.

**Table 4.9.** % Mol and % weight of eliminated ethylene carbonate (EtC) and  $\text{CO}_2$ , as a function of reaction time, during reactive melt blending at 280 °C of equimolar PC-PEN blends in the presence of  $\text{Ti}(\text{OBut})_4$  (0,2% w) as catalyst. The following data are calculated by ( $^1\text{H}$  and  $^{13}\text{C}$ ) NMR and compared to %loss weight by Thermogravimetric Analysis (TGA) of the same initial mixture at 280 °C and in  $\text{N}_2$  flow.

**Table 4.10.** Thermal Properties of PC-PEN copolymer by DSC analysis.

**Table 4.11.** % weight of the component sequences ( $W_A$ ,  $W_B$ ,  $W_C$ ,  $W_D$ ,  $W_E$  and  $W_F$ ), calculated Tg by eq. 19, and experimental Tg, of the equimolar PC-PEN blends.

**Table 4.12.** Viscosity data ( $\eta_{\text{inh}}$ ) and GPC data ( $M_w$ ,  $M_n$  and PD) of the material obtained by reactive melt blending of equimolar PC-PEN blends.

**Table 4.13.** Assignments of the mass peaks observed in the MALDI-TOF spectra of PC-PEN copolymers obtained after 60 min of reactive melt blending at 280 °C of equimolar PC-PEN blends in the presence of  $\text{Ti}(\text{OBut})_4$  (0,2% w) as catalyst.

**Table 4.14.** Assignments of the mass peaks observed in the MALDI-TOF spectra of THF soluble PC-PEN copolymers (20, 30, 45 and 60 min) obtained by reactive melt blending at 280 °C of equimolar PC-PEN blends in the presence of Ti(OBut)<sub>4</sub> (0,2% w) as catalyst.

## List of schemes

**Scheme 3.1.** Exchange reactions that might occur during the melt mixing of PET-MXD6 blends.

**Scheme 3.2.** Outer-outer transamidation reaction;

**Scheme 3.3.** Reactions occurring during the treatment of PET or MXD6 with TA at 285°C.

**Scheme 3.4.** Formation of cyclopentanone end groups during the melt mixing of MXD6.

**Scheme 3.5.** Outer-inner exchange reaction: acidolysis of PET.

**Scheme 4.1.** Formation reaction of polycarbonate (PC).

**Scheme 4.2.** Chemical structures of PEN and PET.

**Scheme 4.3.** Catalyzed Exchange Reactions and consecutive elimination of CO<sub>2</sub> and ethylene carbonate (EtC) in the Melt Mixing of PC with PEN at 280 °C.

**Scheme 4.4.** Formation of diethoxy-bisphenolA sequences (F).

**Scheme 4.5.** Synthesis reactions of poly(bisphenolA naphthalate).

**Scheme 4.6.** Synthesis reactions of copoly(bisphenolA carbonate)-alt-(ethylene carbonate).

**Schema 4.7.** Synthesis reactions of BPAEt and EtBPAEt co-monomers.

**Scheme 4.8.** Reactions synthesis of the monomers diethoxy-bisphenolA.

**Scheme 4.9.** Synthesis reactions of poli(diethoxy-bisphenolA naphthalate).

## Abbreviations

TA	terephthalic acid.
HFIP	hexafluoroisopropanol.
THF	tetrahydrofuran.
HABA	2-(4'-Hydroxybenzeneazo)benzoic acid (matrix)
DHB	2,4-dihydroxy benzoic acid ( matrix)
$\alpha$ -Ciano	4- hidroxicinamic acid (matrix)
MALDI-TOF ms	Matrix Assisted Laser Desorption Ionization- Time of Flight mass spectrometry
PET	poly(ethylene terephthalate).
MXD6	poly( <i>m</i> -Xylene adipamide).
MXDT	poly( <i>m</i> -Xylene terephthalamide).
PEA	poly(ethylene adipate).
PC	poly(bisphenolA carbonate).
PEN	poly(ethylene naphthalate).
pBPAN	poly(bisphenolA naphthalate).
p(BPAC)-alt-(EtC carbonate)	copoly(bisphenolA carbonate)-alt-(ethylene carbonate)
p(BPAEtN)-co-(EtBPAEtN)	poly(ethoxy-bisphenolA naphthalate)-co-(di- ethoxy-bisphenolA naphthalate).
pEtBPAEtN	poly(diethoxy-bisphenolA naphthalate).

# **1. INTRODUCTION**

## **1.1 - Preface**

The modern technology require to macromolecular chemistry the availability of materials able to respond always better to the differen features behavioural demands by designers. The tendency is to obtain materials with innovative properties apparently incompatible: high elastic module together with good impact resistance, ease of fabrication combined with a high resistance to temperature, high permeability and selectivity to gases (membranes for separation of gas mixtures), low permeability to atmospheric gases (O<sub>2</sub> and CO<sub>2</sub>) and good biodegradability (food packaging) etc. In this respect, macromolecular chemists have directed their research in the synthesis of new materials, starting by mixtures of preexisting homopolymers. So arise the field of the “polymeric blends” which today is probably the most effective and convenient method to get innovative and versatile materials having properties which often correspond to the merge of the best characteristics of the starting polymers.

The preparation of polymeric compounds can be performed according to different methods <sup>1,2</sup>:

- Physical mixing;
- Casting by solvent;
- Solution / precipitation by solvent in no-solvent;
- Melt Blending.

The melt blending of polymers is certainly the most interesting technical to develop materials with new properties or improve some already on the source homopolymers. Furthermore, the mixing processes allow you to recycle polymeric materials after use.

The formation of a monophasic blends, where the size of the domains is comparable with the size of individual macromolecules (total miscibility) or a biphasic materials, with total or partial segregation of the components in the two phases (total or partial miscibility), depends of the interactions between different polymer chains.

According to the theory of Flory-Huggins <sup>1, 2</sup>, the miscibility of polymer blends in the molten is dictated by energetic considerations ( $\Delta G_{\text{mix}} = \Delta H_{\text{mix}} - T\Delta S_{\text{mix}}$ ). The change of entropy during the mixing of polymers has a very low value, and gradually becomes negligible with increasing of polymerization degree (molecular weight). The driving factor that indicates the miscibility between two polymers in the molten state is therefore the enthalpy change during the blending<sup>1,2</sup>.

Negative  $\Delta H_{\text{mix}}$  indicate complete miscibility at the molecular level, with small homopolymer clusters randomly dispersed in the blend (monophasic blends). These blends, generally, exhibit very good mechanical properties, in general corresponding to the linear sum of those of the individual components. For biphasic blends, however, the high surface tension does not allow the homogenization of the material, with no interfacial adhesion. Immiscible or partially miscible polymer blends usually show a behavior highly "elastic", which often causes serious problems during processing, such as swelling of the extruded and fracturing under stress. The swelling of the extruded is caused by the shape recovery of the dispersed particles. In general, these problems of the processability can be reduced or completely eliminated by compatibilization. The best compatibilizers agents are block and/or graft copolymers, which usually are added in small percentages to the initial mixture of polymers. As shown in Figure 1.1, these copolymers migrate to the interface of the polymer phases and, by acting as emulsifiers, reducing the repulsive energy between the different domains.

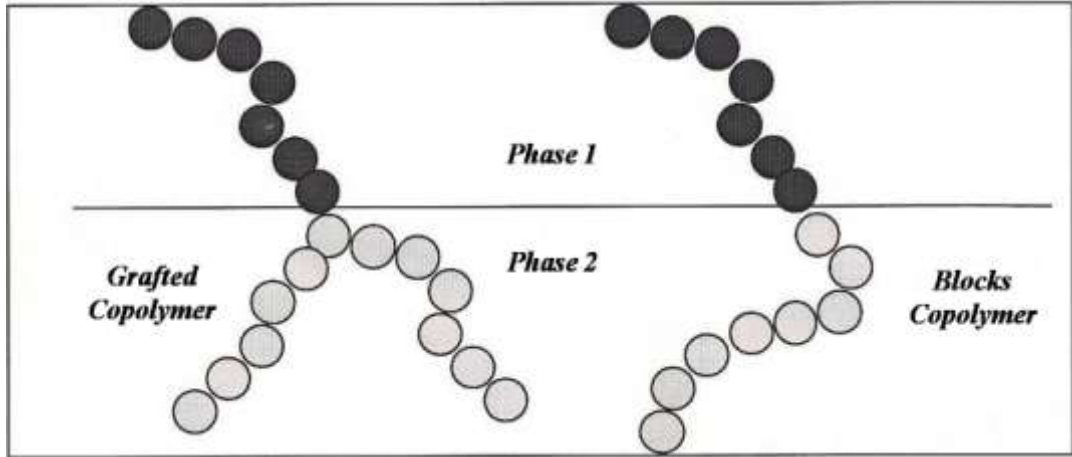


**Figure 1.1.** Copolymer action as compatibilizer.

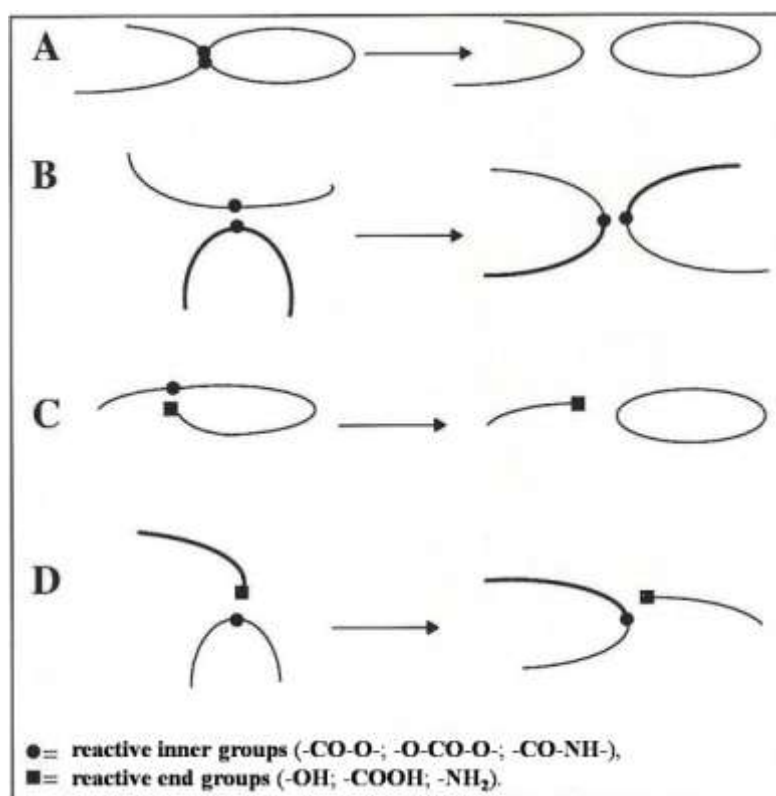
In the grafting and block copolymers is maintained the individuality of the various components, which correspond to segments of polymer of limited length, each characterized by its glass transition temperature ( $T_g$ ). In the block copolymers, the greater the length of the blocks, better are the compatibilizers properties of the copolymer itself. The compatibilization blends, show a single value of  $T_g$ , intermediate between those of the two homopolymers that compose the mixture, in agreement with the classic Fox equation <sup>1,2</sup>.

$$\frac{1}{T_g} = \frac{W_1}{Tg_1} + \frac{W_2}{Tg_2};$$

were  $W_1$ ,  $W_2$  and  $Tg_1$ ,  $Tg_2$  are the weight fractions and the thermal glass transition (in Kelvin) respectively of initial homopolymers.

## 1.2 - Reactive melt blending

Mixtures of polycondensation polymers such as polyesters, polyamides and polycarbonates and, in general, of all polymers containing reactive functional groups within the chain and as terminals, may result in chemical exchange reactions, when mixed in the molten state<sup>1-4</sup>. At these temperatures (200-300°C), may occur chemical interchange reactions induced by catalysts, utilized in the synthesis, and/or by terminal groups (-OH, -NH<sub>2</sub>, -COOH ecc.) present in the polymers or generated by degradation or hydrolytic reactions. In this way can be formed, block, statistical or grafting copolymers, which can act as compatibilizers agents of the initial mixture, sometimes with improving of the mechanical, physical, and chemistry properties. Therefore, the study of the mechanisms and kinetics of exchange and degradation reactions that occur in the molten state, and compositional analysis of materials obtained, it is a necessary step to prepare polymer blends with known and reproducible properties.



**Scheme 1:** Exchange reactions with inner-inner and outer-inner mechanism.



Among the possible processes, we can distinguish reactions between functional groups in the chain (inner-inner, scheme 1, A-B) and reactions that involving terminal groups and those on the chain (outer-inner, scheme 1, C-D).

In figure 2 is shown a schematic representation of the exchange reactions (primary) and degradation (secondary) that may occur in the system consisting of two homopolymers A and B, containing reactive functional groups, depending on the temperature.

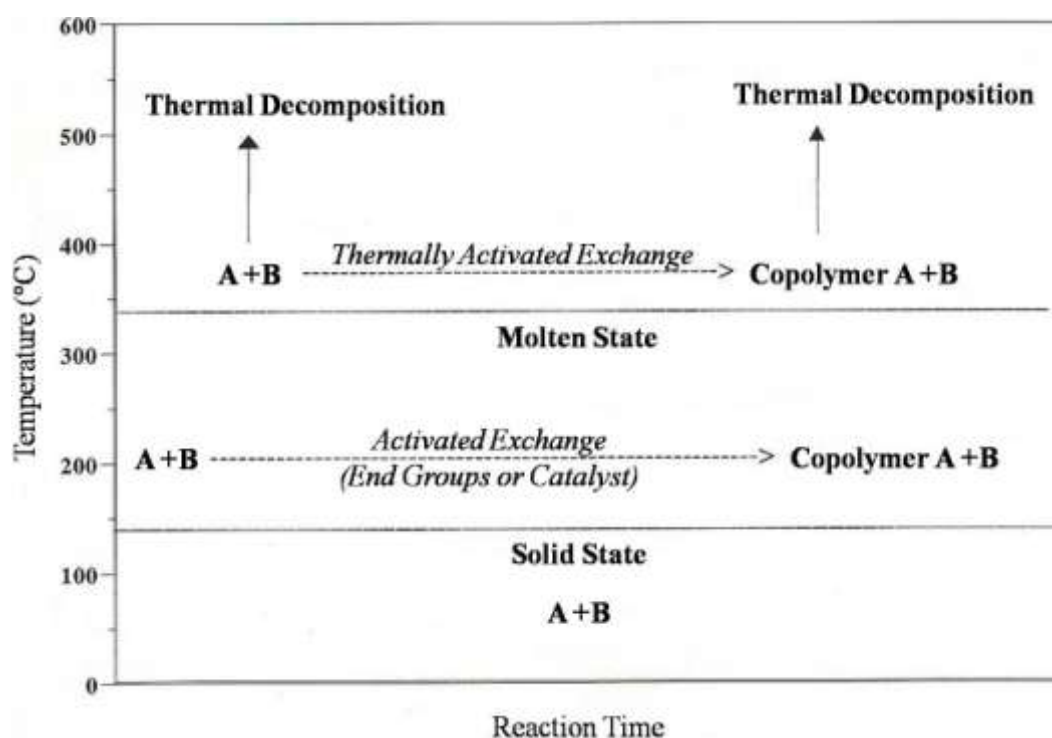


**Figure 1.2.** Schematic representation of the exchange reactions which can occur in polymer blends containing reactive functional groups as a function of temperature.

When the mixture is treated in a temperature range 200-300°C, it forms a copolymer AB as a result of intermolecular reactions induced by the presence of functional groups or traces of catalysts<sup>1, 2 3</sup>, whereas at temperatures higher than 300°C, the exchange reactions are thermally activated, with possibility of simultaneous processes of thermal degradation<sup>5, 6</sup>.

The type of mechanism that allow the chemical exchange reactions depends on the structure of the polymer chains, and therefore by the

presence of reactive functional groups (such as -OH, -COOH and -NH<sub>2</sub>) located within the chain or as terminal groups.

In an equimolar mixture of two homopolymers, A and B, containing reactive functional groups inside, assuming that the reactivity of these groups is the same, every species has equally likely to react with a mechanism like inner-inner, because the concentration of functional groups is the same for both polymers. Therefore, the composition of copolymer AB format must be equal to the initial composition of feed (1:1), regardless of the degree of progress of the reactions, which should proceed until the complete transformation of the two homopolymers.

More complex is the case of reactions that proceed with a mechanism of outer-inner type, because in a equimolar mixture of two homopolymers A and B, both can contain reactive end groups having different reactivity. In any case, the speed of the outer-inner reactions is a function of molecular weight of the homopolymers containing reactive end groups, and therefore of their concentration in the molten.

If only one of the two initial homopolymers possess reactive end groups (ie, the other has a very high molar mass), the reaction rate will depend solely by concentration of these terminals, and the AB copolymer initially formed will contain an excess of units in the reactive polymer.

Therefore, the determination of the nature and composition of the produced copolymer by reactive mixing of two initial homopolymers, may be regarded as a key to understanding the type of reaction occurred.

### 1.3 – Aim of the work

The scientific and industrial literature shows an increase of new studies concerning to polymer blends between polyesters, polyamides and polycarbonates, three important classes of thermoplastic homopolymers, that are immiscible each with other. The compatibilization of the starting polymers, obtained directly during processing (extrusion) or by chemical exchange reactions between the polymer chains, or by adding small amounts of block and or graft copolymers, is certainly one of the key aspects that suggests a macromolecular chemists to study these systems with increasing interest, also because the development of a compatibilized system drastically reduces the costs associated to the production and to the processing of the new materials.

Within of this research topic, the PhD work has been focused on the synthesis and characterization of the following binary blends:

- Polyesters PET (polyethylene terephthalate) with polyamide MXD6 (poly*meta*-xylene adipamide), at 285 °C, in nitrogen flow and in presence of terephthalic acid;
- Polyesters PEN (polyethylene naphthalate) with polycarbonate PC (polybisphenolA carbonate), at 280 °C, in nitrogen flow and in presence of titanium tetra butoxide [Ti(ButO)<sub>4</sub>] as transesterification catalyst.

The aim of research was to have a comprehensive characterization of the interchange reactions that can occur during the reactive blending of PET-MXD6 and PC-PEN blends, in order to establish the possible types of copolymers that can be obtained (blocks, multiblocks, random) on the base of reaction conditions (temperature, time of processing, type of additive, type of mechanical mixer, etc.).

## 1.4 - References:

1. G. Montaudo, C. Puglisi, and S. Samperi, *Transreactions in Condensation Polymers* – Fakirov S, Ed. Wiley-VCH: New York, Chapt.4;
2. AIM “Macromolecole, Scienza e Tecnologia” Vol.1;
3. G. Montaudo, C. Puglisi, F. Samperi, and F. La Mantia, *J Polym Sci, Part A; Polym Chem Ed* - **1996**, 34, 1283;
4. G. Montaudo, C. Puglisi, and F. Samperi, *Macromolecules* – **1998**, 31, 650;
5. B. Plage, H.R. Schulten, *J Anal Appl Pyrolysis* - **1989**, 15, 197;
6. C. C.Huang, F.C. Chang, *Polymer* - **1997**, 38 (9, 179), 2135.

## 2. CHARACTERIZATIONS TECHNIQUES

### 2.1 – Nuclear Magnetic Resonance

Nuclear magnetic resonance (NMR) spectroscopy<sup>1-5</sup> is a very powerful technique for polymer characterisation. It can be used to determine tacticity, branching and structural defects such as the occurrence of head-to-head placement of monomers in vinyl polymers, the sequence of comonomer units in a copolymer chain, and chemical changes such as oxidation states which can be detected at levels as low as one site per 500 repeat units. Although <sup>13</sup>C NMR is commonly used in polymer characterisation, NMR measurements employing other NMR-active nuclei such as <sup>1</sup>H, <sup>15</sup>N, <sup>17</sup>O and <sup>19</sup>F having magnetic moments may have an advantage in the study of some polymers. For example, <sup>29</sup>Si NMR may be used in the characterisation of polysiloxanes, <sup>19</sup>F NMR for fluoropolymers, <sup>15</sup>N NMR for polyamides, and <sup>31</sup>P NMR for polyphosphazenes. A complete listing of important NMR-active nuclei and their natural abundance is given in Table 1<sup>5</sup>.

**Table 1.** Nuclei used in Polymer NMR.

Nuclei	Spin	Natural Abundance (%)	Shift Range (ppm)
<sup>1</sup> H	1/2	99.985	15
<sup>2</sup> H	1	0.0156	15
<sup>13</sup> C	1/2	1.108	220
<sup>14</sup> N	1	99.634	900
<sup>15</sup> N	1/2	0.365	900
<sup>17</sup> O	5/2	0.037	800
<sup>19</sup> F	1/2	100	800
<sup>29</sup> Si	1/2	4.70	250
<sup>31</sup> P	1/2	100	700

Many atomic nuclei behave as if they were spinning. In fact, any atomic nucleus, which possesses either odd mass or odd atomic number, or both, has a quantised spin angular momentum and a magnetic moment.

Among the more common nuclei which possess "spin" one may include  $^1\text{H}$ ,  $^2\text{H}$ ,  $^{13}\text{C}$ ,  $^{14}\text{N}$ ,  $^{17}\text{O}$ , and  $^{19}\text{F}$ . Notice that the nuclei of the ordinary (most abundant) isotopes of carbon and oxygen  $^{12}\text{C}$  and  $^{16}\text{O}$  are not included among those with the spin property. However, the nucleus of the ordinary hydrogen atom, the proton, does have spin. For each of the nuclei with spin, the number of allowed spin states which it may adopt is quantised and is determined by its nuclear spin quantum number,  $\mathbf{I}$ . This number is a physical constant for each nucleus. For a nucleus of spin quantum number  $\mathbf{I}$ , there are  $2\mathbf{I} + 1$  allowed spin states which range with integral differences from  $+\mathbf{I}$  to  $-\mathbf{I}$ . For spin  $\frac{1}{2}$  nuclei the possible magnetic quantum numbers are  $+\frac{1}{2}$  and  $-\frac{1}{2}$ . When placed in a magnetic field, nuclei having spin undergo precession about the field direction. The frequency of this so-called Larmor precession is designated as  $\omega_0$  in radians per second or  $\nu_0$  in Hertz (Hz), cycles per second ( $\omega_0 = 2\pi\nu_0$ ). The nuclei can be made to flip over, i.e. reverse the direction of the spin axis, by applying a second magnetic field (Figure 2.1), designated as  $\mathbf{H}_1$ , at right angles to  $\mathbf{H}_0$ . The Larmor precession frequency or resonance frequency is given by:

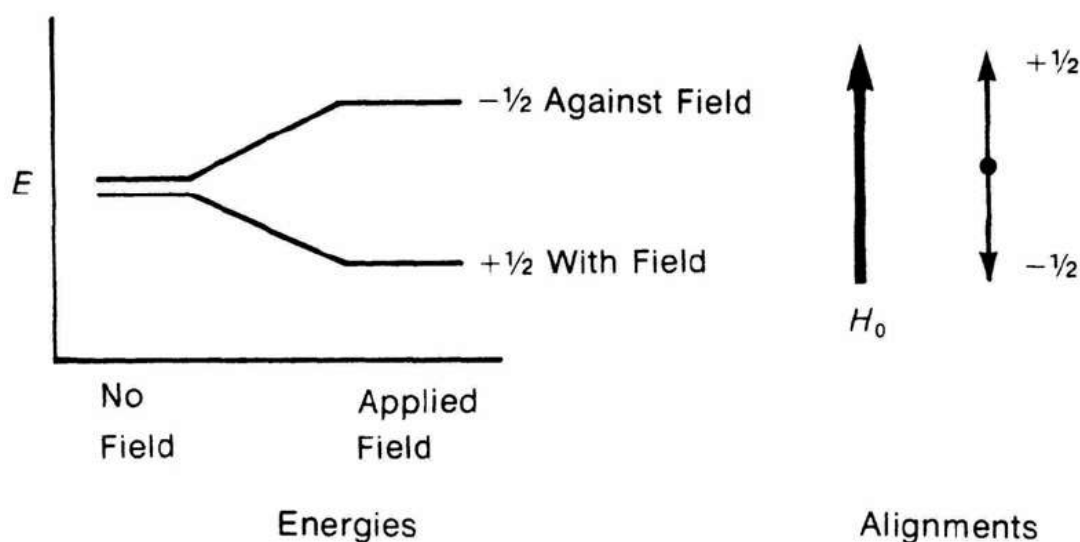


**Figure 2.1.** The spin states of a proton both in the absence and in the presence of applied magnetic field.

where  $\gamma$  is the magnetogyric ratio. The two quantities that determine the observation frequency for NMR signals are the magnetogyric ratio  $\gamma$  and the magnetic field strength  $H_0$ . The sensitivity depends both on the magnetogyric ratio and on the natural abundance of the NMR active nuclei. Protons have the highest sensitivity because they have the highest magnetogyric ratio and natural abundance (Table 1).

The NMR spectrum is usually observed by applying a radio frequency pulse near the resonance frequency and observing a free induction decay (FID). The NMR spectrum, a plot of intensity vs. frequency, is obtained by Fourier transformation of the observed signal. The signal frequency (or chemical shift) is reported relative to some reference compound. The integrated signal intensity is proportional to the number of nuclei. This property is important because it allows us to use NMR as a quantitative tool.

Solution NMR is extremely useful for polymer characterisation because the chemical shifts and relaxation times are sensitive to polymer microstructure. High-resolution spectra are observed because the linewidths are less than the chemical shift variations due to the polymer chain chemical structure and microstructure. The chemical shift resolution results from variations in nuclear shielding arising from variations in electron density that are affected by the presence of nearby electron withdrawing or donating groups. The chemical shift changes can be related to through-bond inductive effects and through-space interactions. The largest effects on the chemical shifts are the chemical type, and the resonances from methyl, methine, methylene and aromatic groups are often well separated in the NMR spectrum. Carbon NMR has been extensively used for the solution characterisation of polymers because it is one of the most common elements in polymers. Carbon has a low natural abundance (1%  $^{13}\text{C}$ ) but most polymers are sufficiently soluble that it is possible to record their NMR spectrum at high concentration ( $[\text{C}] > 0.05$

M). The carbon spectra are often more highly resolved than the proton spectra because the carbon chemical shifts are spread over 200 ppm, rather than the 10 ppm commonly observed for protons.

$^1\text{H}$  and  $^{13}\text{C}$  NMR analyses were performed with a Bruker ACF200 spectrometer at room temperature with deuterated solvent and tetramethylsilane as an internal standard. Two different mixture of deuterated solvent was used:

- $\text{CDCl}_3/(\text{CF}_3\text{CO})_2\text{O}/\text{CF}_3\text{COOD}$  (70:17:13 v/v) for homopolymer models PET, MXD6, PEA, and MXDT, and all the PET-MXD6 melt-mixed blends;
- $\text{CDCl}_3/\text{d-TFA}$  20/20 v:v for all PC-PEN melt-mixed blends and also for the model polymers PC, PEN, pBPAN. p(BPAC)-alt-(EtC), p(BPAEtN)-co-(EtBPAEtN), pEtBPAEtN.

$^{13}\text{C}$  NMR spectra were recorded at 50 MHz using the following acquisition parameters: sweep width, 10,204 Hz and 32.768 data points, giving

a digital resolution of 0.623 Hz per point and an acquisition time of 1.6 s. A pulse width of 3.5  $\mu\text{s}$  and delay of 23 s were used for about 20,000 accumulations. These being the optimized parameters at which peak intensities of carbonyl and methylene carbons most closely match the feed ratio. The acquisition parameters were optimized by the analysis of equimolar PET-MXD6 and PC-PEN physical blends. The data were elaborated with 1D Win-NMR software applying the Lorentz–Gauss enhance function using appropriate line broadening and Gaussian broadening parameters to improve the peaks resolution. The chemical shift resonances were accurately assigned to the specific protons and carbons on the basis of the chemical shifts observed in the spectra for the various model polymers (PET, MXD6, PEA, and MXDT, PC, PEN, pBPAN. p(BPAC)-alt-(EtC), p(BPAEtN)-co-(EtBPAEtN), pEtBPAEtN).



Quantification of the  $^{13}\text{C}$  NMR signals was performed by integration of the area of the corresponding peaks.

## 2.2 – Differential Scanning Calorimeter (DSC)

One of the most widely used techniques to measure  $T_g$  and  $T_m$  is Differential Scanning Calorimetry (DSC) <sup>6-7</sup>. The signal in a DSC experiment is related to the difference between the “thermal response” of a small (5 to 10 mg) polymer sample and reference cell (empty) in two separate aluminium pans. The two are heated and cooled at the same rate or maintained at a constant temperature, as illustrated in Figure 2.2.

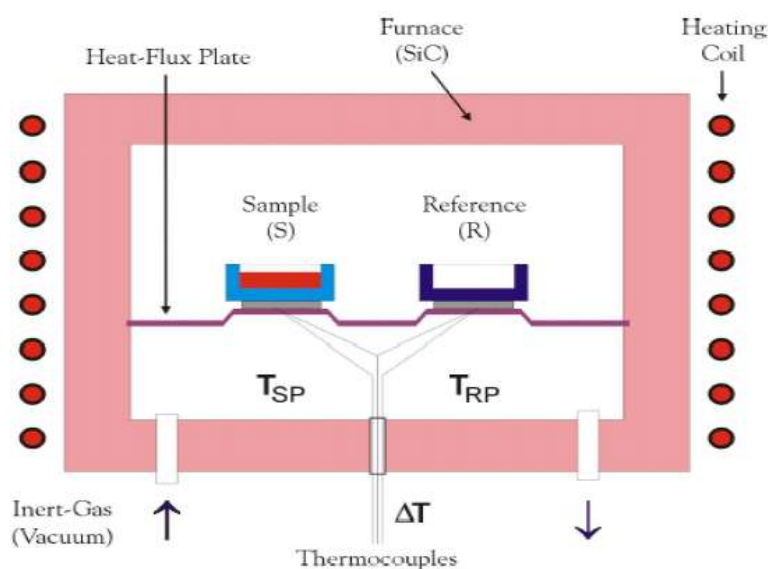


**Figure 2.2.** Schematic representation of a typical DSC sample cell showing the sample (S) and reference (R) pans, as well as the heating and temperature sensing elements.

Thermocouple junctions just underneath each position monitor both the temperature of the sample side  $T_s$ , and the difference between the temperature of sample side  $T_s$  and the temperature of the reference side  $T_r$ ,  $\Delta T = T_r - T_s$ . If the cell is empty and thermally symmetric, the temperature of the reference side will always be the same as the temperature of the sample side irrespective of heating and cooling. The values of specific heat  $C_p$ , may be obtained from the recorded heat-flow rate by calibration with a pure compound such as sapphire for which  $C_p$  is known precisely at different temperatures from Calorimetry measurements.

As illustrated in Figure 2.3, a discontinuity in  $C_p$  (i.e.,  $\Delta C_p = C_p^l - C_p^s$ ), characteristic of a second order transition, is observed at the polymer  $T_g$  that is often identified as the temperature at the midpoint of the step change in  $C_p$  (i.e., at  $\Delta C_p/2$ ).

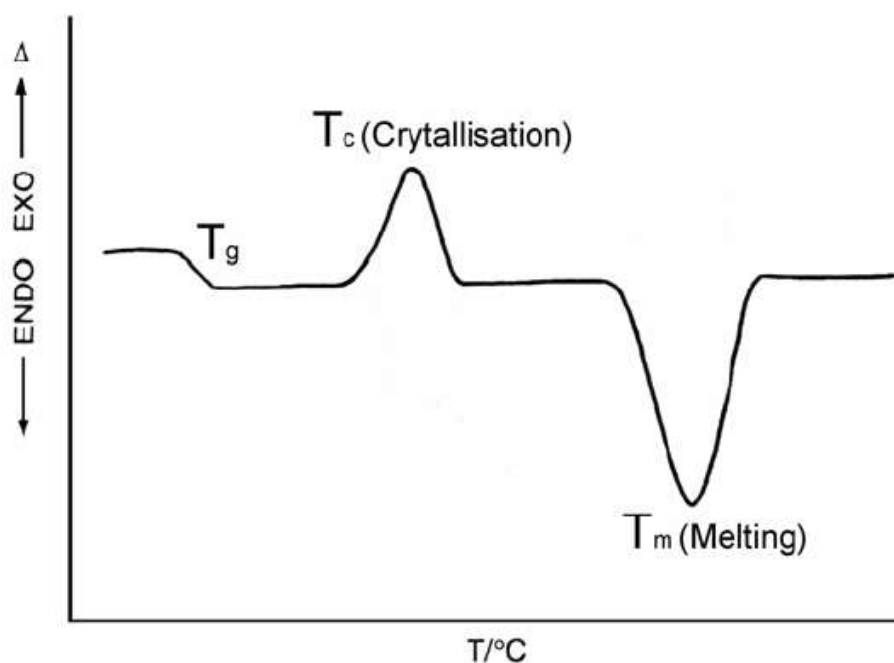


**Figure 2.3.** Typical DSC curve, using convention that endothermic peak goes down.  $\Delta$  indicates the differential signal of temperature between reference and sample.

For many amorphous polymers,  $T_g$  (K) and  $\Delta C_p$  ( $\text{J g}^{-1} \text{K}^{-1}$ ) are related by the approximate relationship that  $\Delta C_p * T_g = 115 \text{ J g}^{-1}$  ( $27.5 \text{ cal g}^{-1}$ )<sup>7</sup>. During heating of a semicrystalline, additional crystallization may occur at temperatures between  $T_g$  and  $T_m$ , as illustrated by the crystallization exotherm in Figure 2.3. At  $T_m$ , which may be defined as the extrapolated temperature of the initial slope of the melt endotherm, crystallites begin to melt over a wide range of temperatures. The breadth of the endotherm is much larger than typically observed for pure low-molecular-weight compounds as a consequence of the lower order of perfection of polymer crystallites. By calibration with a low-molecular-weight standard such as benzoic acid, the heat of fusion ( $\Delta Q$ ) of a

semicrystalline polymer can be determined from measurement of the area under the melt endotherm recorded by DSC.

The thermal behaviors of the all samples (model polymers and of all PET-MXD6 and PC-PEN melt-mixed materials) were investigated in nitrogen atmosphere by TA Instrument Q100 differential scanning Calorimetry (DSC), calibrated with melt purity indium standard (156.6 °C and 28.45 J/g). Samples with a mass of  $5 \pm 1.1$  mg are used. Before any experiment, the baseline is recorded using empty aluminum pan (reference and sample). Each sample was analyzed following the same runs: (i) heating at 10 °C/min from 0 °C to 280 °C; (ii) quenching at 100 °C/ min from 280 °C to 60 °C; (iii) heating at 10 °C/min from 60 °C to 280 °C; and (iv) cooling at 10 °C/min from 280 °C to 60 °C. Three repeated scans were performed to verify the reproducibility of thermal transitions. The T<sub>g</sub> values were measured in the second heating and were computed by midpoint method; the melting point temperatures (T<sub>m</sub>), the cold crystallization (T<sub>cc</sub>), and the crystallization temperatures (T<sub>c</sub>) were taken as the maximum of the specific endothermic and exothermic peaks.

## 2.3 – Thermogravimetry (TGA)

Measurements of changes in sample mass with temperature are made using a thermobalance (sometimes referred to as a thermogravimetric analyzer). A thermobalance is a combination of a suitable electronic microbalance with a furnace, a temperature programmer and computer for control, that allows the sample to be simultaneously weighed and heated or cooled in a controlled manner, and the mass, time, temperature data to be captured. The balance should be in a suitably enclosed system so that the nature and pressure of the atmosphere surrounding the sample can be controlled (see Figure 2.4). Care is usually taken to ensure that the balance mechanism is maintained at, or close to, ambient temperature, in an inert atmosphere.

Thermogravimetric analysis (TGA) was used to assess thermal stability of all samples (the model polymers, PET-MXD6 and PC-PEN

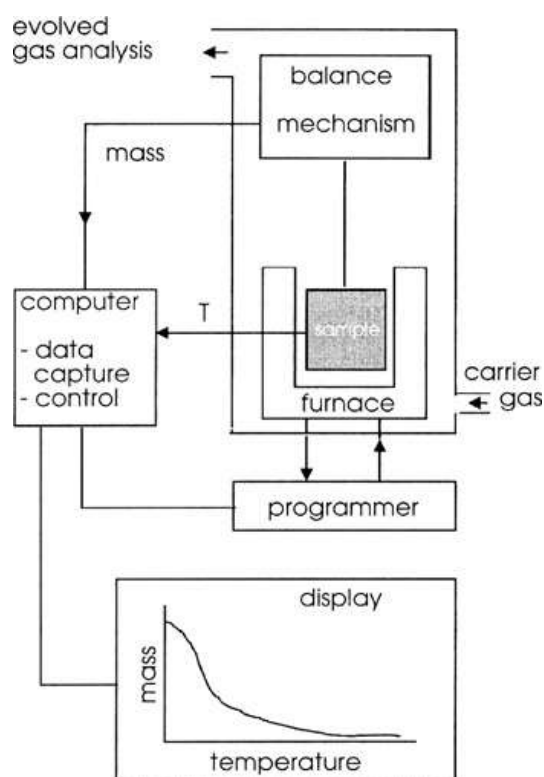


**Figure 2.4.** A schematic thermobalance.

melt-mixed blends) with a TGA-500 V6.7 instrument (TA-INSTRUMENT) coupled with a TA-Instrument Explorer operating software. The analyses were performed under dynamic heating conditions, from 50 °C to 800 °C under nitrogen flow (60 mL min<sup>-1</sup>), at a heating rate of 10 °C min<sup>-1</sup>, using about 2 mg of sample. The weight and temperature of the thermobalance were calibrated using four high-purity magnetic

standards (alumel, nickel, Ni<sub>0.83</sub>Co<sub>0.17</sub> alloy, and Ni<sub>0.63</sub>Co<sub>0.37</sub> alloy) for

the Curie temperature (152.6, 358.2, 554.4, and 746.4 °C, respectively) following both calibration procedure through the instrument control software. Data recorded show the thermal behavior of all samples in terms of weight loss percentage at the increasing of temperature. The slope of degradation curve depends on kind and amount of specific mechanism of degradation during temperature scanning.

## 2.4 – MALDI-TOF mass spectrometry

MALDI-TOF mass spectrometry is an emerging technique offering promise for the fast and accurate determination of a number of polymer characteristics. The MALDI technique is based upon an ultraviolet absorbing matrix pioneered by Hillenkamp and Karas<sup>9</sup>. The matrix and polymer are mixed at a molecular level in an appropriate solvent with a  $\sim 10^4$  molar excess of the matrix. The solvent prevents aggregation of the polymer. The sample/matrix mixture is placed onto a sample probe tip. Under vacuum conditions the solvent is removed, leaving co-crystallized polymer molecules homogeneously dispersed within matrix molecules. When the pulsed laser beam is tuned to the appropriate frequency, the energy is transferred to the matrix which is partially vaporized, carrying intact polymer into the vapor phase and charging the polymer chains (see figure 2.5)<sup>9</sup>.

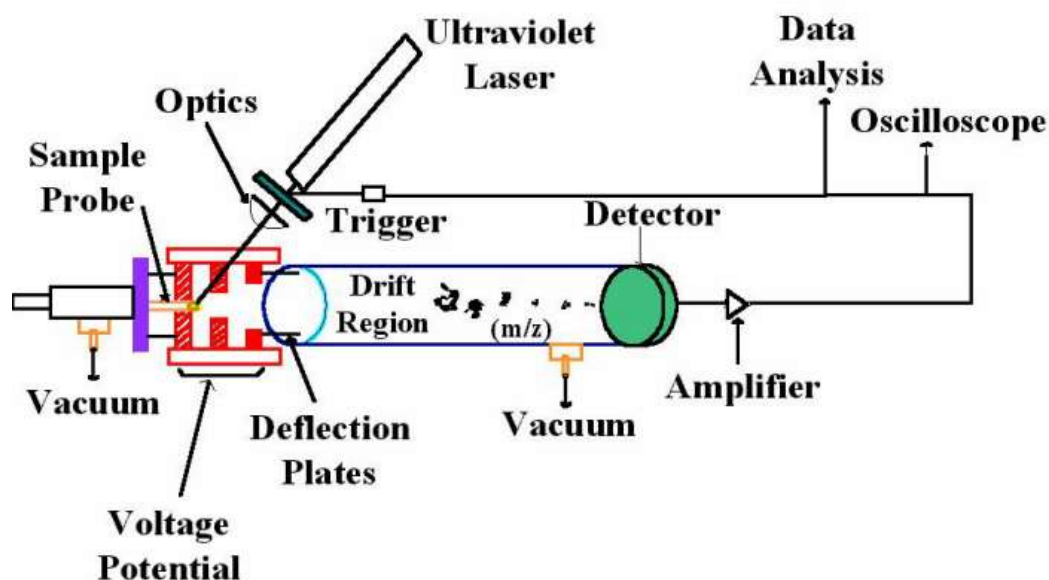


**Figure 2.5.** Schematic of a MALDI-TOF Mass Spectrometer.

Multiple laser shots are used to improve the signal-to-noise ratio and the peak shapes, which increases the accuracy of the molar mass determination<sup>10</sup>. In the linear TOF analyzer (drift region), the distribution

of molecules emanating from a sample are imparted identical translational kinetic energies after (Figure 2.6) being subjected to the same electrical potential energy difference.

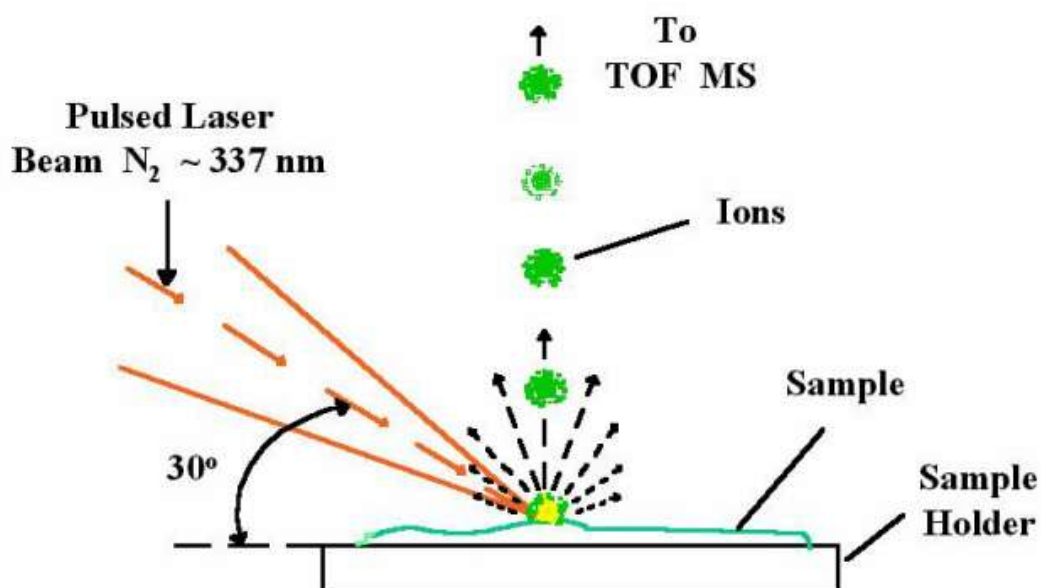


**Figure 2.6.** MALDI-TOF MS Sample Ionization.

These ions will then traverse the same distance down an evacuated field-free drift tube; the smaller ions arrive at the detector in a shorter amount of time than the more massive ions. Separated ion fractions arriving at the end of the drift tube are detected by an appropriate recorder that produces a signal upon impact of each ion group. The digitized data generated from successive laser shots are summed yielding a TOF mass spectrum. The TOF mass spectrum is a recording of the detector signal as a function of time. The time of flight for a molecule of mass  $m$  and charge  $z$  to travel this distance is proportional to  $(m/z)^{1/2}$ . This relationship,  $t \sim (m/z)^{1/2}$ , can be used to calculate the ions mass. Through calculation of the ions mass, conversion of the TOF mass spectrum to a conventional mass spectrum of mass-to-charge axis can be achieved (See Figure 2.7).

MALDI is a ‘soft’ ionization technique in which the energy from the laser is spent in volatilizing the matrix rather than in degrading the polymer. Preparation of an appropriate polymer/matrix mixture is one of the critical limiting factors for the universal application of MALDI to



synthetic polymers. With the advent of MALDI in 1992, the challenge has been to discover appropriate matrix materials for use with synthetic polymers, since previous efforts were centered around biopolymers. Synthetic water-soluble polymers have been shown to be capable of analysis using similar conditions to those of biopolymers. Synthetic, organic-soluble polymers, however, have exhibited analysis complications due to their seeming incompatibility with the matrix materials. Because of this fact, only structurally simplistic synthetic water-soluble and organic-soluble polymers have been investigated to date using MALDI analysis.

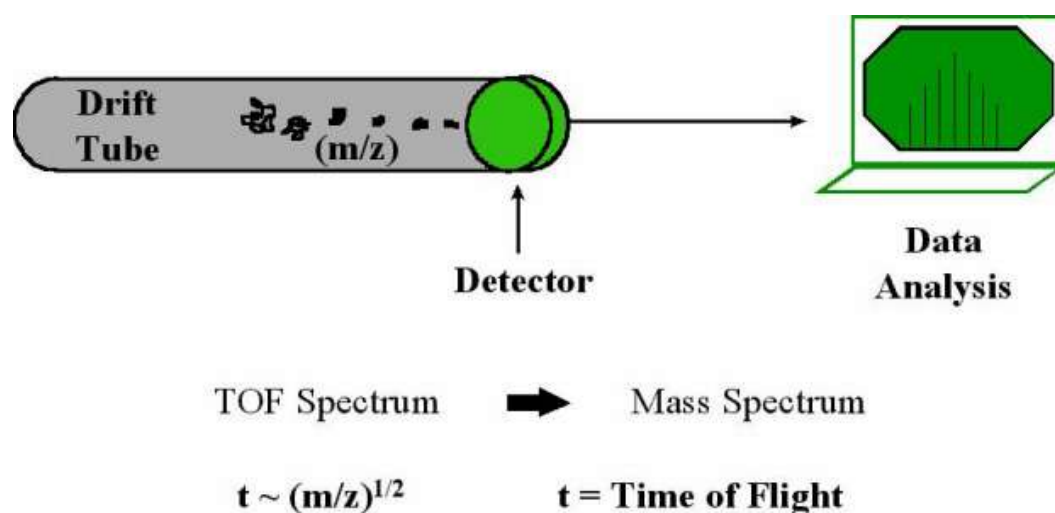


**Figure 2.7.** Conversion from TOF spectra to Conventional Spectra.

The purpose of the matrix material, as alluded to previously, is two-fold: (1) absorption of energy from the laser light, thus preventing polymer decomposition, and (2) isolation of the polymer molecules from one another<sup>10,11,12</sup>. Matrices for biopolymers have traditionally utilized just the biopolymer and the matrix material. Synthetic polymers, particularly organic-soluble polymers, have differing solubilities in the common solvents and often do not have a large concentration of ionized species. Most of the commonly used matrices are 2,5-dihydroxybenzoic acid derivatives, sinapinic acid derivatives, and indoleacrylic acid derivatives. Few compounds are useful as matrix materials due to the numerous stipulations involved: common solubility in a given solvent

(water, acetonitrile, ethanol, etc.), absorption, reactivity, and volatility are conditions that must be considered before an appropriate matrix might be found for a particular synthetic polymer<sup>10,11</sup>. In addition to the matrix material, a cationizing species is often added to increase the concentration of ionized species<sup>13</sup>. Some linear homopolymers and condensation polymers have been shown to yield adequate spectra for analysis without a cationizing species but often alkaline salts (LiCl, NaCl, KCl) or silver trifluoroacetate have been included as the cationizing agent to increase the yield of cationized species and allow a more homogeneous cationization. Surfactants are being investigated<sup>14</sup> for use with organic-soluble polymers where homogenization is not always possible or reproducible. Enhancement of spectra is expected where the surfactant can potentially play a dual role as both a matrix emulsifier and cationization agent.

MALDI-TOF mass spectra were recorded in linear and in reflectron mode with Voyager DE-STR (Perceptive Biosystem) mass spectrometry instrument equipped with nitrogen laser emitting at 337 nm, with a 3 ns pulse width and working in positive mode. The accelerating voltage was 20 kV, and the grid voltage and delay time were optimized for each sample to achieve better resolution. The irradiance was maintained slightly above the threshold. HABA solution 0.5 M in hexafluoro-2-propanol (HFIP or THF) solvent was used as matrices. The concentration of all samples was 5 mg/mL in HFIP (PET, PEN, MXD6, and PET-MXD6 blends) or THF (PC, pBPAN, p(BPAC)-alt-(EtC), p(BPAEtN)-co-(EtBPAEtN), pEtBPAEtN, and PC-PEN blends at 20, 30, 45 and 60 min). Appropriate volume of polymer solution and matrix solution was mixed to obtain a 1:1, 1:2, and 1:3 v/v ratio. About 1  $\mu$ L of each sample/matrix mixture was spotted on the MALDI-TOF sample holder and slowly dried to allow matrix crystallization. Spectra of PET samples were also recorded using DHB (2,4-dihydroxy benzoic acid) as a matrix (0.5 M in

THF) but better spectra were recorded using HABA as the matrix. Indeed the better spectra for PC-PEN blends 20, 30, 45 and 60 min were recorded in reflectron mode using  $\alpha$ -ciano (4- hidroxycinamic acid) as matrix (0.5 M in THF).

## 2.5 – FTIR Spectroscopy

As with other types of energy absorption, molecules are excited to a higher energy state when they absorb infrared radiation<sup>15-17</sup>. The absorption of infrared radiation is, like other absorption processes, a quantised process. Only selected frequencies (energies) of infrared radiation will be absorbed by a molecule. The absorption of infrared radiation corresponds to energy changes on the order of from 2 to 10 kcal/mole. Radiation in this energy range corresponds to the range encompassing the stretching and bending vibrational frequencies of the bonds in most covalent molecules. In the absorption process, those frequencies of infrared radiation, which match the natural vibrational frequencies of the molecule in question, will be absorbed, and the energy absorbed will serve to increase the amplitude of the vibrational motions of the bonds in the molecule. It should be noted, however, that not all bonds in a molecule are capable of absorbing infrared energy, even if the frequency of the radiation exactly matches that of the bond motion. Only those bonds that have a dipole moment are capable of absorbing infrared radiation. Symmetric bonds, like those of H<sub>2</sub>, or Cl<sub>2</sub>, will not absorb infrared radiation. A bond must present an electrical dipole, which is changing at the same frequency as the incoming radiation in order for energy to be transferred. The changing electrical dipole of the bond can then couple with the sinusoidally changing electromagnetic field of the incoming radiation. Thus, symmetric bonds which are symmetrically substituted will not absorb in the infrared. Since every different type of bond has a different natural frequency of vibration, and since the same type of bond in two different compounds is in a slightly different environment, no two molecules of different structures will have exactly the same infrared absorption pattern or infrared spectrum. Although some of the frequencies absorbed in the two cases might be the same, in no case of two different

molecules will their infrared spectra (the patterns of absorption) be identical. Thus, the infrared spectrum can be used for molecules much as a fingerprint can be used for humans. By comparing the infrared spectra of two substances thought to be identical, one can establish whether or not they in fact are identical. If their infrared spectra coincide peak for peak (absorption for absorption), in most cases the two substances will be identical.

In the following are listed all samples analyzed with FTIR:

- PC-PEN copolymers;
- PC;
- PEN;
- pBPAN;
- p(BPAC)-alt-(EtC);
- p(BPAEtN)-co-(EtBPAEtN);
- pEtBPAEtN.

FT-IR spectra of all samples, were recorded on a Perkin-Elmer Instruments, Spectrum One FT-IR Spectrometer. KBr pellets with a sample concentration of 0.5% w/w were prepared by a mechanical press operating at 10 atm

## 2.6 – Viscosimetry

Viscosity of a polymer solution depends on concentration and size (i.e., molecular weight) of the dissolved polymer. By measuring the solution viscosity we should be able to get an idea about molecular weight. Viscosity techniques are very popular because they are experimentally simple. They are, however less accurate and the determined molecular weight, the viscosity average molecular weight, is less precise. For example,  $M_v$  depends on a parameter which depends on the solvent used to measure the viscosity. Therefore the measured molecular weight depends on the solvent used. Despite these drawbacks, viscosity techniques are very valuable.

Several methods exist for characterizing the solution viscosity, or more specifically, the capacity of the solute to increase the viscosity of the solution. That capacity is quantified by using one of several different measures of solution viscosity. The most common solution viscosity terms are:

$$\eta_r = \frac{\eta}{\eta_0} \quad \text{Relative viscosity;}$$

$$\eta_{sp} = \frac{\eta - \eta_0}{\eta_0} = \eta_r - 1 \quad \text{Specific viscosity;}$$

$$\eta_{inh} = \frac{\ln \eta_r}{c} \quad \text{Inherent viscosity;}$$

$$[\eta] = \lim_{c \rightarrow 0} \frac{\eta_{sp}}{c} = \lim_{c \rightarrow 0} \eta_{inh} \quad \text{Intrinsic viscosity;}$$

where  $\eta_0$  is the viscosity of the pure solvent and  $\eta$  is the viscosity of a solution using that solvent. The extrapolated value of  $\eta_{sp}/c$  or  $\eta_{inh}$  at zero concentration is known as the intrinsic viscosity  $[\eta]$  (see Figure 2.8). For dilute polymer solutions, typically 0.5g/dL, Inherent viscosity ( $\eta_{inh}$ ) is approximately equal to Intrinsic viscosity  $[\eta]$ .

Intrinsic viscosity is proportional to average molecular weight of the respective polymer:

$$[\eta] = KM^a \quad \text{Mark-Houwink-Sakurada}$$

where K and a are a function of type of polymer, solvent and temperature.

The most useful kind of viscometer for determining intrinsic viscosity is the "suspended level" or Ubbelohde viscometer, sketched below:

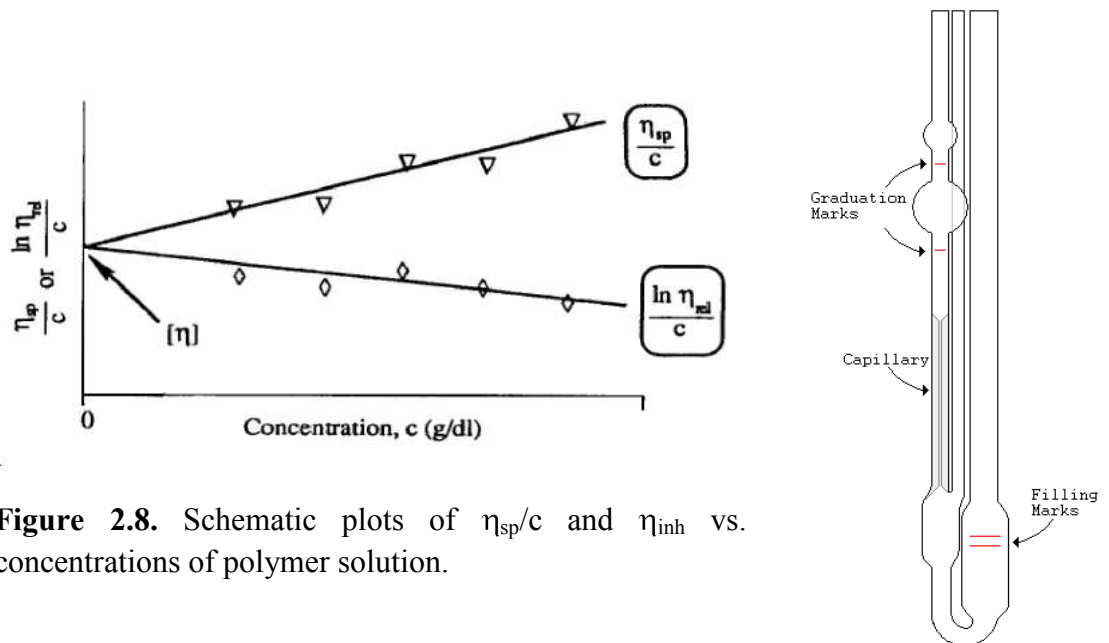


**Figure 2.8.** Schematic plots of  $\eta_{sp}/c$  and  $\eta_{inh}$  vs. concentrations of polymer solution.

The viscometer is called "suspended level" because the liquid initially drawn into the small upper bulb is not connected to the reservoir as it flows down the capillary during measurement. The capillary is suspended above the reservoir. In conjunction with the pressure-equalization tube, this ensures that the only pressure difference between the top of the bulb and the bottom of the capillary is that due to the hydrostatic pressure--i.e., the weight of the liquid.

Capillary viscometry is conceptually simple: the time it takes a volume of polymer solution to flow through a thin capillary is compared to the time for a solvent flow. It turns out that the flow time for either is proportional to the viscosity, and inversely proportional to the density.

$$t_{solvent} = \frac{\eta_{solvent}}{\rho_{solvent}}$$

$$t_{solution} = \frac{\eta_{solution}}{\rho_{solution}}$$

For most polymer solutions at the concentrations of interest,  $\rho_{solution} \cong \rho_{solvent}$ .

Thus, to a very good approximation, the relative viscosity is a simple time ratio:

$$\eta_r = \frac{\eta_{solution}}{\eta_{solvent}}$$

The inherent viscosity ( $\eta_{inh} = \ln \eta_r / C$ ) of all samples was measured at  $30 \pm 0.1$  °C with an Ubbelohde viscometer and at a concentration of 0.5 mg/dL. PET-MXD6 and PC-PEN copolymers, as well as, for PC and PEN, were dissolved in phenol/tetrachloroethane 60/40 w/w, while for the other polymer (pBPAN, PBPAN, p(BPAC)-alt-(EtC), p(BPAEtN)-co-(EtBPAEtN), and pEtBPAEtN) were used only tetrachloroethane.



## 2.7 – Gel Permeation Chromatography (GPC)

Gel-filtration or gel-permeation chromatography (**GPC**), uses porous particles to separate molecules of different sizes. It is generally used to separate biological molecules, to determine molecular weight distributions of polymers (**M<sub>w</sub>**, **M<sub>n</sub>**) and their polydispersity index (**PDI**). Molecules that are smaller than the pore size can enter the gel particles and therefore have a longer path and longer transit time than larger molecules that cannot enter the particles (Figure 2.9).

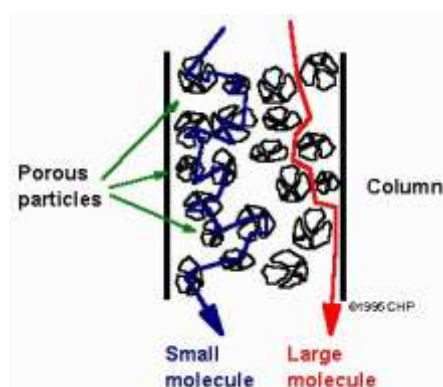
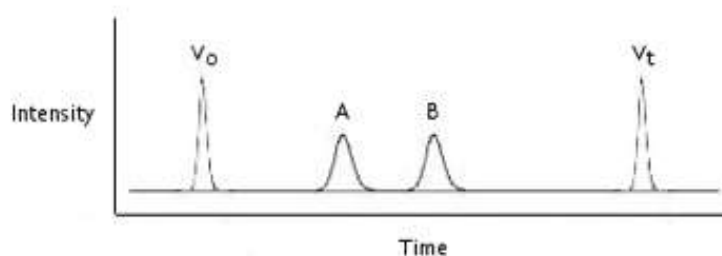


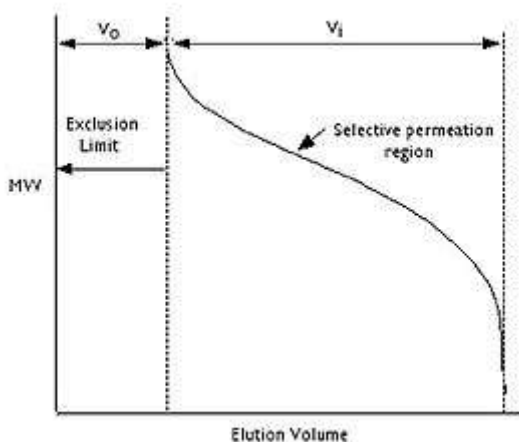
Figure 2.9. Schematic of a gel-permeation chromatography column.

Molecules larger than the pore size can not enter the pores and elute together as the first peak in the chromatogram. This condition is called total exclusion ( $V_0$ ). Molecules that can enter the pores will have an average residence time in the particles that depends on the molecules size and shape. Different molecules therefore have different total transit times through the column. This portion of a chromatogram is called the selective permeation region. Molecules that are smaller than the pore size can enter all pores, and have the longest residence time on the column and elute together as the last peak in the chromatogram ( $V_t$ ).



GPC Chromatogram;  
 $V_0$ = no retention,  $V_t$ =  
complete retention, A  
and B = partial  
retention

This last peak in the chromatogram determines the total permeation limit.



The total volume can be considered by the following equation<sup>18</sup>, where  $V_g$  is the volume of the polymer gel and  $V_t$  is the total volume:  $V_t = V_g + V_i + V_o$ . Analytes that are not retained are eluted with the free volume outside of the particles ( $V_o$ ), while analytes that are completely retained are eluted with volume of solvent held in the pores ( $V_i$ ).

It can be shown that hydrodynamic volume is proportional to the product  $[\eta]M$  where  $[\eta]$  is the intrinsic viscosity and  $M$  is the molecular weight<sup>19</sup>. A plot of  $\log [\eta]M$  versus elution volume (or elution time) for a particular solvent, column, and instrument provides a universal calibration curve which can be used for any polymer in that solvent so long as the Mark-Houwink constants are known for the polymer-solvent pair. Such a calibration curve is obtained by determining the retention volumes (or times) of monodisperse polymer standards. Once the calibration is obtained, the gel permeation chromatogram of any other polymer can be obtained in the same solvent and the molecular weights (usually  $M_n$  and  $M_w$ ) and the complete molecular weight distribution for the polymer can be determined. If the polymer to be analyzed is the same polymer as that used in obtaining the calibration, a plot of  $\log M$  versus elution volume (or time) can be used since the Mark-Houwink constants for the sample are the same as those for the standards.

The average molar mass ( $M_w$  and  $M_n$ ) values of PC and of the PC-PEN copolymers soluble in THF (20, 30, 45 and 60 min mixing) were calculated by GPC analysis using relative calibration curve derived by linear narrow polystyrene (PS) standards. In a typical analysis, 100  $\mu\text{L}$  of

a polymer solution in THF (2–3 mg/mL) was injected and eluted at a flow rate of 1mL/min, using THF as eluent and *o*-dichlorobenzene (1  $\mu$ L) as flow marker.

## 2.8 – References

1. D. L. Pavia, G. M. Lampman and J. George S. Kriz, "Introduction to Spectroscopy", W.B Saunders Company, 1979, p.81.
2. E. D. Becker, "High resolution NMR: theory and chemical applications", Academic Press, 1980, p.3.
3. C. D. Craver and J. Chares E Carraher, "Applied Polymer Science 21st Century", Elsevier, 2000, p.787.
4. W. Kemp, "NMR in chemistry: a multinuclear introduction", Macmillan Education, 1986, p.2.
5. J. R. Fried, "Polymer Science and Technology", Prentice Hall PTR, 1995, p.66.
6. P. J. Haines, "Thermal Methods of Analysis", Blackie Academic and Professional, 1995, p.63.
7. J. R. Fried, "Polymer Science and Technology", Prentice Hall PTR, 1995, p.153.
8. M. P. Stevens, "Polymer Chemistry", Oxford University Press, 1999, p.149.
9. Karas, M.; Hillencamp, F. Anal. Chem., 1988, 60, 2301.
10. Karas, M.; Hillencamp, F.; Beavis, R. C.; Chait, B. T. Anal. Chem., 1991, 63(24), 1193A.
11. Beavis, R. C. Org. Mass Spec., 1992, 27, 653.
12. Creel, H. S. Trends Poly. Sci., 1993, 1(11), 336.
13. Bahr, U.; Deppe, A.; Karas, M.; Hillencamp, F. Anal. Chem., 1992, 64, 2866.
14. Kassis, C. M.; Belu, A. M.; DeSimone, J. M.; Linton, R. W.; Lange, G. W.; Friedman, R. M. Poly. Prep., 1996, 37(1), 833.
15. D. L. Pavia, G. M. Lampman and J. George S. Kriz, "Introduction to Spectroscopy", W.B Saunders Company, 1979, p.13.

16. C. D. Craver and J. Chares E Carraher, "Applied Polymer Science 21st Century", Elsevier, 2000, p.709.
17. P. C. Painter and M. M. Coleman, "Fundamentals of polymer science", Technomic Publishing Company, Inc., 1997, p.145.
18. Skoog, D.A. Principles of Instrumental Analysis, 6th ed.; Thompson Brooks/Cole: Belmont, CA, 2006, Chapter 28.

Painter and Coleman, Fundamentals of Polymer Science, pp.

**PART (I)**

**CHARACTERIZATION OF COPOLYESTERAMIDES FROM**  
**REACTIVE BLENDING OF PET AND MXD6 IN THE**  
**MOLTEN STATE**

### 3.1 – Introduction

Blends of condensation polymers such as polyesters, polyamides, and polymers bearing reactive functional groups in the backbone or at the chain ends may yield chemical exchange reactions when they are mixed in the molten state, leading to the formation of block, segmented, random, or grafted copolymers, affecting the properties of the original blends.<sup>1–29</sup> An exchange reaction may be proceeded by the direct exchange between two functional groups located inside the polymer chains (referred to inner–inner exchange) and by the attack of reactive chain ends on inner groups (referred to inner–outer exchange).<sup>1–7</sup> Exchange reactions may be induced by the presence of catalyst residues used in the polymerization or may be caused by reactive terminal groups (i.e., OH, COOH, and NH<sub>2</sub>), originally present in the polymers or generated *in situ* by thermal-and/or hydrolytic degradation reactions.<sup>1–29</sup> In the past 18 years, we have investigated exchange reactions occurring in the melt-mixing processes of several condensation polymer blends with both end-capped polymer samples and polymers possessing specific reactive chain end groups.<sup>1–7</sup>

Polyester/polyamide blends such as poly(ethylene terephthalate)/nylon-6 (PET-Ny6), poly(butylene terephthalate)/nylon-6 (PBT-Ny6), PET-nylon-66 (PET-Ny66), and PET-poly-(m-xylene adipamide) (PET-MXD6) have been investigated.<sup>5,6,8–22,30–35</sup> Several literature reports assert that exchange reactions occurring in polyester/polyamide blends can be induced with an appropriate catalyst.<sup>9,16,18,19,22,30</sup> Some researchers<sup>16,18,19</sup> have stated that p-toluene sulfonic acid (TsOH) is an efficient catalyst for amide–ester exchange reactions in PET-Ny6 and PET-Ny66 blends, whereas others<sup>21</sup> have suggested that TsOH catalyzes the outer–inner exchange reaction of an amino end group with an inner ester group of PET. On contrary, in a previous work investigating the role of TsOH and the activity of the

reactive chain ends in the melt mixing of Ny6-PET blends,<sup>5</sup> we have found that the role of TsOH is not that of a catalyst but of a reactant; it reacts with PET yielding PET oligomers terminated with carboxyl groups.<sup>5,36</sup> Then, these oligomers quickly react with Ny6 producing Ny6-PET copolymers. Our studies have revealed the essential role of carboxyl end groups in the exchange reaction between Ny6 and PET and allowed a detailed mechanism for this reaction, based on the structural identification of the PET-Ny6 copolymers produced in the exchange reactions. In other studies, we have also shown the essential role of active -COOH end groups in the exchange reactions occurring during the melt mixing of PBT-Ny6<sup>6</sup> and aliphatic polyamide/polyamide blends.<sup>2,7</sup>

In this work, we extend our mechanistic studies on the PET-MXD6 melt-mixed blends. These blends have attracted scientific,<sup>30-35</sup> technical,<sup>37</sup> and commercial interest, in particular, in the area of food packaging because of their potential for combining the low O<sub>2</sub> and CO<sub>2</sub> permeability of the MXD6 (and order of magnitude higher than that of PET<sup>38-39</sup>) with the good toughness, clarity, and economics of PET. However, PET and MXD6 give incompatible blends with low optical clarity and an undesirable yellow color when processed in the molten state.<sup>40</sup> PET-MXD6 blends have been studied to improve their transparency when stretched,<sup>31,32</sup> to improve gas barrier of PET,<sup>33</sup> and to address the mechanism of color generation.<sup>34</sup> Compatibilized PET-MXD6 (90/10 w/w) blend was obtained through the incorporation of small amount of sodium 5-sulfisophthalate (SIPE) in the PET matrix.<sup>35</sup> The authors found that the O<sub>2</sub> permeability at 43% relative humidity was reduced by a factor of 3, in comparison of PET, in the biaxially oriented film of the compatibilized blends. Compatibilized blends were also obtained using ionomers.<sup>41</sup> The goal of the studies on the PET-MXD6 blends is to achieve the improved gas barrier, while maintaining good optical clarity, inducing the interchange reaction between PET and MXD6



to produce *in situ* their copolymers and, thus to overcome their incompatibility. Xie et al. reported that the interchange reaction in PET-MXD6 blends (90/10 w/w) in the molten state (290–310 °C) occurs only in the presence of sodium *p*-toluenesulfonate (*p*-TSONa).<sup>30</sup> They have characterized the melt-mixed blends by <sup>1</sup>H-NMR in deuterated sulfuric acid (D<sub>2</sub>SO<sub>4</sub>) to degrade selectively the PET components of reacted blends, and applying a mathematical model have calculated the degree of randomness of PET-MXD6 copolymers. However, the researchers did not report the molar composition of the sequences (dyads and triads) in the formed copolymers, and also a systematic study of the catalytic activity of *p*-TSONa, especially the activity of the end chains initially present in the homopolymers or generated during their melt mixing. Moreover, the authors did not report any measure of properties as a function of reaction conditions, which correlate with the average molar masses of the melt-mixed PET-MXD6 investigated. In accordance with our previous studies on the PET-Ny6 melt-mixed blends,<sup>5</sup> we believe, contrary to the Xie et al.,<sup>30</sup> that *p*-TSONa and *p*-TSOH<sup>5</sup> are reagents and not catalysts and that exchange reactions between PET and MXD6 occur via the attack of reactive carboxylic acid end groups on ester and amide inner groups. Carboxylic acid end groups can be produced *in situ* by the reaction of *p*-TSONa with PET homopolymer, which has been confirmed by the preliminary studies performed in the present work.

Here, equimolar mixtures (respect to the repeat units) of PET and MXD6 were melt mixed at 285 °C under N<sub>2</sub> flow for different times with and without terephthalic acid (TA; 1 wt %). All melt-mixed materials were characterized by <sup>13</sup>C and <sup>1</sup>H-NMR, DSC, TGA, and viscosimetric measurements, without any purification or removal of possible nonreacted homopolymers. The NMR analysis of the crude melt-mixed blends were performed in a mixture of CDCl<sub>3</sub>/(CF<sub>3</sub>CO)<sub>2</sub>O/CF<sub>3</sub>COOD (70/17/13 V/V) to obtain reliable information on the molar composition of the sequences

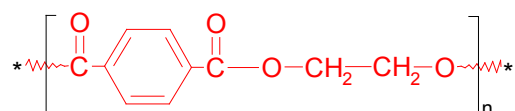
(dyads and tryads), average sequences lengths, and degree of randomness in the formed PET-MXD6 copolymers, as a function of the reaction times. These data were calculated applying an appropriate statistic model to the corresponding NMR spectra. A modified FOX equation was used to calculate the theoretical glass transition ( $T_g$ ) of the four components PET-MXD6 copolymers formed by melt mixing of PET-MXD6 in the presence of TA (1 wt %) at different reaction time.

## 3.2 – Materials

PET and MXD6 resin used for melt blending are commercial products useful for packaging with extended shelf life. The PET was supplied by Equipolymers with light C93 commercial grade (ISO viscosity Number ISO 1628/5, 93 mL/g), whereas the Polyamide MXD6 was supplied by Mistubishi Gas Chemical with S6007 commercial grade (M.F.R. 2.0 g/10 min—ASTM D1238 method). Poly(ethylene adipate) (PEA) with Mw 10,000 by GPC, supplied by Sigma Aldrich, was used as polymer model for NMR assignments and DSC characterization. All solvents and reagents: terephthalic acid (TA), *m*-xylenediamine, phenol, terephthaloyl dichloride, tetrachloroethane, triethylamine, tricaprilmethylammonium chloride (Aliquat 336), methanol, CHCl<sub>3</sub>, hexafluoroisopropanol (HFIP), anhydride trifluoroacetic (CF<sub>3</sub>CO)<sub>2</sub>O, n-hexane, CDCl<sub>3</sub>, with analytical grade used were purchased from Sigma Aldrich (Italy). Deuterated solvents CDCl<sub>3</sub> and CF<sub>3</sub>COOD were supplied by Merck. Poly(*m*-xylene terephthalamide) (MXDT) polymer model was also synthesized and characterized in our laboratory.<sup>42</sup>

### 3.3 - Poly(ethylene terephthalate) - PET

The polyethylene terephthalate is certainly the best known of the aromatic polyesters<sup>2-7</sup>. is a thermoplastic resin obtained by polycondensation between terephthalic acid (or its dimethyl ester) and the ethylene glycol. is certainly one of the most versatile resins. Its repeat unit may be so indicated:



The wide range of products covering applications in the field of textile and technical fibers, packaging, engineering plastics. The properties of PET are determined by an appropriate arrangement of amorphous and crystalline areas. The mechanical and gas barrier characteristics are achieved through the orientation of polymer chains and their simultaneous crystallization.

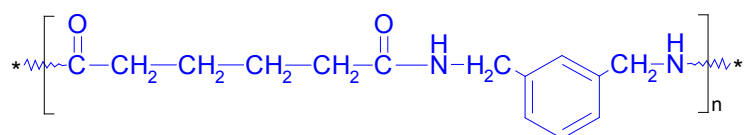
PET has a glass transition temperature of about 72-74 °C and a melting temperature of about 250 °C. Depending on the greater or lesser molecular weight of PET, expressed by intrinsic viscosity, it determines its uses. This polyester is characterized by high mechanical properties and good tenacity; also has good thermal and chemical resistance, excellent transparency and gloss and barrier properties to O<sub>2</sub> and CO<sub>2</sub>. The main applications of polyethylene terephthalate concern the field of packaging: PET is in fact used for the production of bottles for water and soft drinks, although during this process, the PET can undergo phenomena degradation to volatile products (as formaldehyde) that can greatly affect the organoleptic properties of drinks such as mineral not carbonated water<sup>8</sup>.

PET is also used for the production of bottles for household cleaners, trays, blister thermoforming and for support film of multilayer

materials. Moreover, it is also used like synthetic fibers (for clothing, furniture, upholstery, ropes, geotextile use, etc.), or decorative films for graphic arts, as well as radiographic and photographic plates and audio tapes and video.

#### 4.4 - Poly(*m*-xylene adipamide) - MXD6

Poly(*m*-xylene adipamide) is one of the crystalline polyamide resins. It has many distinguished properties compared with other conventional polyamide resins such as nylon 6 and nylon 6,6<sup>9</sup>. MXD6 is produced through polycondensation of meta-xylene diamine with adipic acid. Its repeat unit may be so indicated:



The study of this polyamide as fiber, began in Chevron in 1956 and went on some years later in Snia Viscosa, but without any success. Initially, the *m*-xylenediamine was impure of the para isomer until 1970 when the MGC made possible the separation of the two isomers (para and meta). However MXD6 failed to establish itself as a fiber because of the slow crystallization process that undergoes when is the dry state, even under optimal conditions of temperature (160-170 °C).

A major positive feature, enhanced by Mitsubishi Gas Chemical is the high impermeability to atmospheric gases (particularly oxygen) that manifests in biaxially oriented films. In particular MXD6 exhibits gas barrier properties against dioxygen and carbon dioxide better than those of ethylene-vinylalcohol copolymers (EVOH), acrylonitrile copolymers (PAN) and vinylidenechloride copolymers (PVDC) under practical conditions. For these reasons, the MXD6 has been widely applied for packaging materials and molding compounds<sup>10</sup>. For instance, it is used by multilayer techniques<sup>11</sup> to improve the gas barrier properties of poly(ethylene terephthalate) (PET) in bottling industries.

### **3.5 – Reactive blending procedure**

The starting homopolymers (both in pellet form) were dried overnight in a vacuum system at 140 °C before use. Equimolar mixture (with respect to the repeat units) of PET and MXD6 were melt mixed with and without TA (1 wt %) at 285 °C for different times (from 5 to 120 min), under N<sub>2</sub> flow. The melt mixing was performed in a twin-screw mixer 330AEV Brabender under N<sub>2</sub> flow and with a stirring rate of 30 rpm. For comparison, the blending was also performed in a round bottom, three-neck flask equipped with a stirrer, inert gas inlet and outlet, and a thermometer for measuring the temperature of the melt. The reaction vessel was thermostated at 285 °C. As very similar results were obtained for melt-mixed blends in both experimental apparatus, here we will discuss only the melt-mixed materials obtained by the Brabender mixer.

Both the homopolymers were also treated in the same experimental conditions in the Brabender mixer to investigate their thermal behavior and also the role of TA.

### 3.6 – Synthesis of poly(*m*-xylene terephthalamide) - MXDT

Poly(*m*-xylene terephthalamide) (MXDT) was synthesized by interfacial polymerization of *m*-xylenediamine and terephthaloyl dichloride, with tricaprilmethylammonium chloride (Aliquat 336) as phase transfer agent and triethylamine as base acceptor of hydrochloric acid liberate in the reaction.<sup>42</sup> A mixture of 3.4 g (0.025 mol) of *m*-xylenediamine, 5.55 g (0.055 mol) of triethylamine, and 1 mmol of Aliquat 336 in 30 mL of water was vigorously stirred in a precooled blender with 5.05 g (0.025 mol) of terephthaloyl dichloride in 40 mL CHCl<sub>3</sub>. The reaction was carried out for 5 min, and the organic phase was separated in a separating funnel and rotoevaporated to eliminate the solvent. The white solid was dissolved in 30 mL of CHCl<sub>3</sub>/(CF<sub>3</sub>CO)<sub>2</sub>O (80/20 v:v) solvent mixture and then added dropwise to 300 mL of CH<sub>3</sub>OH. The precipitate polymer was filtered, washed twice with CH<sub>3</sub>OH, and dried overnight under vacuum at 60 °C (yield 83%).



### 3.7 – Characterization of samples

All PET-MXD6 blends and model polymers were characterized with the following technical of analysis:

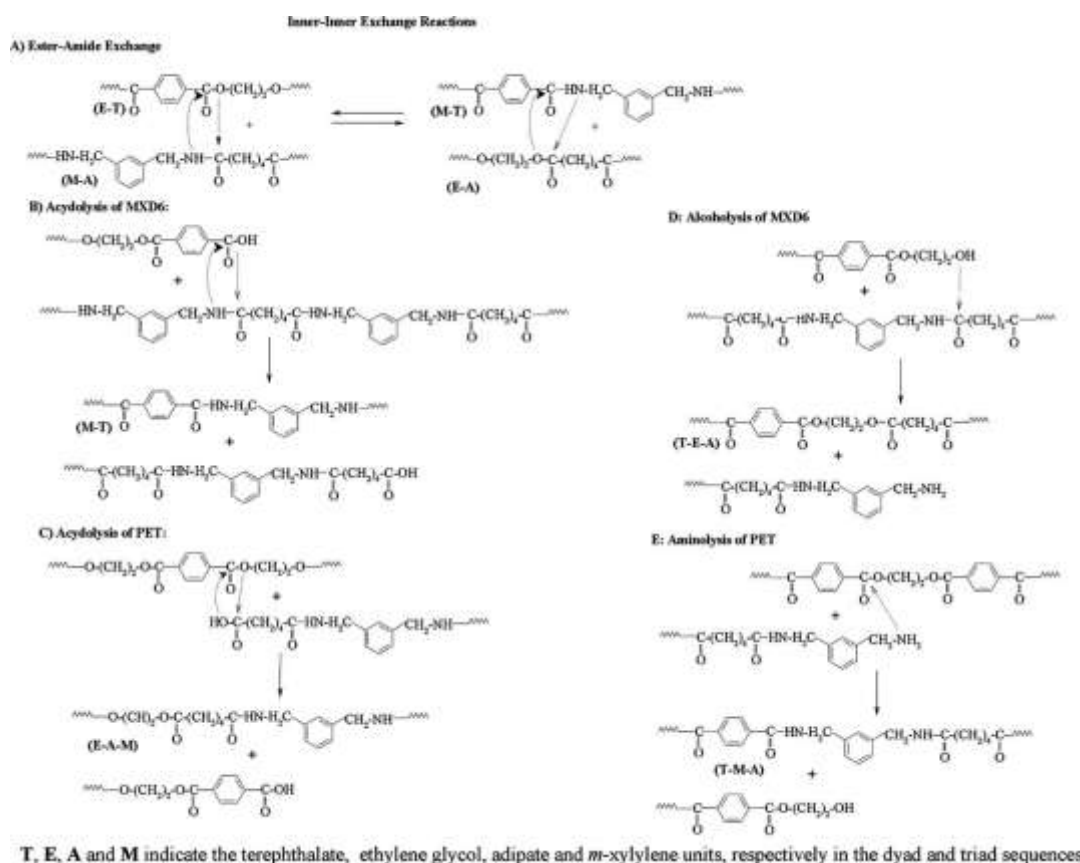
- Nuclear Magnetic Resonance –  $^1\text{H}$  and  $^{13}\text{C}$  NMR (*Figures 3.3, 3.4, 3.5, Tables 3.4, 3.5*);
- Differential Scanning Calorimetry – DSC (*Tables 3., 3.7*);
- Thermogravimetric analysis – TGA (*Table 3.7*);
- MALDI-TOF mass spectrometry (*Figures 3.1, 3.2, 3.7 Tables 3.2, 3.7*);
- Viscosimetry (*Table 3.1*);

The aim of these studies is a fully elucidation of microstructures and composition of new PET-MXD6 copolymers as well as the kinetic mechanism of the catalyzed exchange reactions ester-carbonate that occurring between PC and PEN homopolymers in the molten state.

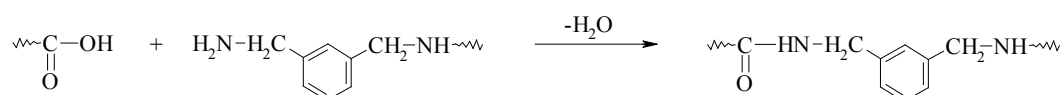
### 3.8 – Results and discussion

PET and MXD6 are incompatible in the molten state, and the challenge is to achieve compatible PET-MXD6 blends through the enhancement of the interchange reaction between the homopolymers favoring the *in situ* formation of their copolymers that can act as compatibilizers. The possible exchange reactions, which might occur during the melt mixing of PET-MXD6 blends, are highlighted in Scheme 3.1. Outer–outer transamidation reaction is also possible between carboxylic acid end chains and amine ends of MXD6 chains (Scheme 3.2). These exchange reactions are allowed to PET-MXD6 copolymers with two new structural units beside those of initial homopolymers as schematized in Chart 1. The progress of the exchange reactions can be followed by  $^1\text{H}$  and  $^{13}\text{C}$  NMR analysis and also by investigation of thermal properties of the melt-mixed materials. In accordance with our previous studies on the polyester/polyamide<sup>5,6</sup> and polyamide/polyamide<sup>2,7</sup> incompatible blends, here we have performed the melt mixing of equimolar mixtures of PET and MXD6 at 285 °C for different times, ranging from 15 to 120 min, with TA (1 wt %) and from 5 to 60 min without TA, under  $\text{N}_2$  flow. All melt-mixed materials were studied without any purification or removal of possibility unaffected homopolymers, by  $^1\text{H}$  and  $^{13}\text{C}$  NMR, DSC, and viscosity tools. Preliminary studies were also performed onto PET and MXD6 heated at 285 °C with and without TA (1 wt %) for different time durations under  $\text{N}_2$  flow to ascertain if thermal degradative and/or hydrolysis reactions occur and, in particular, to investigate the neat effect of TA onto PET and MXD6 in the melt-mixing conditions used for their reactive melt blending. Both homopolymers were also treated with *p*-TSONa (1 wt %), because some authors<sup>30</sup> believed that it is a catalyst of chemical reaction between these homopolymers in the melt. However, in accordance with

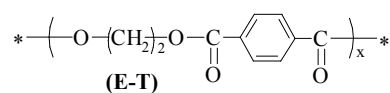
our previous study onto the PET-Ny6 blends melt mixed in the presence of *p*-TSOH,<sup>5</sup> our studies reveal that *p*-TSO<sub>Na</sub> react only with the ester groups of the PET chains, yielding PET oligomers terminated with carboxyl groups, whereas the MXD6 remains unaffected.



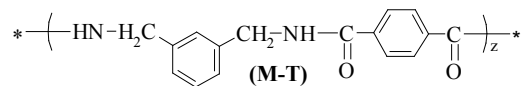
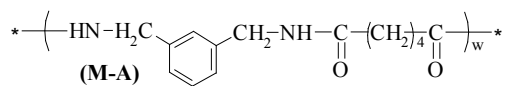
**Scheme 3.1.** Exchange reactions that might occur during the melt mixing of PET-MXD6 blends.



**Scheme 3.2.** Outer–outer transamidation reaction.



**(E-A)**



$$(x + y + z + w) = 1$$

**Chart 3.1.** Structural units expected in the PET-MXD6 copolymers formed by exchange reactions.

### 3.9 – Studies on PET and MXD6 Samples

Values of inherent viscosities ( $\eta_{inh}$ ) and calorimetric data of the heated PET and MXD6 samples are summarized in Table 3.1. It shows that the neat PET remains almost unaltered at 285 °C, because its  $\eta_{inh}$  and calorimetric data do not change, whereas a dramatic decrement of the  $\eta_{inh}$  and then of its molar mass is observed when 1% TA is added, as well as has been observed in the presence of *p*-TSOH.<sup>5,36</sup> Heated PET samples were characterized by MALDI-TOF technique that is able to look each molecule even in a complex mixture<sup>43–45</sup> to obtain information on the end groups as a function of the heating conditions. MALDI spectra of PET samples show a series of peaks ranging from  $m/z$  1000 (where a mass cutoff was applied) to about  $m/z$  9000–10,000, and in [Figure 3.1(b) and 3.1(c)] the MALDI spectra of the unheated and heated PET sample at 285 °C for 5 min with and without TA are shown; the peaks present are assigned as in Table 3.2. The spectrum of the unheated PET [Figure 3.1(a)] shows intense signals because of the sodiated ions of cycles (species  $A_n$ ) that dominate in the mass range  $m/z$  1000–5000 and to the linear oligomers that dominate in the mass range higher than  $m/z$  4000. From these spectra, we identified linear oligomers terminated with hydroxyl groups at both the ends (species  $C_n$ ), linear oligomers terminated with carboxyl and hydroxyl groups (species  $B_n$ ). Peaks corresponding to both linear and cyclic oligomers having one or two diethylene glycol units along the chains were also observed (species  $A_n^1$ ,  $A_n^2$ ,  $B_n^1$ , and  $C_n^1$  in Table 3.2). The presence of the diethylene glycol units has been also confirmed by <sup>1</sup>H-NMR analysis, because they give two unresolved triplet at 4.15 ppm [proton signals labeled with the symbol \* in Figure 3.3(a)] and at 4.70 ppm. Therefore, according to the MALDI spectrum of neat PET sample [Figure 3.1(a)], its linear chains are mostly terminated with

hydroxyl groups, and these groups could give exchange reaction with MXD6 chains [Scheme 3.1(D)].

**Table 3.1.** Some properties of polymer models and of heated PET and MXD6 samples with and without TA at 285 °C.

Sample	TA (%w)	Time (min)	$\eta_{inh}$	Tg (°C)	Tcc (°C)	Tm (°C)	Tc (°C)
PET_1	0	0	0,65	79	165	246	172
PET_2	0	5	0,66	79	136	247	180
PET_3	0	15	0,66	79	137	248	180
PET_4	0	30	0,66	80	138	247	179
PET_5	0	45	0,66	80	139	247	179
PET_6	0	60	0,67	80	140	247	179
PET_7	0	75	0,66	80	139	247	180
PET_8	0	90	0,64	79	138	247	182
PET_9	0	105	0,62	79	138	248	183
PET_10	0	120	0,62	79	136	248	186
PET_11	1	0	0,65	79	165	246	172
PET_12	1	5	0,29	81	-	250	208
PET_13	1	15	0,29	81	-	250	207
PET_14	1	30	0,29	81	-	250	206
PET_15	1	45	0,30	82	-	250	206
PET_16	1	60	0,30	81	-	250	205
PET_17	1	75	0,29	81	-	250	205
PET_18	1	90	0,29	82	-	250	205
PET_19	1	105	0,28	81	-	250	205
PET_20	1	120	0,28	81	-	250	204
MXD6_1	0	0	1,05	86	153	236	169
MXD6_2	0	5	1,02	87	144	237	167
MXD6_3	0	15	0,94	87	144	237	167
MXD6_4	0	30	0,89	86	145	237	165
MXD6_5	0	45	0,85	86	144	236	164
MXD6_6	0	60	0,81	85	143	235	167
MXD6_7	0	75	0,78	85	143	235	167
MXD6_8	0	90	0,76	85	143	235	165
MXD6_9	0	105	0,72	84	142	233	164
MXD6_10	0	120	0,70	84	142	233	185
MXD6_11	1	0	1,05	86	153	236	169
MXD6_12	1	5	0,48	84	141	235	172
MXD6_13	1	15	0,48	84	142	234	164
MXD6_14	1	30	0,48	84	143	233	160
MXD6_15	1	45	0,50	84	144	232	161
MXD6_16	1	60	0,52	85	144	232	168
MXD6_17	1	75	0,54	84	144	231	163
MXD6_18	1	90	0,57	85	143	230	160
MXD6_19	1	105	0,62	85	143	230	169
MXD6_20	1	120	0,67	85	144	229	155

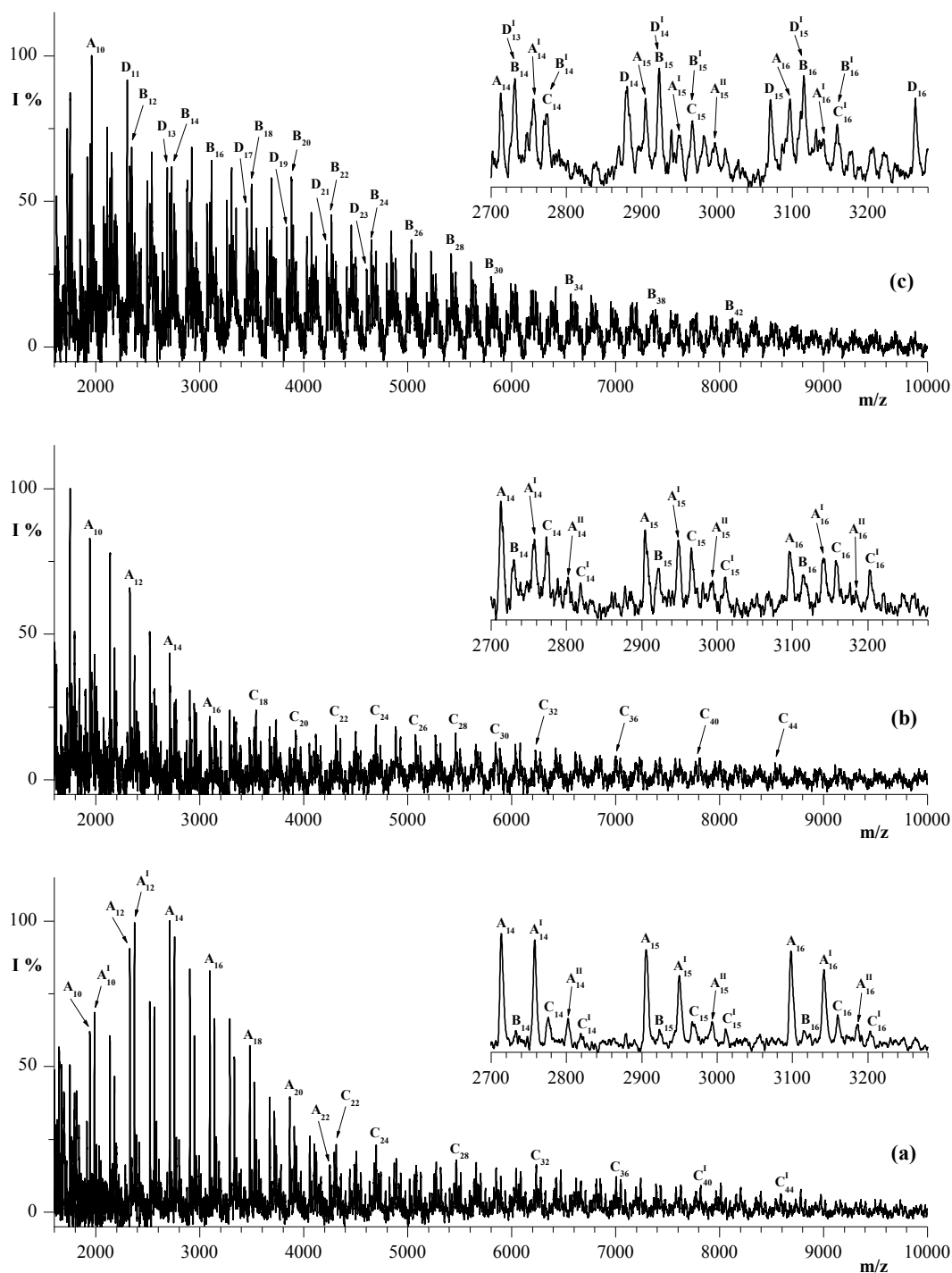


**Figure 3.1.** MALDI-TOF mass spectra of PET heated at 285 °C for (a) 0 min, (b) 5 min, and (c) 5 min in the presence of TA (1 wt%).

**Table 3.2.** Mass assignments of peaks present in the MALDI spectra of un-processed and processed PET and MXD6 samples, reported in Figures 3.1 and 3.2.

SPECIES	STRUCTURES	n	$[M_n+Na^+]^{(a)}$
$A_n$		14	2713,8
		15	2906,0
		16	3098,2
$B_n$		14	2731,8
		15	2924,0
		16	3116,2
$C_n$		14	2775,4
		15	2968,0
		16	3160,2
$D_n$		14	2879,8
		15	3072,0
		16	3264,2
$A_n^I$		14	2757,8
		15	2950,0
		16	3142,2
$A_n^{II}$		14	2801,8
		15	2994,0
		16	3186,2
$B_n^I$		14	2775,4
		15	2968,0
		16	3160,2
$C_n^I$		14	2819,8
		15	3012,0
		16	3204,2
$D_n^I$		13	2731,6
		14	2923,8
		15	3116,0
$\alpha_n$		9	2239,7
		10	2486,0
$\beta_n$		9	2257,7
		10	2504,0
$\chi_n$		9	2375,7
		10	2622,0
$\delta_n$		9	2385,7
		10	2632,0
$\epsilon_n$		9	2405,7
		10	2652,0
$\iota_n$		9	2367,7
		10	2614,0
$\beta_n^I$		9	2279,7
		10	2526,0
$\delta_n^I$		9	2407,7
		10	2654,0
$\delta_n^{II}$		9	2429,7
		10	2676,0
$\epsilon_n^I$		9	2427,7
		10	2674,0
$\epsilon_n^{II}$		9	2449,7
		10	2696,0

(a) The mass accuracy was better than  $\Delta m = \pm 0,4-0,7$  Da.



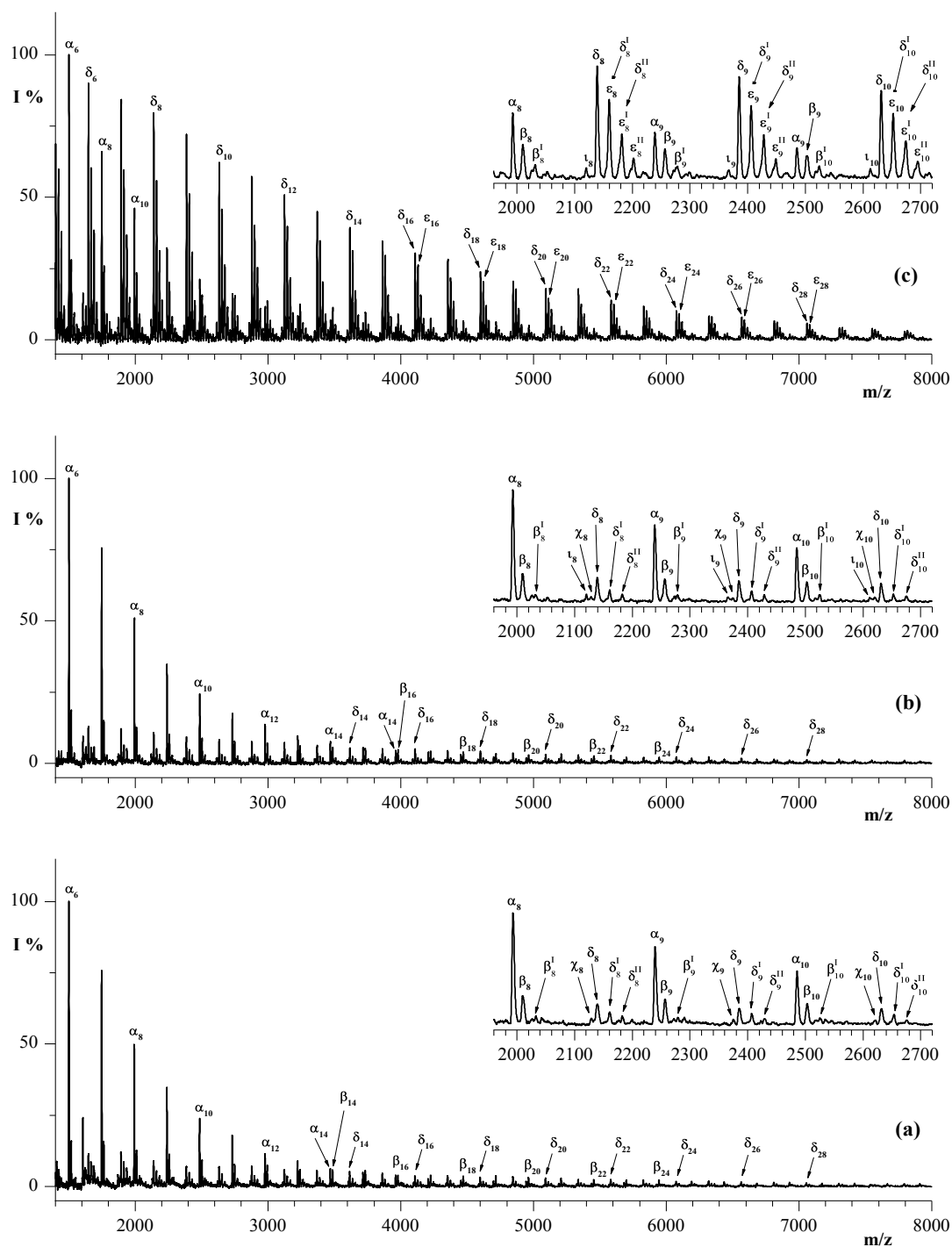
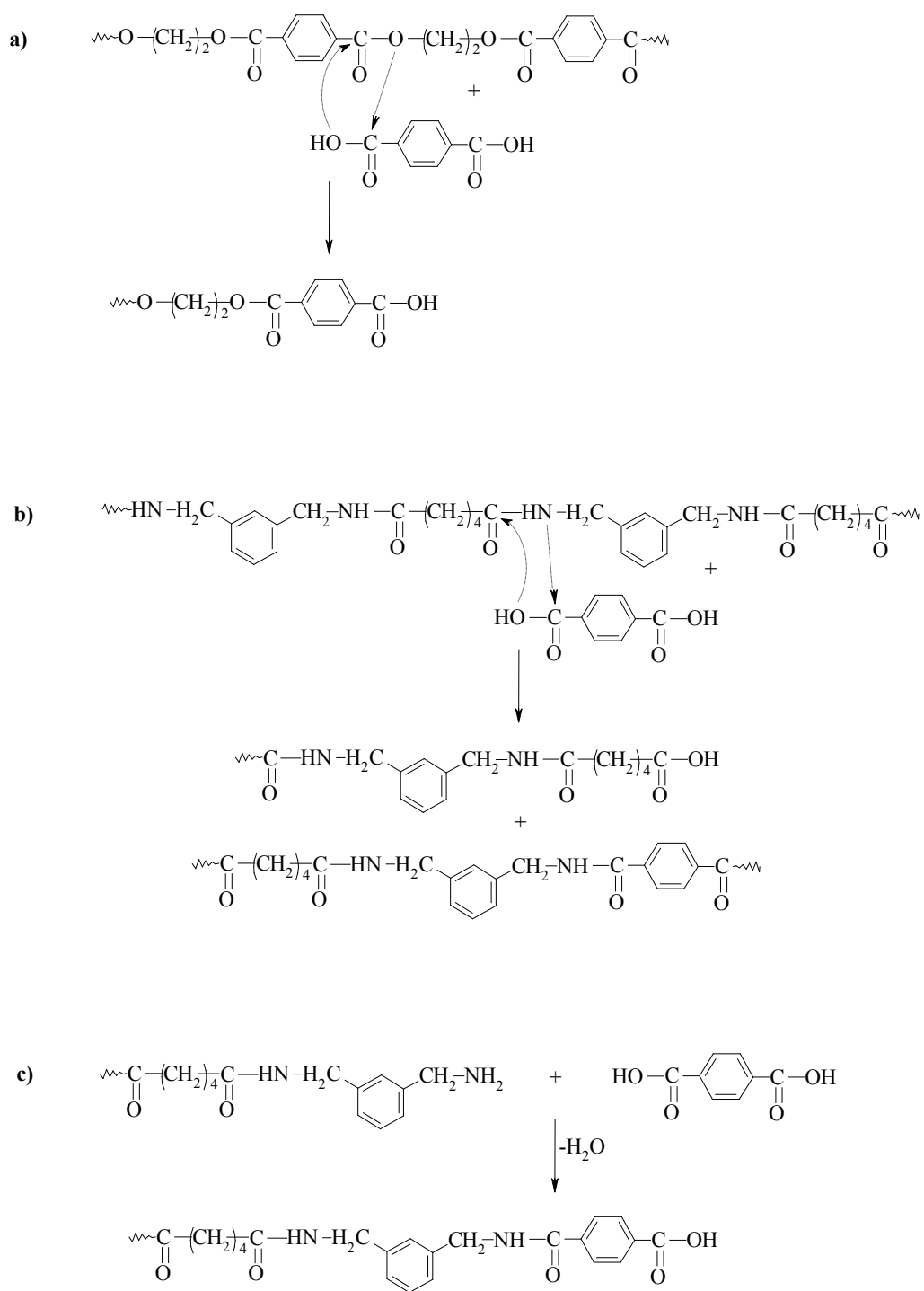


**Figure 3.2.** MALDI-TOF mass spectra of MXD6 heated at 285 °C for (a) 0 min, (b) 5 min, and (c) 5 min in the presence of TA (1 wt%).

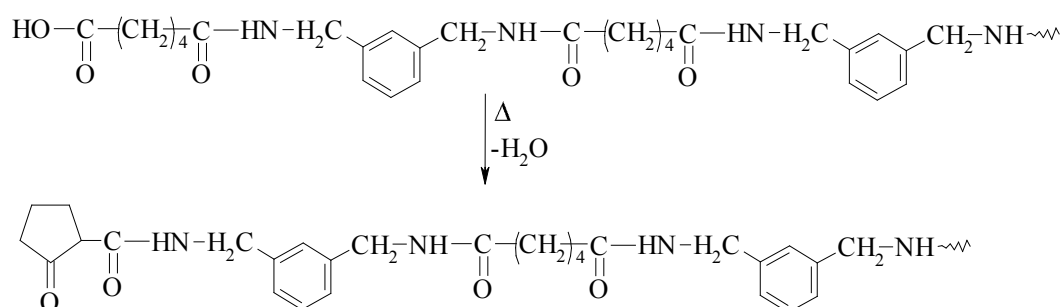
MALDI spectra of PET heated at 285 °C as well of that heated for 5 min [Figure 3.1(b)] are very similar to that of the neat unheated sample [Figure 3.1(a)], confirming that PET is stable at 285 °C under nitrogen flow for long time (60 min). When PET is heated at 285 °C for various time intervals in the presence of TA (1 wt %), the MALDI spectra show distinct changes in the relative intensity of peaks present in the neat PET [Figure 3.1(a)] and new peaks also appear due to the linear chains terminated with terephthalic units at both the ends [species  $D_n$  and  $D_n^1$  in Figure. 3.1(c) and in Table 3.2] formed by acidolysis reaction of PET with TA [Scheme 3.3(a)]. The relative intensity of these peaks increases with respect to those of PET oligomers belonging to the families  $A_n$  and  $C_n$ , as the reaction time increases due to progress of the acidolysis reactions. Therefore, the acidolysis reaction [Scheme 3.3(a)] occurs in the presence of TA with the consequent increase of carboxyl-terminated chains as confirmed by the MALDI-TOF mass spectrum in Figure 3.1(c). From the data in Table 3.1, we can observe that the  $T_m$  and  $T_g$  values of the heated MXD6 samples decrease from 236 to 233 °C and from 86 to 84 °C, respectively. Slight decrease in  $\eta_{inh}$  indicates the occurrence of some degradative hydrolysis reactions. Its  $\eta_{inh}$  dramatically decrease when it was heated with TA at shorter reaction time (5 min) and then slightly increases as the reaction time increases. These data suggest that in the first step the TA attack onto amide inner groups of the MXD6 sample [Scheme 3.3(B)] occurs, yielding MXD6 chains terminated with aromatic and aliphatic carboxylic acid groups. In the successive second step, these end chains may react with the amine ends initially present in the MXD6 sample giving an outer–inner coupling transamidation reaction (Scheme 3.2), thus determining the increase of the molar masses and then of the viscosities of heated MXD6 samples. Therefore, the acidolysis and transamidation reactions of the MXD6 chains could be competitive during the melt mixing of MXD6 sample in presence of TA.



**Scheme 3.3.** Reaction occurring during the treatment of PET or MXD6 with TA at 285 °C.

Neat and heated MXD6 samples at 285 °C with and without TA were analyzed by MALDI-TOF ms. A MALDI-TOF mass spectrum of a MXD6 sample was already published,<sup>46</sup> and in Figure 3.2(a), we report the MXD6 sample that we have used in the melt mixing with PET; the mass peak series present are assigned as in Table 3.2. It shows peaks due to the cyclic oligomers (species  $\alpha_n$  in Table 3.2), the linear oligomers terminated with carboxyl and amine groups (species  $\beta_n$  in Table 3.2), the linear oligomers bearing amine groups at both ends (species  $\chi_n$  in Table 3.2), and the oligomers terminated with adipic acid units at both ends (species  $\delta_n$  in Table 3.2). Peaks from cyclic oligomers dominate in the mass range lower than  $m/z$  3500, whereas peaks from linear oligomers dominate in the mass range higher than  $m/z$  3500. At high mass range, the most intense peaks correspond to MXD6 oligomer series  $\delta_n$  suggesting that the used MXD6 polyamide is essentially terminated with aliphatic carboxylic acid groups. MALDI-TOF mass spectra of the heated polyamide show other series of peaks besides those present in the unheated MXD6 [Figure 3.2(a)]; Figure 3.2(b) reports the mass spectrum of the sample heated for 5 min. These new peaks labeled as  $\tau_n$  in Table 3.2 and in Figure 3.2 correspond to the linear MXD6 chains terminated with the cyclopentanone units. These peaks are growing in intensity with increasing heating time, which is due to the thermal decomposition reactions that take place at longer heating times involving the adipic end units of the polyamide chains as depicted in Scheme 3.4. This degradation reaction was studied previously in the Ny66 heated at about 290 °C.<sup>2,47</sup> The formation of cyclopentanone-ended MXD6 chains was also observed in the MXD6 sample treated with TA, which can be observed in Figure 3.2(c) that portrays the MALDI-TOF mass spectrum of the compounds obtained after 5 min of reaction. As expected, in this mass spectrum, the most intense peaks correspond to the sodiated ions of MXD6 oligomers

bearing aliphatic and aromatic carboxylic acid end groups (species  $\epsilon$  and  $\delta$  in Figure 3.2(c) and in Table 3.2).



**Scheme 3.4.** Formation of cyclopentanone end groups during the melt mixing of

In this mass spectrum, the sodiated ions of the sodiated salts of these acid-ended oligomers also appear [mass series  $\epsilon^{\text{I}}$ ,  $\epsilon^{\text{II}}$ ,  $\delta^{\text{I}}$  and  $\delta^{\text{II}}$  in Figure 3.2(c) and in Table 3.2], which were formed during the preparation of matrix/analyte mixture for MALDI analysis. The peaks due to the initial MXD6 oligomers terminated with amine groups at both ends (mass series  $\chi_n$  in Table 3.2 and in Figure 3.2(a) and 3.2(b)] disappear in the mass spectrum of the MXD6 melt mixed with TA at 285 °C, suggesting that TA also react with the amine end chains [Scheme 3.3(c)] and that outer–inner transamidation reaction between two different polyamide chains terminated one with TA and one with amine groups (Scheme 3.2). Therefore, the slight increment of the  $\eta_{\text{inh}}$  with the increase in the reaction time (see Table 3.2) should be due at the last reaction.

### 3.10 – Characterization of PET-MXD6 melt-mixed blends

PET-MXD6 blends melt mixed at 285 °C with and without TA (1 wt %) were well characterized by  $^1\text{H}$  and  $^{13}\text{C}$  NMR analyses to follow the exchange reactions, which occurring and to evaluate the structure (block, random) and the molar composition of the PET-MXD6 copolymers eventually formed, as a function of the reaction time. Both protons and carbons NMR spectra of PET-MXD6 blends melt mixed without TA show that no significant exchange reaction occurs between anhydrous PET and MXD6 at 285 °C, under inert controlled atmosphere, even at longer reaction time (60 min). This result suggest that, as well as in the PET-Ny6<sup>5</sup> and PBT-Ny6<sup>6</sup> blends, the direct ester–amide exchange reaction [Scheme 3.1(A)] does not occurs in incompatible PET-MXD6 blends, confirming also the studies of Prattipati et al..<sup>35</sup> Therefore, because the PET and MXD6 samples used in this study are essentially terminated with hydroxyl and aliphatic carboxylic acid end groups, the outer–inner reactions schematized in Scheme 3.1 (routes B-E) do not occur in the incompatible polyeter/polyamide melt blend, as already observed for PET-Ny6<sup>5</sup> and PBT-Ny6 blends.<sup>6</sup>  $^1\text{H}$ -NMR spectra of PET-MXD6 blends melt mixed in presence the of TA (1 wt %; referred thereafter as PET-MXD6-(1 wt %)TA) for 30, 45, 75, and 120 min are displayed in Figure 3.3; the peaks present are assigned as in Table 3.3 and in accordance with the chemical shifts of the homopolymers models (PET, MXD6, PEA, and MXDT). Figure 3.3 also shows the proton spectra of the four polymer models to facilitate the assignments of the new signals because of the heterosequences (**E-A** and **M-T** in Chart 3.1) that should be formed by exchange reactions. The proton spectra of melt-mixed blends at time higher than 20 min are more complex with respect to that of the initial physical blend, indicating that copolymers may be formed by exchange reactions. The assignments of the sequences (dyads or triads)

corresponding to the signals of the  $^1\text{H-NMR}$  spectra in Figure 3.3 are reported in Table 3.3.

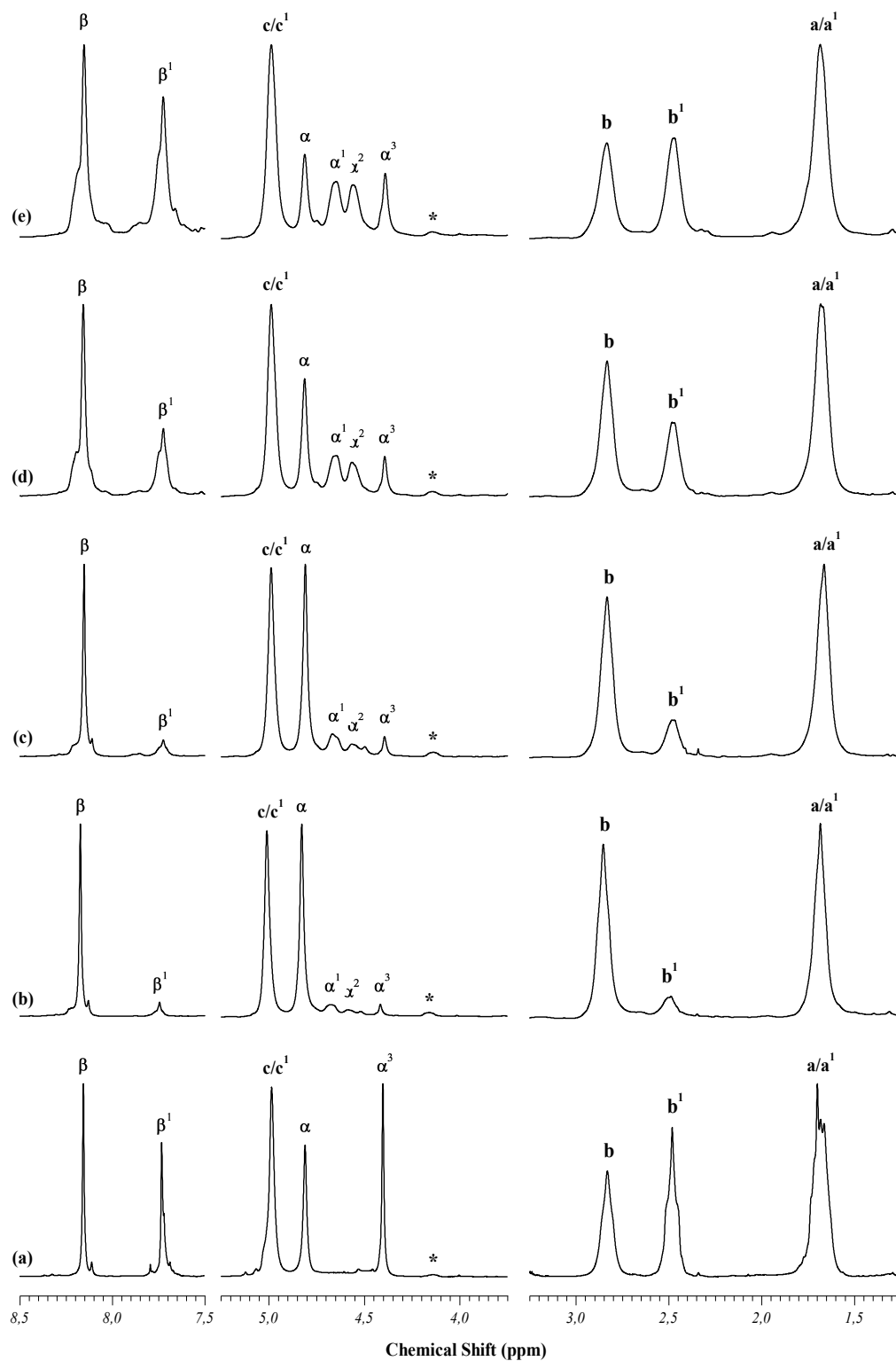


**Figure 3.3.** Sections of the  $^1\text{H-NMR}$  spectra of (a) an equimolar mixture (with respect of the repeat units) of the polymer models (PET, MXD6, MXDT, and PEA) and of PET-MXD6-(1 wt%)TA melt-mixed blends at 285 °C for: (b) 30 min, (c) 45 min, (d) 75 min, and (e) 120 min.

**Table 3.3.** Assignments of chemical shifts due to the protons and carbons belonging to sequences centered on the ethylene glycol, terephthalate and adipate structural units along the PET-MXD6 copolymer chains, as observed in their NMR spectra portrayed in Figures 3.3 and 3.4.

Sequences <sup>(a)</sup>	Structures	Chemical Shift <sup>(b)</sup> (ppm)		
		Proton	Carbon	
T-E-T		$\alpha$	4,81	64,03
A-E-T		$\alpha^2$ $\alpha^1$	4,56 4,65	63,30 64,03
A-E-A		$\alpha^3$	4,40	63,30
E-T-E		$\beta$ $\delta$	8,16 -----	130,22 167,70
E-T-M		$c^1$ $\beta^1$ $\beta$ $\delta^1$ $\delta^2$	4,98 7,72 8,14 ----- -----	50,72 ----- ----- 167,11 172,46
M-T-M		$c^1$ $\beta^1$ $\delta^3$	4,98 7,72 -----	50,72 ----- 172,03
M-A-M		$a$ $b$ $c$ $h$	1,66 2,83 4,98 -----	23,67 37,72 47,88 177,45
E-A-M		$a^1$ $a^2$ $b^1$ $b$ $c$ $h^1$ $h^2$	1,66 1,66 2,48 2,83 4,98 ----- -----	23,83 23,88 33,84 37,72 47,88 177,38 177,15
E-A-E		$a^3$ $b^1$ $h^3$	1,66 2,49 -----	24,03 33,84 177,04

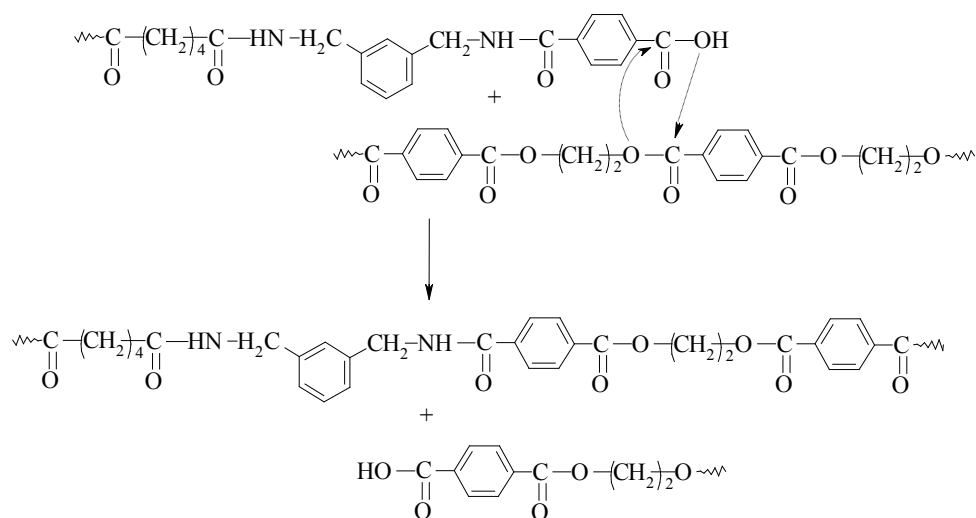
- (a) A = adipic units; E = ethyleneglycol units; M = m-Xylene diamine units; T = terephthalic units;  
 (b) The chemical shifts were measure with an accuracy of  $\pm 0.02$  ppm.



These spectra, beside the signals due to the resonances of the protons belong to the initial homosequences ethylene-terephthalate (**E-T**) and *m*-xylene adipamide (**M-A**), belonging initially to the homopolymers PET and MXD6, respectively, may show new signals due to the cosequences generated by the exchange occurring in the melt mixing. The unresolved triplet at 2.48 ppm was assigned to the methylene protons  $b^1$  (Table 3.3) of the adipate units belonging to the formed ethylene adipate (**E-A**) units, whereas the peak at 7.74 ppm was assigned at the aromatic protons  $\beta^1$  of the terephthalate unit belonging to the generated dyad *m*-xylene terephthalamide (**M-T**; Table 3.3). The presence of these new signals confirms the formation of the PET-MXD6 copolymers. The peaks in the range from 6.8 to 7.4 ppm, because of the resonance of the aromatic protons of the *m*-xylene units, are very complex and do not permit the unequivocal assignments of the corresponding sequences. The spectra in the range from 4.0 to 5.1 ppm are complex as the methylene protons  $\alpha^i$  and  $c^i$  belonging to the ethylene glycol units and to the *m*-xylene units, respectively, (Table 3.3) resonate. However, some structural information can be derived from these signals that we have tentatively assigned as reported in Figure 3.3. In particular, the signals at 4.4 ppm ( $\alpha^3$ ) were assigned at the symmetric triads **A-E-A**, the signals at 4.56 ppm ( $\alpha^2$ ) and 4.65 ppm ( $\alpha^1$ ) were assigned at the asymmetric triads **T-E-A**, and the signal at 4.81 ppm (a) were assigned at the symmetric triads **T-E-T**. The signals at 4.98 ppm (c) are due to the **M-A** dyads. The peak at 8.16 ppm ( $\beta$ ) that in the initial blend is due to the aromatic protons of PET chains, in the spectra of the melt-mixed blend is due to the same protons belonging to the dyad and triad sequences **E-T** and **E-T-E** in the copolymer chains. The formation of **M-T** sequences that link PET and MXD6 blocks in the initially formed block copolymers confirms that the carboxylic ends of PET are able to attack the amide groups along the MXD6 chains [Scheme

3.1(B)]. However, the surprising presence of the **E-A** sequences in the copolymer formed at shorter reaction time (15 min) is diagnostic of the exchange reaction due to the attack of aliphatic carboxyl ends of MXD6 at the inner ester groups of PET chains [Scheme 3.1(C)]. Therefore, although MXD6 chains with aliphatic carboxyl groups are unreactive in the initial incompatible PET-MXD6 blends, as discussed before and as already observed for Ny6/polyester blends,<sup>5,6</sup> when the blend become partial or totally compatible, the aliphatic carboxylic may promote the exchange reactions determining their progress.

The exchange reactions due to the attack of the generated in situ terephthalic end groups of MXD6 [Scheme 3.3(B)] onto the inner ester groups of PET (Scheme 3.5) contribute to the formation of copolyesteramide.



**Scheme 3.5.** Outer-inner Exchange reaction: acydolysis of PET.

The kinetics and the progress of the exchange reactions can be followed from the change in intensity of the peaks belonging to dyads **E-T**, **M-A**, **E-A**, and **M-T** (see Chart 3.1) with respect to the reaction time. To establish the effect of the interchange reactions on the microstructure of the PET-MXD6 copolymers, we have used the intensities of proton

resonances peaks at 2.49, 2.83, 7.74, and 8.16 ppm and applied an appropriate statistical model,<sup>2,5-7,23,24,48</sup> and we have calculated the molar fractions of dyad sequences ( $C_{E-T}$ ,  $C_{M-A}$ ,  $C_{E-A}$ , and  $C_{M-T}$ ), their average sequence lengths ( $L_{E-T}$ ,  $L_{M-A}$ ,  $L_{E-A}$ , and  $L_{M-T}$ ), the degree of exchange (**DE**), and the degree of randomness (**DR**) in the PET-MXD6 copolymers formed at different reaction time. For these purposes, the following eq 1–10 were used:

$$C_{E-T} = \frac{I_{8,16}}{I_{8,16}+I_{7,74}} * C_{PET} \quad (1)$$

$$C_{M-A} = \frac{I_{2,49}}{I_{2,49}+I_{2,83}} * C_{MXD6} \quad (2)$$

$$C_{M-T} = \frac{I_{7,74}}{I_{8,16}+I_{7,74}} * C_{PET} \quad (3)$$

$$C_{E-A} = \frac{I_{2,83}}{I_{2,49}+I_{2,83}} * C_{MXD6} \quad (4)$$

$$L_{E-T} = \left( \frac{C_{E-T}}{C_{M-T}} \right) + 1 \quad (5)$$

$$L_{M-A} = \left( \frac{C_{M-A}}{C_{E-A}} \right) + 1 \quad (6)$$

$$L_{M-T} = \left( \frac{C_{M-T}}{C_{E-T}} \right) + 1 \quad (7)$$

$$L_{E-A} = \left( \frac{C_{E-A}}{C_{M-A}} \right) + 1 \quad (8)$$

$$DE = (C_{E-A} + C_{M-T}) * 100 \quad (9)$$

$$DR = \frac{1}{L_{E-T}} + \frac{1}{L_{M-A}} \quad (10)$$

where  $C_{PET} = 0.5$  and  $C_{MXD6} = 0.5$  are the initial compositions of the homopolymers components.

The calculated values are listed in Table 3.4. It shows that PET-MXD6 block copolymers were formed just at shorter reaction time (15, 20, and 30 min), and owing the progress of the exchange reactions, a random copolymer was formed at 120-min mixing.

Generally, the structural characterization of the copolyamides, copolyesters, and the copolyesteramides were performed by <sup>13</sup>C-NMR analysis,<sup>2-8,16,23-29</sup> because often their carbonyl resonance signals are

sensitive to changes in their environment and then on the sequence length distributions. Therefore, we have also used the powerful  $^{13}\text{C}$ -NMR tool to obtain more reliable information about the chemical microstructure of the melt-mixed PET-MXD6–(1 wt %)TA materials.

**Table 3.4.** Material balance, molar fraction of dyads, their Average Sequence Lengths, Degree of Exchange (DE) and Degree of Randomness (DR) calculated from  $^1\text{H}$ -NMR spectra of equimolar PET-MXD6 - (1%w)TA blend melt mixed at 285 °C for different time.

Time (min)	Molar Fraction of Dyads <sup>a</sup>				Average Sequence Lengths <sup>a</sup>				DE <sup>a</sup>	DR <sup>a</sup>
	C <sub>E-T</sub>	C <sub>E-A</sub>	C <sub>M-A</sub>	C <sub>M-T</sub>	L <sub>E-T</sub>	L <sub>M-A</sub>	L <sub>E-A</sub>	L <sub>M-T</sub>		
0'	0,500	-	0,500	-	-	-	-	-	-	-
15'	0.480	0.020	0.481	0.025	20.2	25.0	1.04	1.05	4.5	0.090
20'	0.463	0.034	0.466	0.037	13.5	14.7	1.07	1.08	7.0	0.140
30'	0.442	0.055	0.445	0.058	8.60	9.10	1.12	1.13	11.3	0.224
45'	0.410	0.102	0.398	0.090	5.60	4.90	1.25	1.22	19.2	0.384
60'	0.370	0.140	0.370	0.138	3.70	3.65	1.38	1.37	27.8	0.555
75'	0.318	0.179	0.321	0.182	2.74	2.80	1.56	1.57	36.1	0.722
90'	0.300	0.210	0.300	0.200	2.50	2.50	1.67	1.67	41.0	0.818
105'	0.267	0.224	0.276	0.233	2.25	2.23	1.81	1.87	45.7	0.914
120'	0.243	0.253	0.247	0.257	1.95	1.97	2.02	2.06	51.0	1.020

(a) Calculated by eqs 1-10.

Figure 3.4 portrays relevant peaks for PET-MXD6–(1 wt %)TA melt mixed at 285 °C for 20, 30, 60, 75, 90, and 120 min, and also of an equimolar mixture of the four polymer models (PET, MXD6, PEA, and MXDT). Peaks present in the carbon spectra of all PET-MXD6–(1 wt %)TA melt-mixed products were assigned in accordance with the chemical shifts of the polymer models and our interpretation. The chemical shifts of the most important carbons were reported in Table 3.3. As expected and as can be observed in Figure 3.4, the  $^{13}\text{C}$ -NMR spectra show well-resolved peaks, in particular, in the carbonyl regions between

166 and 179 ppm. Well resolved peaks were also observed in upper field (in the range between 23 and 66 ppm), where the methylene carbons belonging to the adipate and ethylene glycol units resonate.

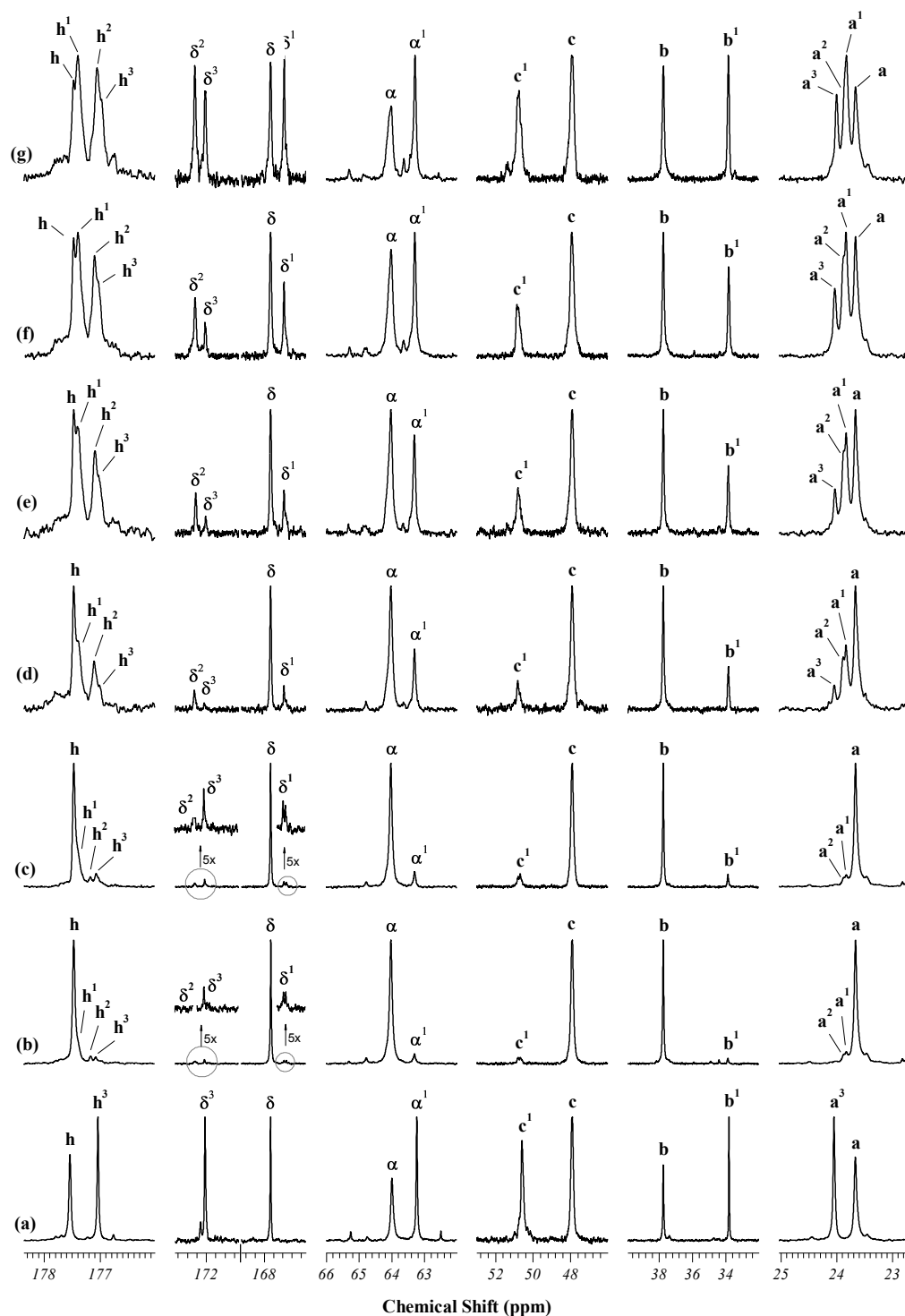


**Figure 3.4.** Sections of the  $^{13}\text{C}$ -NMR spectra of (a) an equimolar mixture (with respect of the repeat units) of the polymer models (PET, MXD6, MXDT, and PEA) and of PET-MXD6-(1 wt%)TA melt-mixed blends at 285 °C for: (b) 20 min, (c) 30 min, (d) 60 min, (e) 75 min, (f) 90 min, and (e) 120 min.

The aromatic carbons belong to the terephthalate (**T**) and *m*-xylene (**M**) units, which resonate in the range 120–135 ppm, appear poorly resolved, and do not permit unequivocal assignments of the corresponding dyad and triad sequences. In the carbonyl regions between 166 and 174 ppm, beside the peak at 167.63 ppm due to the carbonyls of PET units (carbons  $\delta$ ) in the initial blends, three new carbonyl peaks ( $\delta^1$ ,  $\delta^2$ , and  $\delta^3$ ) are observed in the spectra of the melt-mixed blends for time higher than 15 min. These signals were assigned to the triads centered on terephthalate units, as in Table 3.3. The signal at 167.70 ppm ( $\delta$ ) belongs to the symmetric triads **E-T-E** that at 172.03 ppm ( $\delta^3$ ) is due to the symmetric triads **M-T-M**, whereas those at 167.11 ppm ( $\delta^1$ ) and at 172.46 ( $\delta^2$ ) are due to the two nonequivalent carbonyls belong to the asymmetric triads **E-T-M**. In the range between 176 and 178 ppm, beside the signal at 177.45 ppm initially due to the resonance of carbonyl of the MXD6 chains (carbons h in Table 3.3 and in Figure 3.4), appear another signal at about 177.15 ppm (carbons  $h^2$ ) whose relative intensity increases as reaction time increases. By expanding this section of the spectra, a shoulder emerges at both the peaks, and therefore, these four peaks that are not well-resolved can be assigned to the three triads centered on the adipate units. In particular, the carbonyl resonance peak h at 177.45 ppm was assigned to the symmetric triads **M-A-M**, and the signal  $h^3$  at 177.04 ppm was assigned at the symmetric triads **E-A-E**, while the carbonyl signals  $h^1$  and  $h^2$  at 177.38 and 177.15 ppm, respectively, were assigned at the asymmetric triads **E-A-M**. Therefore, analyzing the signals due to the resonance of the carbonyls can be characterized from the triad sequences along the PET-MXD6 copolymer chains. The **M-A-M**, **E-A-E**, and **E-A-M** triad sequences along the copolymer chains can be also characterized looking at the methylene carbons in  $\beta$  with respect to the amide and ester

carbonyl of the adipate units, which resonated between 23 and 25 ppm (signals a, a<sup>1</sup>, a<sup>2</sup>, and a<sup>3</sup> in Figure 3.4).

**Table 3.5.** Molar fraction of dyads and triads, Average Sequence Lengths, Degree of Exchange (DE) and Degree of Randomness (DR) from  $^{13}\text{C}$ -NMR spectra of PET-MXD6- (1%w)TA melt mixed blend at 285 °C for different time.

Time (min)	Molar Fraction of Triads <sup>(a)</sup>						Molar Fraction of Dyads <sup>(b)</sup>				Average Sequence Lengths <sup>(c)</sup>				DE <sup>(d)</sup>	DR <sup>(e)</sup>
	C <sub>E-T-E</sub>	C <sub>E-T-M</sub>	C <sub>M-T-M</sub>	C <sub>M-A-M</sub>	C <sub>E-A-M</sub>	C <sub>E-A-E</sub>	C <sub>E-T</sub>	C <sub>E-A</sub>	C <sub>M-A</sub>	C <sub>M-T</sub>	L <sub>E-T</sub>	L <sub>M-A</sub>	L <sub>E-A</sub>	L <sub>M-T</sub>		
0	0.500	-	-	0.500	-	-	0.500	-	0.500	-	-	-	-	-	-	-
15	0.460	0.026	0.013	0.470	n.d.	n.d.	0.480	0.020	0.470	0.030	17.0	24.5	1.04	1.06	5.00	0.100
20	0.450	0.035	0.015	0.480	0.020	n.d.	0.477	0.023	0.472	0.028	18.0	21.5	1.06	1.05	5.10	0.102
30	0.424	0.050	0.030	0.427	0.070	0.005	0.453	0.047	0.444	0.056	9.09	10.4	1.11	1.12	10.3	0.206
45	0.396	0.070	0.040	0.366	0.110	0.023	0.418	0.082	0.410	0.090	5.06	6.00	1.20	1.25	17.2	0.364
60	0.350	0.110	0.042	0.313	0.154	0.033	0.360	0.140	0.350	0.150	3.40	3.50	1.40	1.42	29.0	0.580
75	0.300	0.160	0.043	0.225	0.206	0.070	0.330	0.170	0.320	0.180	2.83	2.88	1.53	1.55	0.350	0.700
90	0.228	0.230	0.043	0.202	0.210	0.088	0.304	0.196	0.290	0.210	2.45	2.48	1.68	1.69	40.6	0.810
105	0.181	0.260	0.060	0.176	0.230	0.095	0.272	0.228	0.270	0.230	2.18	2.18	1.84	1.84	46.0	0.920
120	0.153	0.250	0.100	0.155	0.245	0.102	0.264	0.236	0.253	0.247	2.07	2.07	1.93	1.94	48.3	0.970

(a) calculated by equations 15-20; (b) calculated using equations 11-14; (c) calculated by equations 5-8; (d) calculated by equation 9; (e) calculated by equation 10.



Signals at 23.67 ppm (carbons  $\alpha$ ) are due to the triads **M-A-M**; low resolved peaks  $\alpha^1$  and  $\alpha^2$  at about 23.85 ppm were assigned to the **E-A-M** triads; signals  $\alpha^3$  at 24.03 ppm were assigned to the **E-A-E** triads. Further information about the dyad sequences in the copolymers can be obtained following the evolution versus the reaction time of the peaks in range 35– 66 ppm due to the resonances of: the two methylene carbons of the ethylene glycol units (peaks  $\alpha$  and  $\alpha^1$  in Figure 3.4; the methylene carbons of the adipate units linked to the carbonyls (signals  $b$  and  $b^1$ ); the methylene carbons of the *m*xylene units (signals  $c$  and  $c^1$ ). Comparing proton and carbon spectra is clear that more information on the microstructure of the copolymer versus the reaction time can be obtained from  $^{13}\text{C}$ -NMR spectra. Using the relative intensities of the methylene carbon peaks  $b$ ,  $b^1$ ,  $\alpha$ , and  $\alpha^1$  in Figure 3.4 and applying the statistical model applied to the proton spectra, we have calculated the molar fractions of dyad sequences ( $C_{E-T}$ ,  $C_{M-A}$ ,  $C_{E-A}$ , and  $C_{M-T}$ ), their average sequence lengths ( $L_{E-T}$ ,  $L_{M-A}$ ,  $L_{E-A}$ , and  $L_{M-T}$ ), the degree of exchange (**DE**), and the degree of randomness (**DR**) in the PET-MXD6 copolymers formed at different reaction time, using the following eqs 11–14 and the eqs 5–10 discussed before.

$$C_{E-T} = \left( \frac{I_{\alpha^0}}{I_{\alpha^0} + I_{\alpha^1}} \right) * C_{PET} \quad (11)$$

$$C_{E-A} = \left( \frac{I_{\alpha^1}}{I_{\alpha^0} + I_{\alpha^1}} \right) * C_{PET} \quad (12)$$

$$C_{M-A} = \left( \frac{I_C}{I_C + I_{C^1}} \right) * C_{MXD6} \quad (13)$$

$$C_{M-T} = \left( \frac{I_{C^1}}{I_C + I_{C^1}} \right) * C_{MXD6} \quad (14)$$

The calculated values are reported in Table 3.5. Very similar values were calculated using the relative intensities of the carbonyl carbon peaks  $h$ ,  $h^1$ ,  $h^2$ ,  $h^3$ ,  $\delta$ ,  $\delta^1$ ,  $\delta^2$ , and  $\delta^3$  applying the same statistical method and the appropriate equations. Using the intensities of the carbon peaks  $a$ ,  $a^1$ ,  $a^2$ ,  $a^3$ ,  $\delta$ ,  $\delta^1$ ,  $\delta^2$ , and

$\delta^3$ , we have also calculated the molar fractions of triad sequences ( $C_{E-T-E}$ ,  $C_{E-T-M}$ ,  $C_{M-T-M}$ ,  $C_{M-A-M}$ ,  $C_{E-A-M}$ , and  $C_{E-A-E}$ ) by the following eqs 15–20.

$$C_{E-T-E} = \left( \frac{I_{\delta}}{\sum_{i=0}^3 I_{\delta^i}} \right) * C_{PET} \quad (15)$$

$$C_{E-T-M} = \left( \frac{I_{\delta^1} + I_{\delta^2}}{\sum_{i=0}^3 I_{\delta^i}} \right) * C_{PET} \quad (16)$$

$$C_{E-T-M} = \left( \frac{I_{\delta^2}}{\sum_{i=0}^3 I_{\delta^i}} \right) * C_{PET} \quad (17)$$

$$C_{M-A-M} = \left( \frac{I_a}{\sum_{i=0}^3 I_{a^i}} \right) * C_{MXD6} \quad (18)$$

$$C_{E-A-M} = \left( \frac{I_{a^{1,2}}}{\sum_{i=0}^3 I_{a^i}} \right) * C_{MXD6} \quad (19)$$

$$C_{E-A-E} = \left( \frac{I_{a^3}}{\sum_{i=0}^3 I_{a^i}} \right) * C_{MXD6} \quad (20)$$

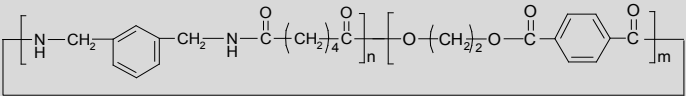
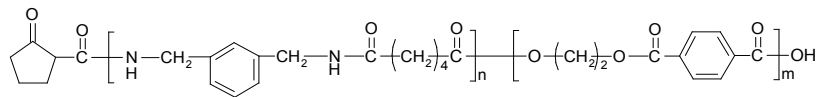
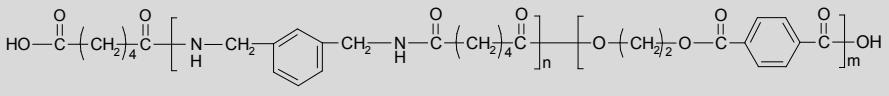
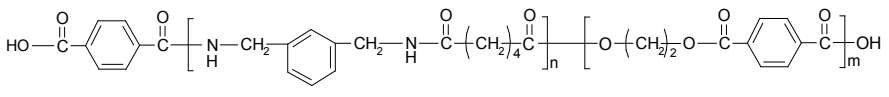
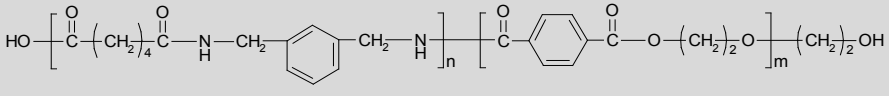
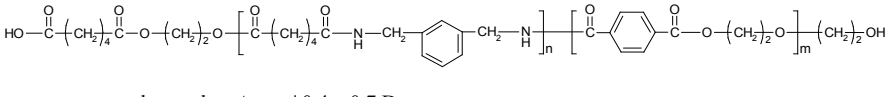
Calculated values are collected in Table 3.5. Microstructure data determined from  $^{13}\text{C}$ -NMR spectra confirm that PET-MXD6 block copolymers were formed at shorter reaction time 15 and 20 min. The average sequence lengths of the PET ( $L_{E-T}$ ) and MXD6 ( $L_{M-A}$ ) blocks decrease as the reaction time, and a random copolymer was formed at 120 min mixing. These indicate that exchange reactions progress to a thermodynamic equilibrium producing a random PET-MXD6 copolymer at longer reaction time (120 min). The agreement of the molar and the structural data calculated from  $^1\text{H}$  and  $^{13}\text{C}$ -NMR spectra of PET-MXD6-(1 wt %)TA melt-mixed blends suggests that structural information on the PET-MXD6 copolymers can be obtained from their NMR spectra using mixture of  $\text{CDCl}_3/\text{TFA}/(\text{CF}_3\text{CO})_2\text{O}$  solvent instead of the  $\text{D}_2\text{SO}_4$ , which has been used by other researchers,<sup>30</sup> that degrades the ester  $\text{C}=\text{O}$  groups belonging to the ester-ester and ester-amide sequences, which resulted in the consequent loss of information on the distribution of their dyads and triads sequences along the copolymer chains. An important factor that influences the correctness in the determination of the homopolymers block lengths would be the presence in the copolymers of PET and/or MXD6

unaffected by exchange reactions at shorter reaction time (15–20 min). In the present studies, we used an equimolar ratio of homopolymers and relatively high temperature of reactive blending (285 °C), hence it is expected that the amounts of residual homopolymers in all melt-mixed materials studied are low enough so as not to affect significantly the accuracy of the sequential analysis, in particular for copolymer formed at high reaction time. However, for melt-mixed products with a **DR** < 0.2 cannot exclude the presence of the PET and MXD6 copolymers from NMR analysis because it is an averaging technique and is not possible to distinguish each component. To overcome this problem, all PET-MXD6–(1 wt %)TA melt-mixed materials will be further studied by MALDI-TOF MS; for example, here we report the experimental and calculated MALDI mass spectra of the random copolymer formed at 120 min mixing (namely PET-MXD6-(120)). The MALDI-TOF mass spectra of other melt-mixed materials are actually studied to obtain further information about the composition and structure of the components.

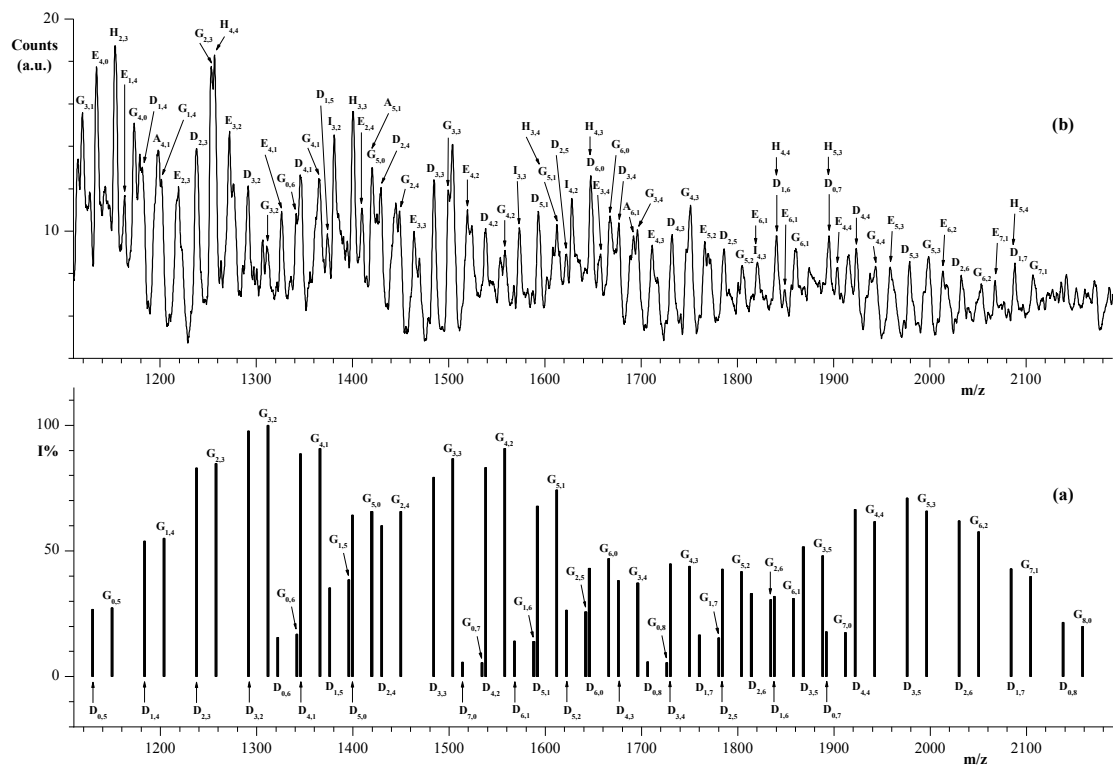
### 3.11 – MALDI-TOF ms characterization

Figure 3.5(a) reports the MALDI TOF mass spectrum of the copolymer sample PET-MXD6-(120) in the mass range  $m/z$  1100–2200; the peaks present are assigned as in Table 3.6. It can be seen that all peaks are due to sodiated oligomers. As expected, the most intense peaks are due to chains terminated with adipic acid groups, labeled as  $D_{n,m}$  and to chains terminated with TA, labeled as  $G_{n,m}$ ; as well as for the heated MXD6 [Figure 3.2(b) and 2(c)], copolymer chains terminated with cyclopentanone units (species  $E_{n,m}$  in Table 3.5) were also observed. These end groups were formed by degradative reactions involving the adipic acid end moieties (Scheme 3.4). The indexes “ $m$  and  $n$ ” indicate the number of MXD6 (**M-A**) and PET (**E-T**) repeat units present in the macromolecular chains. As a matter of fact, heating PET-MXD6, new units are formed, namely units **M-T** (*m*-xylylendiamine terephthalate) and units **E-A** (ethylene adipate). Unfortunately these units are mixed with PET and MXD6 units, and they are hidden in the spectrum. We considered 60 peaks due to pentamers, hexamers, heptamers, and octamers of the type  $D_{n,m}$  and  $G_{n,m}$ . The intensity of the 60 peaks was given as an input to the DROPO program<sup>49</sup> and a minimization was launched. The result was  $P_{M-A} = 0.57$ ,  $P_{M-T} = 0.43$ ,  $P_{E-A} = 0.50$ , and  $P_{E-T} = 0.50$ . Figure 3.5(b) also reports the calculated mass spectrum and the agreement is fine ( $AF = 0.4$ ). The degree of randomness associated with these values is 0.93, which compares well with the NMR values reported in Tables 3.4 and 3.5.

**Table 3.6.** Mass assignments of peaks present in the experimental and calculated MALDI mass spectra of the PET-MXD6-(120) random copolymer reported in Figure 3.5.

Species	Structures	$[M+Na]^+(n,m)^{(a)}$
$A_{n,m}$		1200(4,1); 1446.2 (5,1); 1692.4 (6,1)
$E_{n,m}$		1135.8 (4,0); 1166.1 (1,4); 1328.1 (4,1); 1220.1 (2,3); 1274.1 (3,2); 1574.3 (5,1); 1412.3 (2,4); 1466.3 (3,3); 1520.3 (4,2); 1658.5 (3,4); 1712.5 (4,3); 1766.5 (5,2); 1820.5 (6,1); 1904.7 (3,5); 1959.7 (4,4); 2012.7 (5,3); 2066.7 (6,2); 2120.6 (7,1)
$D_{n,m}$		1099.9 (3,1); 1045.9 (2,2); 1184.1 (1,4); 1238.1 (2,3); 1292.1 (3,2); 1346.1 (4,1); 1376.3 (1,5); 1430.3 (2,4); 1484.3 (3,3); 1538.3 (4,2); 1622.5 (2,5); 1676.5 (3,4); 1730.5 (4,3); 1784.5 (5,2); 1868.7 (3,5); 1922.7 (4,4); 1976.7 (5,3); 2030.7 (6,2)
$G_{n,m}$		1119.9 (3,1); 1173.8 (4,0); 1204.1 (1,4); 1258.1 (2,3); 1312.1 (3,2); 1366.1 (4,1); 1420.1 (5,0); 1450.3 (2,4); 1504.3 (3,3); 1558.3 (4,2); 1612.3 (5,1); 1696.5 (3,4); 1750.5 (4,3); 1804.5 (5,2); 1878.7 (6,1); 1912.4 (7,0); 1942.7 (4,4); 1996.7 (5,3); 2050.7 (6,2).
$H_{n,m}$		1154 (2,3); 1402.2 (3,3); 1592.3 (3,4); 1648.4 (4,3); 1840.6 (4,4); 1894.6 (5,3); 2084.8 (5,4)
$I_{n,m}$		1382.2 (3,2); 1574.4 (3,3); 1628.4 (4,2); 1820.6 (4,3)

(a) The Mass accuracy was better than  $\Delta m = \pm 0.4 - 0.7$  Da.



**Figure 3.5.** (a) Theoretical and (b) experimental MALDI-TOF mass spectra of PET-MXD6 (120 min) random copolymer, in the mass range 1100–2200 Da.

### 3.12 – DSC analysis

The progress of PET-MXD6 copolymer formation could be followed also by the following thermal properties ( $T_g$ ,  $T_m$ ,  $T_{cc}$ , and  $T_c$ ) of the melt reacted blends as a function of the melt-mixing time, measured by means of DSC. DSC data obtained by analysis of the equimolar PET-MXD6–(1 wt %)TA melt-mixed blends were summarized in Table 3.7. It shows that the initial blend melt mixed for 0 min exhibits two endothermic melting peaks at 247 and 238 °C and two second-order transitions ( $T_g$ ) at 80 and 89 °C, almost identical to the values obtained for the neat PET and MXD6 homopolymers, confirming that these polymers are incompatible in the molten state. It also shows a broad cold crystallization exotherm ( $T_{cc}$ ) with a maximum at about 147 °C. The reacted products at 15, 20, and 30 min show two melting peaks  $T_m$ , which one at about 247–245 °C and one that progressively shift from 238 to 208 °C. They also present a very broad cold crystallization exothermic peak lying between 120 and 160 °C and a single  $T_g$ . This data suggest that block copolymers were formed at shorter reaction time in accordance with the NMR data in Tables 3.4 and 3.5. The presence of two melting process can be ascribed at the PET and MXD6 blocks. By comparison with the  $T_m$  value of initial polymer components, the second melting at about 245 °C should be due to the PET blocks, whereas the first melting should be due to the MXD6 blocks. As this is shifted at lower temperature from 238 to 208 °C with the increase in reaction time (from 0 to 30 min), we believe that the melting of MXD6 blocks can be influenced of the presence of the PET blocks and/or above all from the heterosequences (dyads **E-A** and **M-T**) formed by exchange reactions. The copolymer formed at 45 min reacting shows only one endothermic melting peak with a maximum at 239 °C, it also gives a cold crystallization exotherm at 131 °C. A similar behavior was observed for PET-Ny6 copolymers formed by melt mixing of PET-Ny6 blends (1:1 mol) in the presence of TsOH (0.5 wt %t).<sup>5</sup>

**Table 3.7.** Viscosity ( $\eta_{inh}$ ), thermal properties ( $T_g$ ,  $T_{cc}$ ,  $T_c$  and  $T_m$ ) and TGA data (PDT) of PET-MXD6-(1%w)TA blend melt mixed at 285 °C for different times. Thermal properties were determined by DSC analysis.

Reaction Time (min)	$\eta_{inh}^{(a)}$ (dL/g)	$T_g$ exp (°C)	$T_g$ calc <sup>(b)</sup> (°C)	$T_{cc}$ (°C)	$T_c$ (°C)	$T_m$ (°C)	$\Delta H_m$ (J/g)	PDT (°C)
0	1.13	80 / 89	--	140	147	238 / 247	29.00 / 4.70	400
15	0.86	81	82.1	152	157	216 / 247	13.70 / 26.70	396
20	0.87	80	81.5	144	147	215 / 247	14.20 / 26.10	395
30	0.88	79	80.0	131	146	208 / 245	13.44 / 15.07	392
45	0.88	78	77.3	131	146	239	10.94	392
60	0.88	73	73.0	--	--	225	2.84	391
75	0.86	70	70.9	--	--	--	--	392
90	0.86	68	68.2	--	--	--	--	392
105	0.84	65	66.1	--	--	--	--	392
120	0.84	64	64.7	--	--	--	--	393

(a)  $\eta_{inh}$  data were obtained at 30°C with a phenol/tetrachloroethane (60/40 w/w) mixture as a solvent.

(b) calculated by Eq. 22. Thermal properties were determined by DSC analyses.

The copolymer composition data in Tables 3.4 and 3.5 show that the average sequence lengths of PET ( $L_{E-T}$ ) MXD6 ( $L_{M-A}$ ) blocks decrease as increase the reaction time. The  $L_{E-T}$  in the PET-MXD6 copolymer formed at 45 min is 5.06, very similar to the  $L_{M-A}$  values that is 6. Based on these data, the presence of only one melting point in the block copolymers formed at 45 min heating could be explained as the following hypothesis: (i) when E-T (PET) and M-A (MXD6) blocks reach an average sequence length of about 6 or less can cocrystallize and accommodate themselves in the same crystal structure; (ii) probably when the MXD6 blocks reach an average sequence length lower than 10 are not able to crystallize. Obviously, other studies are necessary to explain this behavior and clarify each double correlate with our hypotheses.



The PET-MXD6 copolymers formed at reaction time higher than 45 min does not show any crystallization and melting process, indicating that a totally amorphous sample is formed. Being the average sequence lengths of PET and MXD6 blocks ( $L_{E-T}$  and  $L_{M-A}$ , respectively, in Table 3.5) about 2.8 in the copolymer formed at 60 min of melt mixing, its thermal behavior can be interpreted as a proof that also the PET or both PET and MXD6 blocks have reached some critical lengths making them unable to crystallize. All PET-MXD6 copolymers formed by melt mixing of PET-MXD6 blends in the presence of TA show only one glass transition temperature ( $T_g$ ) that decrease from 81 °C (intermediate to those of the initial homopolymers) to 63.2 °C. This result confirms that the microstructure and composition of PET-MXD6 copolymers change with the progress of the exchange reaction as increase the reaction time, in accordance with the molar composition data obtained from NMR analyses. NMR data in Tables 3.4 and 3.5 show that a random copolymers was formed at 120 min heating, and we have tentatively applied the empirical Fox equation (eq 21) to calculate its  $T_g$  value.

$$\frac{1}{T_g} = \frac{W_1}{T_{g1}} + \frac{W_2}{T_{g2}} \quad (21)$$

where  $W_1$  (0.4384) and  $W_2$  (0.5616) are the weight fraction of PET and MXD6 initial components;  $T_{g1}$  (352 °K) and  $T_{g2}$  (359 °K) are the glass transitions of PET and MXD6 samples, respectively. By this equation, generally used to calculate the  $T_g$  values of random copolymers formed by melt mixing of binary A/B blends,<sup>2,5-7</sup> we obtain a value of 82.9 °C that is very different from that measured (63.4 °C). First, we have believed that this difference was due to the lower molar masses of the copolymer with respect to the initial PET-MXD6 blend, but the inherent viscosity values in Table 3.7 show that it decrease from 1.133 g/dL (0 min) to 0.856 g/dL until 15 min and remain almost constant as the melt-mixing time increase, indicating that mostly the average molar masses of the formed copolymers does not have much varying. Therefore, due to exchange reactions (Schemes 3.1 and 3.5) two new heterosequences were

formed: the aliphatic ester ethyleneadipate (**E-A**) units and the aromatic amide *m*-xylylene terphthalamide (**M-T**) units, we believe that their different stiffness, with respect to semiaromatic **E-T** (PET) and **M-A** (MXD6) sequences, might influence the thermal properties, in particular, the  $T_g$  of the corresponding PET-MXD6 copolymers. This hypothesis can be supported by the calorimetric data of the corresponding polymer models PEA and MXDT. The aliphatic polyester PEA is a semicrystalline polymer with a  $T_g$  of 224 °K (48 °C), a cold crystallization  $T_{cc}$  at 278 °K (5 °C), and a  $T_m$  at 321 °K (48 °C), whereas the thermally stable aromatic polyamide MXDT polymer is amorphous with a  $T_g$  of 445 °K (172 °C). These polymers show  $T_g$  values very different from those the PET and MXD6 homopolymers. As we have determined the molar composition of dyads in the PET-MXD6 formed copolymers (Tables 3.4 and 3.5) by NMR studies, we have expanded the two-component Fox equation in a new fourcomponent equation (eq 22) that take into account the composition of the copolymer analyzed.

$$\frac{1}{T_g} = \frac{W_1}{T_{g1}} + \frac{W_2}{T_{g2}} + \frac{W_3}{T_{g3}} + \frac{W_4}{T_{g4}} \quad (22)$$

where:  $W_1$ ,  $W_2$ ,  $W_3$ , and  $W_4$  are the weight fractions of the dyads **E-T**, **M-A**, **E-A**, and **M-T**, respectively;  $T_{g1}$ ,  $T_{g2}$ ,  $T_{g3}$ , and  $T_{g4}$  are glass transition values in °K of the corresponding homopolymers PET, MXD6, PEA, and MXDT, respectively. The weight fraction of each dyad was calculated by the following eq 23.

$$W_i = \frac{C_i * m_i}{\sum_{i=1}^4 C_i * m_i} \quad (23)$$

where  $C_i$  is the molar fraction of the corresponding dyad and  $m_i$  is the molecular mass (192 g/mol for the dyad **E-T**, 226 g/mol for the dyad **M-A**, 172 g/mol for the dyad **E-A**, and 266 g/mol for the dyad **M-T**). Applying these equation at a theoretical random four-component copolyesteramide formed from an equimolar PET-MXD6 reacted blend being 0.25 the molar composition of each dyad, we calculate a  $T_g$  of 64.7 °C that match with that of

the random copolymer formed at 120 min mixing (64 °C), confirming the validity of our equation. Using the molar fraction values determined from  $^{13}\text{C}$ -NMR analyses (Table 3.5), we have calculated the  $T_g$  of the all copolymers, and the values are summarized in Table 3.7. The agreement of calculated and experimental values indicates that structural and molar compositions of each sequence influence the glass transition of the PET-MXD6 copolymers and that the dominant components of the melt mixed materials taken at lower reaction times (15 and 20 min) are PET-MXD6 block copolymers with a negligible amount of unreacted homopolymers.

### 3.13 – Thermogravimetric analysis (TGA)

Thermal stabilities of the homopolymer models and of the PET-MXD6–(1 wt %)TA melt-mixed materials were investigated by thermogravimetric analysis (TGA). All samples exhibit a single degradation step. PET decompose in the range 340–500 °C with a polymer decomposition temperature (PDT), that correspond to the maximum rate of polymer degradation) of 434 °C, leaving a char residue at 800 °C of 10%. MXD6 decomposes in the range 320–480 °C with a PDT of 400 °C, producing a char residue of 15% at 800 °C. MXDT decomposes in the same range with a PDT of 400 °C, leaving a char residue at 800 °C of 32%, whereas the PEA decomposes in the range 270–400 °C with a PDT of 364 °C, giving a char residue at 800 °C of 2%. All PET-MXD6–(1 wt %)TA melt-mixed materials decompose in the range 350–450 °C with a single PDT, leaving a char residue at 800 °C of about 14–15%. Their PDT values slight decrease from 400 to 393 °C as increases the reaction time of the PET-MXD6–(1 wt %)TA samples (see data in Table 3.7), indicating that the thermal stability of the PET-MXD6 copolymers should depend on the molar composition of their four components.

### 3.14 – Conclusions

Our results show that hydrolytic reaction of PET chains occurs when a catalytic amount of TA is added during the melt mixing of PET-MXD6 blends, yielding linear PET and MXD6 chains terminated with reactive aromatic carboxyl groups (Scheme 3 a and 3b). These oligomers can react with inner amide and ester groups leading to the formation of PET-MXD6 block copolymers that can compatibilize the blends. In this homogeneous environment, the aliphatic carboxyl-terminated MXD6 chains, inactive in the initial biphasic blend, may promote the exchange reactions (Scheme 1C) as shown by the formation of E-A sequence in the copolyesteramides. The progress of exchange reactions and the microstructure of the formed copolymers was followed by  $^1\text{H}$  and  $^{13}\text{C}$  NMR analyses using a  $\text{CDCl}_3/\text{TFA-d}/(\text{CF}_3\text{CO})_2\text{O}$  mixture as solvent at room temperature and applying appropriate mathematical equations. The data reveal that random copolymers were formed at reaction time higher than 75 min, whereas block copolymers were formed at shorter reaction time (15–30 min). Therefore, reliable information on the microstructure of the PET-MXD6 copolymers can be obtained by  $^1\text{H}$  NMR and/or  $^{13}\text{C}$ -NMR analyses, using nondegradative solvents, instead of the  $\text{D}_2\text{SO}_4$ .<sup>30</sup> Combining viscosities and NMR data emerge that the exchange reactions prevail enough on the acid hydrolysis at mixing time higher than 15 min. The thermal properties ( $T_g$ ,  $T_m$ ,  $T_{cc}$ , and  $T_c$ ) of the copolymers change as a function of their dyads' molar composition, their average sequence lengths, and their degree of randomness. All copolymers present a single  $T_g$ , which value decrease as increase the melt mixing time of the blends. The measured  $T_g$  values match with those calculated by our proposed modified Fox equation (eq 22) that take into account of the molar composition of the four structural units (dyads) component the formed PET-MXD6 copolymers at the different reaction time. The agreement of calculated and experimental  $T_g$  values confirms the validity of the proposed equation. MALDI-TOF analysis of the

heated MXD6 and of the PET-MXD6 melt-mixed blends reveals also the formation cyclopentanone ended chains, owing to the degradative reaction involving the adipic acid end groups.

### 3.15 – References

- 1 Montaudo, G.; Puglisi, C.; Samperi, F. *Transreactions in Condensation Polymers*; Fakirov, S., Ed.; Wiley-VCH: Weinheim, 1998; Chapter 4, p 159, and references therein;
- 2 Puglisi, C.; Samperi, F.; Di Giorgi, S.; Montando, G. *Macromolecules* 2003, 36, 1098–1107;
- 3 Montaudo, G.; Puglisi, C.; Samperi, F. *Macromolecules* 1998, 31, 650–661, and references therein;
- 4 Montaudo, G.; Montaudo, M. S.; Scamporrino, E.; Vitalini, D. *Macromolecules* 1992, 25, 5099–5107;
- 5 Samperi, F.; Puglisi, C.; Alicata, R.; Montaudo, G. *J Polym Sci Part A: Polym Chem* 2003, 41, 2778–2793;
- 6 Samperi, F.; Montaudo, M.; Puglisi, C.; Alicata, R.; Montaudo, G. *Macromolecules* 2003, 36, 7143–7154;
- 7 Samperi, F.; Montaudo, M.; Puglisi, C.; Di Giorgi, S.; Montando, G. *Macromolecules* 2004, 37, 6449–6459;
- 8 Fakirov, S.; Evstatiev, M.; Petrovich, S. *Macromolecules* 1993, 26, 5219–5226;
- 9 Evstatiev, M.; Schultz, J. M.; Petrovich, S.; Georgiev, G.; Fakirov, S.; Friedrich, K. *J Appl Polym Sci* 1998, 67, 723–737;
- 10 Fakirov, S.; Evstatiev, M.; Schultz, J. M. *Polymer* 1993, 34, 4669–4679.
- 11 Chiou, K.-C.; Chang, F.-C. *J Polym Sci Part B: Polym Phys* 2000, 38, 23–33;
- 12 An, J.; Ge, J.; Liu, Y. *J Appl Polym Sci* 1996, 6, 1803–1810;
- 13 Jin, X. M.; Li, W. *J Macromol Sci Rev Macromol Chem Phys* 1995, 35, 1–13;
- 14 Huang, C. C.; Chang, F. C. *Polymer* 1997, 38, 2135–2141;
- 15 Haberstroh, E.; Prollius, E. J. *Polym Eng Sci* 2001, 21, 239–250;
- 16 Denchev, Z.; Kricheldorf, H. R.; Fakirov, S. *Macromol Chem Phys* 2001, 202, 574;

- 17 Samios, C. K.; Kalfoglou, N. K. *Polymer* 1999, 40, 4811–4819;
- 18 Pillon, L. Z.; Utracki, L. A. *Polym Eng Sci* 1984, 24, 1300–1305;
- 19 Pillon, L. Z.; Utracki, L. A. *Polym Eng Sci* 1987, 27, 562–567;
- 20 Inoshita, K.; Terekawa, M.; Yasuda, T. *Jpn Pat.* 7,228,916, 1972;
- 21 Brown, S. B. In *Reactive Extrusion*; Xanthos, M., Ed.; Hanser: Munich, 1992; Chapter 4;
- 22 Van Bennekom, A. C. M.; Willemsen, P. A. A. T.; Gaymans, R. J. *Polymer* 1996, 37, 5447–5467;
- 23 Devaux, J.; Godard, P.; Mercier, J. P. *J Polym Sci Polym Phys Ed* 1982, 20, 1875–1880;
- 24 Devaux, J. *Transreactions in Condensation Polymers*; Fakirov, S., Ed.; Wiley-VCH: Weinheim, 1999; Chapter 3, p 125, and references therein;
- 25 Kricheldorf, H. R.; Leppert, E.; Schilling, G. *Makromol Chem* 1975, 176, 81–95;
- 26 Schilling, G.; Kricheldorf, H. R. *Makromol Chem* 1975, 176, 3341–3348;
- 27 Kricheldorf, H. R.; Muehlhaupt, R. *Angew Makromol Chem* 1977, 65, 185–192;
- 28 Kricheldorf, H. R.; Hull, W. E. *J Macromol Sci Chem A* 1977, 11, 2281–2292;
- 29 Kricheldorf, H. R. *Pure Appl Chem* 1982, 54, 467–481;
- 30 Xie, F.; Kim, Y. W.; Jabarin, S. A. *J Appl Polym Sci* 2009, 112, 3449–3461;
- 31 Hu, Y. S.; Prattipati, V.; Hiltner, A.; Baer, E.; Mehta, S. *Polymer* 2005, 46, 5202–5210;
- 32 Prattipati, V.; Hu, Y. S.; Bandi, S.; Mehta, S.; Schiraldi, D. A.; Hiltner, A.; Baer, E. *J Appl Polym Sci* 2005, 99, 225–235;
- 33 Hu, Y. S.; Prattipati, V.; Mehta, S.; Schiraldi, D. A.; Hiltner, A.; Baer, E. *Polymer* 2005, 46, 2685–2698;
- 34 Bandi, S.; Mehta, S.; Mehta, S. *Polym Deg Stab* 2005, 88, 341–348;



- 35 Prattipati, V.; Hu, Y. S.; Bandi, S.; Schiraldi, D. A.; Hiltner, A.; Baer, E.; Mehta, S. *J Appl Polym Sci* 2005, 99, 1361–1370;
- 36 Samperi, F.; Puglisi, C.; Alicata, R.; Montaudo, G. *Polym Degrad Stab* 2004, 83, 3–10;
- 37 (a) Okudaira, T.; Tsuboi, A.; Sugihara, S.; Hama, Y. U.S. Pat. 4,398,642, 1983; (b) Okudaira, T.; Hama, Y., et al. U.S. Pat; 4,535,901, 1985;
- 38 Takashima, M.; Yamamoto, K.; Shimazaki, H.; Maruyama, K. Mitsubishi Gas Chemical Co., Ltd., Japan. JP11,246,686, Jpn. Kokai Tokio Koho, 1999;
- 39 Rajagopalan, P.; Kim, J. S.; Brack, H. P.; Lu, X.; Eisenberg, A.; Weiss, R. A.; Risen, W. M., Jr. *J Polym Sci Polym Phys Ed* 1995, 33, 495–503;
- 40 Bell, E. T.; Bradley, J. R.; Long, T. E.; Stafford, S. L. Pat. 6,239,233, 2001;
- 41 Maruhashi, Y.; Iida, S. *Polym Eng Sci* 2001, 41, 1987–1996;
- 42 Samperi, F.; Battiato, S. 2010, in preparation;
- 43 Montaudo, G.; Montaudo, M. S.; Samperi, F. In *Mass Spectrometry of Polymers*; Montaudo, G.; Lattimer, R. P., Eds.; CRC Press: Boca Raton, 2002; Chapters 2 and 10;
- 44 Montaudo, G.; Montaudo, M. S.; Samperi, F. *Rev Prog Polym Sci* 2006, 31, 277–357;
- 45 Pasch, H.; Schrepp, W. *MALDI-TOF Mass Spectrometry of Synthetic Polymers*; Springer-Verlag: Berlin, 2003; p 298;
- 46 Singletary, N.; Bates, R. B.; Jacobsen, N.; Lee, A. K.; Guangxin, L.; Somogyi, A.; Streeter, M. J.; Hall, H. K., Jr. *Macromolecules* 2009, 42, 2336–2343;
- 47 Puglisi, C.; Samperi, F.; Di Giorgi, S.; Montaudo, G. *Polym Deg Stab* 2002, 78, 369–378;
- 48 Yamadera, R.; Murano, M. *J Polym Sci A* 1966, 5, 2259–2268;
- 49 Montaudo, M. S. *J Am Soc Mass Spectrom* 2004, 15, 37.

**PART (II)**

**REACTIVE MELT MIXING OF PC-PEN BLENDS:**  
**STRUCTURAL CHARACTERIZATION OF REACTION**  
**PRODUCTS**

## 4.1 – Introduction

Polyesters are a major class of polymers that have been extensively studied in Reactive Blending. In particular, most of the scientific and industrial interest has been focused on the binary blends based on the polyester polyethylene terephthalate (PET). In fact, although the PET is nowadays one of the versatile polymers used for production of gas barrier and clear packages, however in some cases, such as demand of high barrier levels to gases or improved mechanical properties, and dimensional stability at elevated temperatures cannot be reached by it. A possible route to develop new materials with improved barrier properties involves melt blending of PET with thermoplastics polymer like poly(*m*-xylene adipamide) (MXD6) or poly(ethylene-2,6-naphthalate) (PEN). The polyamide MXD6 and the polyester PEN are very expensive polymer materials that exhibits excellent gas barrier properties to O<sub>2</sub> and CO<sub>2</sub>. The PET-MXD6 system has previous studied in the first year of this PhD course with aim to elucidate the nature and kinetics of the ester/amide interchange reactions between PET and MXD6<sup>5</sup>. On the other hand numerous studies have also been devoted to blends of PET and PEN from which one would expect to make potential packaging materials with improved thermal and barrier properties<sup>6-15</sup>. The system PET-PC represent an important example of materials based to PET that exhibits improved mechanical properties. The semicrystalline PET provides chemical resistance, thermal stability and high barrier to gases, while the amorphous PC provides impact resistance, toughness, and dimensional stability at elevated temperatures<sup>1, 2, 3-4</sup>.

PEN is another important polyester that could replace to PET for packaging applications. PEN differs from PET in that the acid component of its polymer chain is naphthalene 2,6-dicarboxylic acid, replacing the terephthalic acid of PET. The two aromatic rings of PEN confer on it

improvements in strength and modulus, chemical and hydrolytic resistance, gaseous barrier, thermal and thermo-oxidative resistance and ultraviolet light resistance compared to PET. However a main limiting factor in the use of the PEN is its high cost with respect to PET. Therefore, in order to make good use of PEN's excellent barrier properties, it is necessary to mix it with other polymers, so that new materials with an adequate properties/price relationship can be obtained. Poly(bisphenolA carbonate) (PC) represents an attractive candidate for blending with PEN in order to produce materials with applications in packaging of foods and electronic devices. PC is an amorphous polymer with attractive engineering properties, including high impact strength, low moisture absorption, low combustibility, good dimensional stability, and high light transmittance (88%). However, despite the evident scientific and industrial interest in PC-PEN blends, the literature reports fewer studies dealing with melt blending of PC with PEN, such as Maiza<sup>16</sup> and Kallitsis<sup>17</sup>, in which are not fully elucidated either the nature and kinetics of the reaction occurring between PC and PEN and the composition of the melt mixed materials. The miscibility of these polyester/polycarbonate blends, near and above the melting point of PEN (about 270 °C) is increased through exchange reactions, involving the formation of block copolymer units that lead to compatibilization of this system.

Maiza<sup>16</sup> and coworkers present evidence of the existence of interchange reactions in the system PC-PEN free catalyst, as determined by solubility measurements, FTIR and <sup>1</sup>H-NMR spectroscopy, as well as Differential Scanning Calorimetry (DSC). However, as reported by the same authors, it is necessary to model compounds in order to establish an accurate elucidation of all new structures resulting from the exchange reactions ester/carbonate.

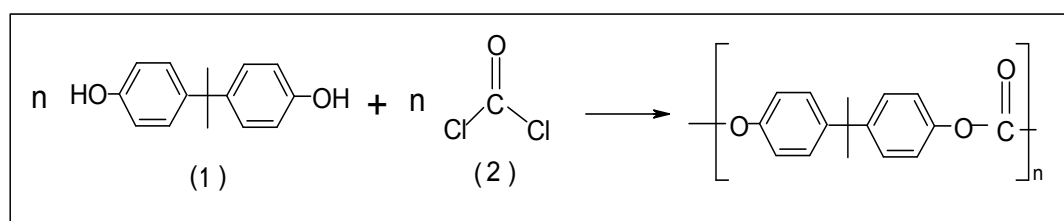
Kallitsis<sup>17</sup> and coworkers have studied the Melt Blending of the system PC-PEN free catalyst, at 290 °C, under a blanket of argon, and at

various composition of initial feed. All the blends prepared exhibited a biphasic character (SEM and DSC) and has very good mechanical properties (tensile tests and DMA), in some cases, even better than those of the respective pure constituents. This behavior was attributed to a copolymer formation in the mesophase, which effectively compatibilizes the system. The formation of a PC-PEN block copolymer was considered to be due to transesterification reactions between PC and PEN and was verified by extractions experiments and examination of the soluble and insoluble fractions in chloroform by various spectroscopic techniques (FTIR, FT-Raman, and  $^1\text{H-NMR}$ ).

In the second and third year of PhD work has been investigated the reactive blending of equimolar mixture of PC-PEN blends in presence of 0,1% (w/w) of  $\text{Ti}(\text{ButO})_4$ , under nitrogen flow, and for different mixing times. The aim of these studies was focused on the characterization of the microstructure and kinetic mechanisms of interchange reactions ester/carbonate occurring between initial homopolymers (PC and PEN), and on the chemical composition of the melt mixed materials. The characterization by  $^1\text{H}$  and  $^{13}\text{C}$  NMR was crucial both for determining the structure and composition of PC-PEN copolymers produced at different mixing times and also for the identification of reactions that produce these materials. This system behaves similarly to other systems polycarbonate/polyester, such as PC-PBT and PC-PET, already extensively studied and characterized<sup>1, 18, 19</sup>. Until now, fewer investigations have performed to elucidate the nature and kinetics of the ester interchange reaction between PC and PEN<sup>16, 17</sup>.

## 4.2 – Poly(bisphenolA carbonate) - PC

There are several types of aromatic and aliphatic polycarbonates; and the polycarbonate of 2,2-bis-(4 - hydroxyphenyl) propane, commonly known as polycarbonate bisphenolA (PC), it is the most commercially important. The synthesis of this polymer is shown in Scheme 4.1.



**Scheme 4.1.** Formation reaction of polycarbonate (PC) 1) bisphenolA, 2) phosgene.

PC is amorphous materials that has a glass transition ( $T_g$ ) between 145-155 °C depending on molecular weight. This so high  $T_g$  value depends on the structure bulky and from preventing the movement of various segments of the molecules. These characteristics together transparency, excellent toughness, thermal stability, a very good dimensional stability, and low moisture absorption make PC one of the most widely used engineering thermoplastics<sup>16, 17</sup>.

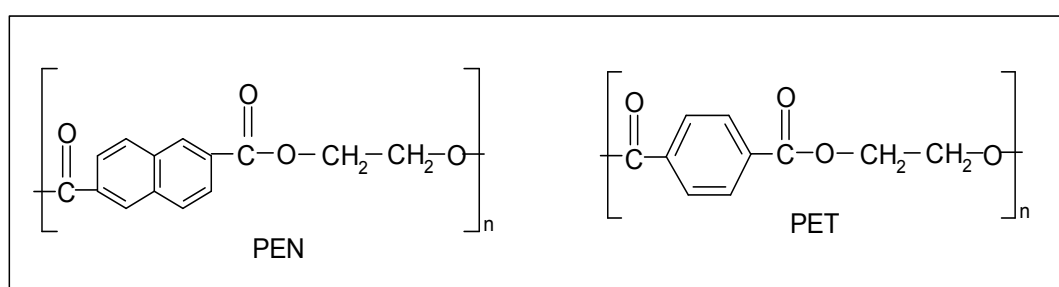
Constraints to the use of polycarbonate include limited chemical (solvents like Tetrahydrofuran and Chloroform) and scratch resistance and it's tendency to yellow upon long term exposure to UV light. However these constraints can be readily overcome by adding the right additives to the compound or processing through a co-extrusion process.

Typical PC and PC-blend applications include: compact disc (CD and DVD), riot shield, vandal proof glazing, electrical components, automobiles components, safety helmets, lenses and headlamp lenses, medical devices, sports safety equipment, baby feeding bottles, and food storage containers.

In recent years PC-blends have become increasingly commercially important. Typical blends include PC-ABS (PC plus acrylonitrile-butadiene-styrene), PC-PBT and PC-PET. The first one blends exhibit high melt flow, very high toughness at low temperature and improved stresscrack resistance compared to PC homopolymer. Blends between PC with PBT combine the impact-toughness, dimensional stability and heat resistance of PC with chemical resistance and high melt flow typical of aromatic polyesters. PC-PET blends are preferred when improving of chemical resistance and dimensional stability respect to PC-PBT are required.

### 4.3 – Poly(ethylene naphthalate) - PEN

The poly(ethylene naphthalate) (PEN) is the molecular evolution of poly(ethylene terephthalate) (PET), aimed at resolving the limits of the properties and applications of PET. As is known, the low  $T_g$ , which prevents the sterilization, and too high permeability, which prevents applications such as bottles for beer, are the main limits recognized for PET. Scheme 4.2, shows the repeat units of PET and PEN with the respective values of  $T_g$  and  $T_m$ .



**Scheme 4.2.** Chemical structures of PEN and PET.

The two polymers are similar chemical structure and either are semi-crystalline materials (PEN:  $T_g = 120\text{ }^\circ\text{C}$ ,  $T_m = 262\text{ }^\circ\text{C}$  and PET:-  $T_g = 75\text{ }^\circ\text{C}$ ,  $T_m = 265\text{ }^\circ\text{C}$ )<sup>20</sup>. The naphthalate group gives to PEN good rigidity (more higher  $T_g$  to PET) and then better thermal and mechanical properties, chemical resistance and barrier properties respect to PET. Barrier properties of PEN are five times better than PET. These characteristics make PEN particularly suitable for applications in food packaging<sup>21-27</sup>.

One factor limiting the use of highly PEN such as large scale is its high cost. This has necessitated its blending with other polymers in order to synthesize new materials with better value for money<sup>16</sup>. This objective has been achieved also prepare new copolymers with other co-monomers such as ethylene terephthalate (PET). The PET-PEN copolymers with molar compositions between 8 and 20% (w/w) in PEN found widespread



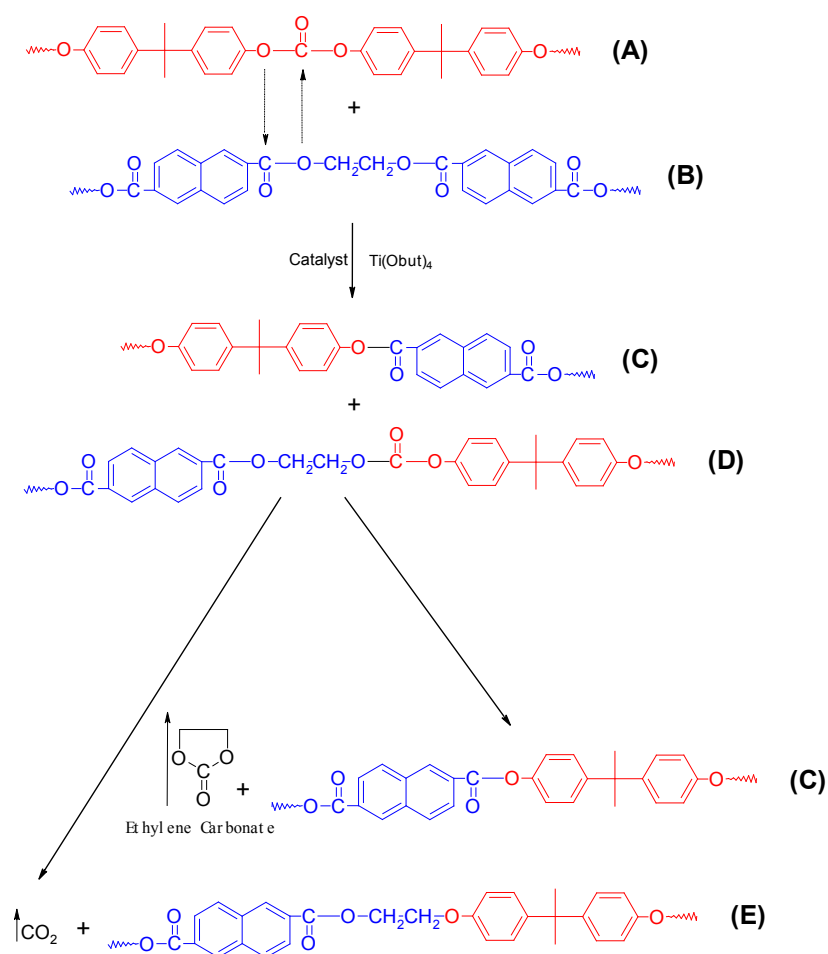
use in the fields of food packaging, for the best gas barrier properties than PET, which is widely used for storage and transport of liquids: H<sub>2</sub>O and fizzy drinks. For this reason the PET-PEN blends is the one most studied among polymer blends based of PEN in the last decade, while there are still few studies on PC-PEN<sup>16,17</sup>.

#### **4.4 – Reactive blending procedure**

The starting homopolymers (both in pellet form) were dried for 48 hours in a vacuum system at 120 °C before their use. Typically, 50 g of equimolar mixture (with respect to the repeat unit) of PC and PEN were melt mixed with Ti(OBut)<sub>4</sub> as trans-esterification catalyst, for different times (2, 5, 8, 10, 15, 20, 30, 45, and 60 min) at 280 °C under nitrogen flow. The catalyst (0,2%w) was added after one min of mixing and this was considered as time zero. The melt-mixing were performed in a twin-screw mixer 330 AEV Brabender using a rotor speed of 20 rpm.

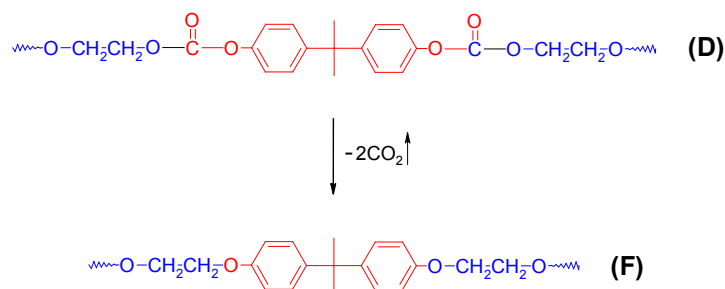
## 4.5 – Synthesis of polymer models

Previous studies on PC-PET blends shown that during the processing in the molten state (280-300 °C) occur elimination reactions of molecules of CO<sub>2</sub> and Ethylene Carbonate (EtC) involving rearrangement of repeat units of the polymer with formation of new structural units cannot be predicted from the stoichiometry of typical of direct exchange reactions ester-carbonate<sup>9</sup>. Since PEN has a similar structure at the PET is a predictable a similar reaction mechanism and hence the formation of four other possible structural units beyond those of the initial homopolymers PC and PEN, respectively **A** and **B** units. Two sequences, **C** and **D** are produced by catalyzed transesterification reactions (Scheme 4.3).



**Scheme 4.3.** Catalyzed Exchange Reactions and consecutive elimination of CO<sub>2</sub> and ethylene carbonate (EtC) in the Melt Mixing of PC with PEN at 280 °C.

Other two structural units, **E** and **F**, are obtained by elimination of CO<sub>2</sub> (Schemes 4.3 and 4.4).



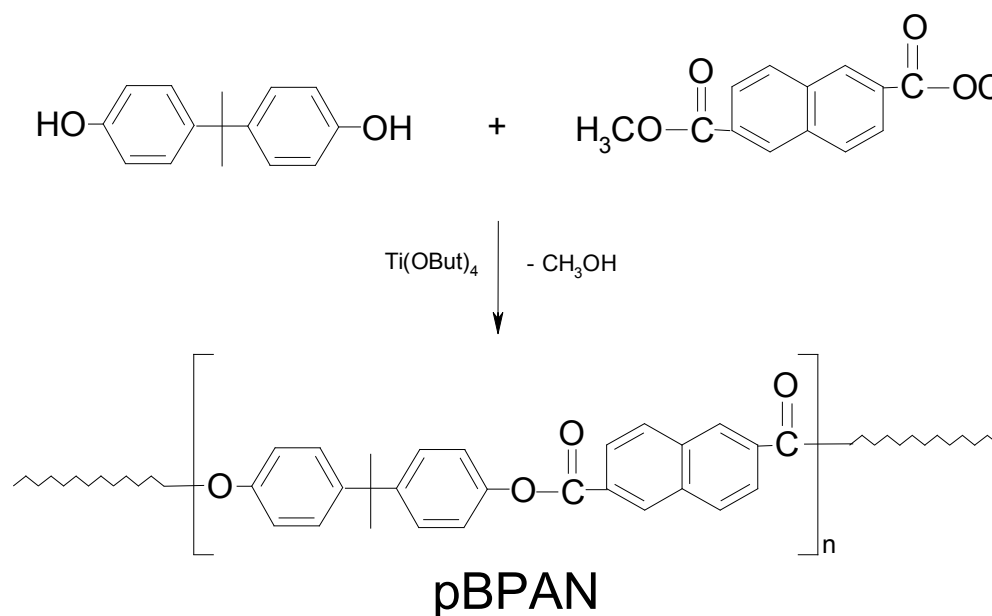
**Scheme 4.4.** Formation of diethoxy-bisphenolA sequences (**F**).

For this reason it was synthesized and characterized four polymer models with equal structures at predicted units **C**, **D**, **E** and **F**.

Predicted Structural Units	Corresponding Polymer Models synthesized	Symbol
<b>C</b>	poly(bisphenolA naphthalate) $* \left[ \text{C}_6\text{H}_4\text{-C(CH}_3\text{)}_2\text{-C}_6\text{H}_4\text{-O-C(=O)-C}_6\text{H}_4\text{-C(=O)-O} \right]_n *$	<b>pBPAN</b>
<b>D</b>	copoly(bisphenolA carbonate)-alt-(ethylene carbonate) $* \left[ \text{O-C}_6\text{H}_4\text{-C(CH}_3\text{)}_2\text{-C}_6\text{H}_4\text{-O-C(=O)-O-CH}_2\text{CH}_2\text{O-C(=O)-O} \right]_n *$	<b>p(BPAC)-alt-(EtC)</b>
<b>E-co-F</b>	poly(ethoxy-bisphenolA naphthalate)-co-(diethoxy-bisphenolA naphthalate) $* \left[ \text{C}_6\text{H}_4\text{-C(CH}_3\text{)}_2\text{-C}_6\text{H}_4\text{-O-C(=O)-O-CH}_2\text{CH}_2\text{O-C}_6\text{H}_4\text{-C(CH}_3\text{)}_2\text{-C}_6\text{H}_4\text{-O-C(=O)-O-CH}_2\text{CH}_2\text{O-C}_6\text{H}_4\text{-C(CH}_3\text{)}_2\text{-C}_6\text{H}_4\text{-O-C(=O)-O-CH}_2\text{CH}_2\text{O} \right]_{j_0} *$	<b>p(BPAEtN)-co-(EtBPAEtN)</b>
<b>F</b>	poly(diethoxy-bisphenolA naphthalate) $* \left[ \text{C}_6\text{H}_4\text{-C(CH}_3\text{)}_2\text{-C}_6\text{H}_4\text{-O-CH}_2\text{CH}_2\text{O-C}_6\text{H}_4\text{-C(CH}_3\text{)}_2\text{-C}_6\text{H}_4\text{-O-CH}_2\text{CH}_2\text{O} \right]_n *$	<b>pEtBPAEtN</b>

## 4.6 – Synthesis of poly(bisphenolA-naphthalate)

Poly(bisphenolA-naphthalate) was synthesized by polycondensation starting by dimethyl-naphthalate (DMT) and bisphenolA (BPA) in presence of  $\text{Ti}(\text{OBut})_4$  (0,2%w) as esterification catalyst (Scheme 4.5).



**Scheme 4.5.** Synthesis reactions of poly(bisphenolA-naphthalate).

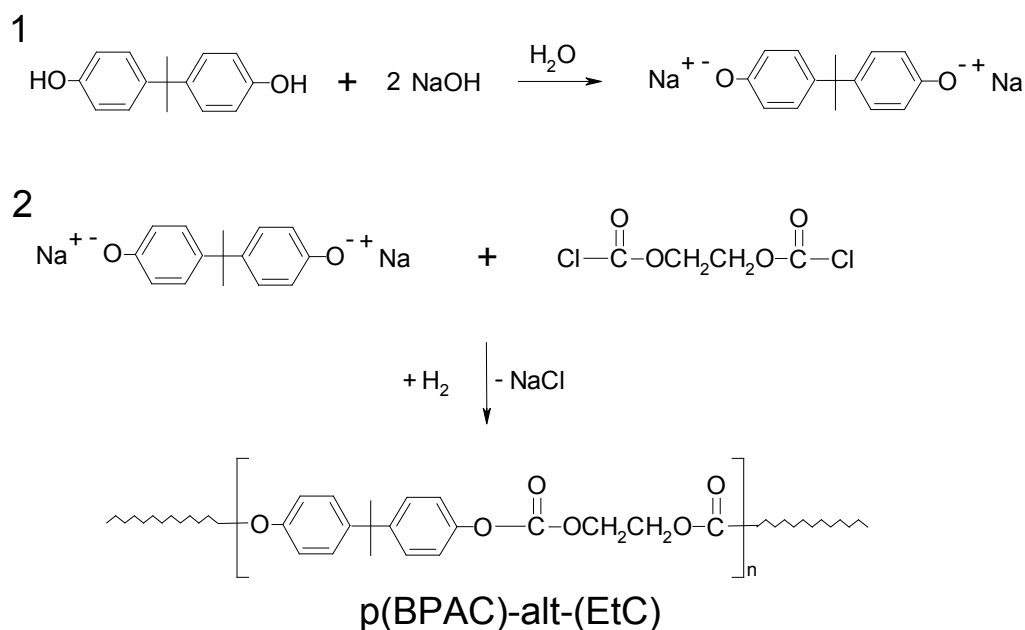
The reaction temperature was chosen on the basis of melting temperatures of individual monomers ( $T_{\text{m}(\text{BPA})} = 131 \text{ }^\circ\text{C}$ ,  $T_{\text{m}(\text{DMT})} = 187 \text{ }^\circ\text{C}$ ). Therefore, the reaction was conducted in three stages: the first one at  $190\text{-}200 \text{ }^\circ\text{C}$  for 3 hours under  $\text{N}_2$  flow; in the second and third step at  $240 \text{ }^\circ\text{C}$  and  $270 \text{ }^\circ\text{C}$ , respectively, for 1 h under vacuum (1-2 mm Hg).

The synthesis was carried out by reacting 0.041 mol (10.00 g) DMT with 0.045 mol (28.10 g) of BPA in the presence of 20 mg of  $\text{Ti}(\text{OBut})_4$  (0.2% by weight compared to BPA). The final product obtained was dissolved in  $\text{CHCl}_3$ , precipitated in a large excess of acetone, filtered and washed with acetone and finally dried in vacuum oven at  $60 \text{ }^\circ\text{C}$  for 24 hours, obtaining 32.35 g (yield 92%).

P(BPA-N) was characterized by NMR spectroscopy, MALDI-TOF mass spectrometry (MALDI), FTIR spectroscopy, Differential Scanning Calorimetry (DSC), Thermogravimetry (TGA) and viscosity.

## 4.7 – Synthesis of copoly(bisphenolA carbonate)-alt-(ethylene-carbonate)

Copoly(bisphenolA carbonate)-alt-(ethylene carbonate) - p(BPAC)-alt-(EtC) was synthesized by an interfacial polymerization process of Ethylene-bis-chloroformate (EBCF) and bisphenolA (BPA) in the presence of tricapril methylammonium chloride ("Aliquat 336") as phase transfer agent (Scheme 4.6).



**Scheme 4.6.** Synthesis reactions of copoly(bisphenolA carbonate)-alt (ethylene-carbonate).

The two monomers, EBCF and BPA, were respectively dissolved in CH<sub>2</sub>Cl<sub>2</sub> and H<sub>2</sub>O (both at 10% w). In addition, in the aqueous solution containing BPA was dissolved NaOH in 2:1 molar ratio compared to monomer (the yellowish of the solution indicate the formation of phenate). At this point the aqueous solution was poured into a mixer pre-cooled in the freezer (0 °C) to which the organic solution was added quickly under vigorous agitation. After leaving the system to react for 5 minutes, the organic phase was separated from water by separating funnel and washed twice with aqueous 10% HCl and then several times with

H<sub>2</sub>O until neutral. At this point the organic solution was treated with anhydrous Na<sub>2</sub>SO<sub>4</sub> and then precipitate into a large excess of C<sub>2</sub>H<sub>5</sub>OH (10 times), resulting in copoly(bisphenolA carbonate)-alt-(ethylene-carbonate) as a white precipitate.

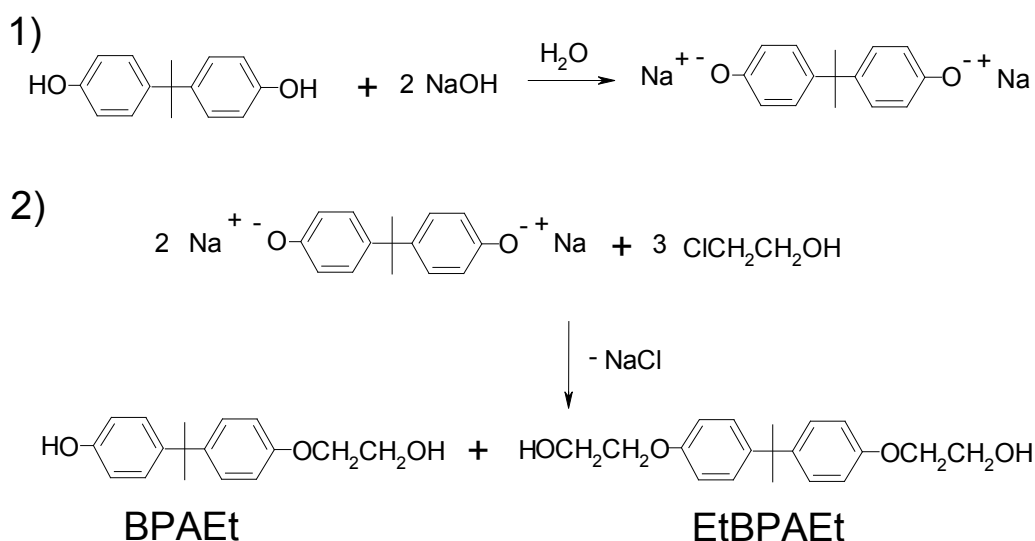
Then the product was dried in vacuum oven at 60 °C for 24 hours (2.64 g with a yield of 90%) and characterized.



## 4.8 – Synthesis of poly(ethoxy-bisphenolA naphthalate)-co-(diethoxy-bisphenolA naphthalate)

The initial step of the synthesis of the poly(ethoxy-bisphenolA naphthalate)-co-(diethoxy-bisphenolA naphthalate) - p(BPAEtN)-co-(EtBPAEtN) copolymer implies as initial step the preparation of aliphatic mixture co-monomers corresponding to *mono* and *di* aliphatic ether (Et) of bisphenolA (BPA), respectively indicated as BPAEt and EtBPAEt.

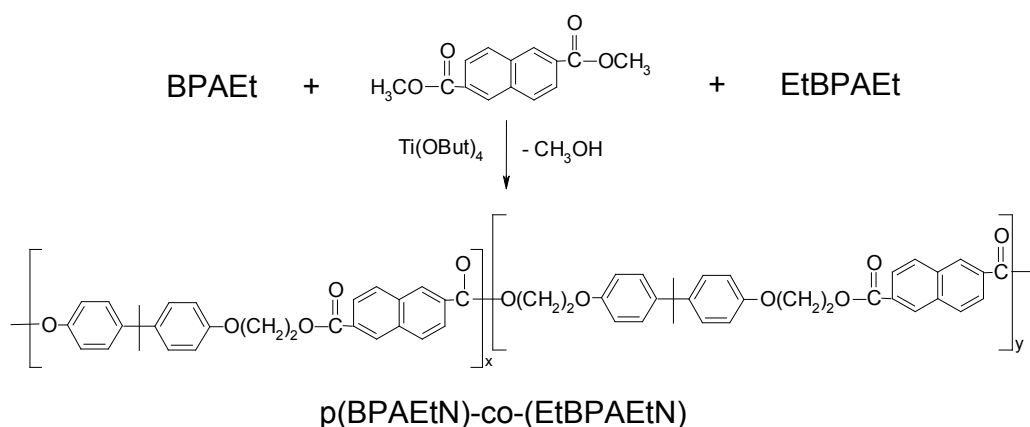
BPA in aqueous basic solution for NaOH (molar ratio 1:2) react with 2-chloro-ethanol in a molar ratio of 2:3, in a total volume of 100 ml of H<sub>2</sub>O. The general mechanism of the reaction is summarized in Scheme 4.7.



**Schema 4.7.** Synthesis reactions of BPAEt and EtBPAEt co-monomers.

The synthesis of the mixture of the two co-monomers was realized through two step: first one step at 40-50 °C for 30 min, in which the BPA is dissolved in H<sub>2</sub>O in the presence of NaOH under continuous magnetic stirring (the yellowish of the solution indicate the formation of phenate); second step with addition of 2 chloro ethanol and gradually heated up to 100 °C for 3 hours under N<sub>2</sub> flow.

At the end of reaction, the solution containing the two comonomers was distilled by rotary evaporation and treated with a mix water/acetone (50:50 – v/v), obtaining a dark precipitate. The precipitate was properly filtered and dried in vacuum oven at a temperature of 50 °C for 12 hours. By <sup>1</sup>H-NMR spectroscopy resulting a mixture of mono and diethoxy-bisphenolA with molar ratio 40:60. The mixture of comonomers (BPAEt and EtBPAEt) was used in the synthesis of the corresponding copolymer by reaction with DMT (0.00325 mol) in 1:1 ratio in moles (Scheme 8) under N<sub>2</sub> flow and in the presence of Ti(OBut)<sub>4</sub> (0.2% w )

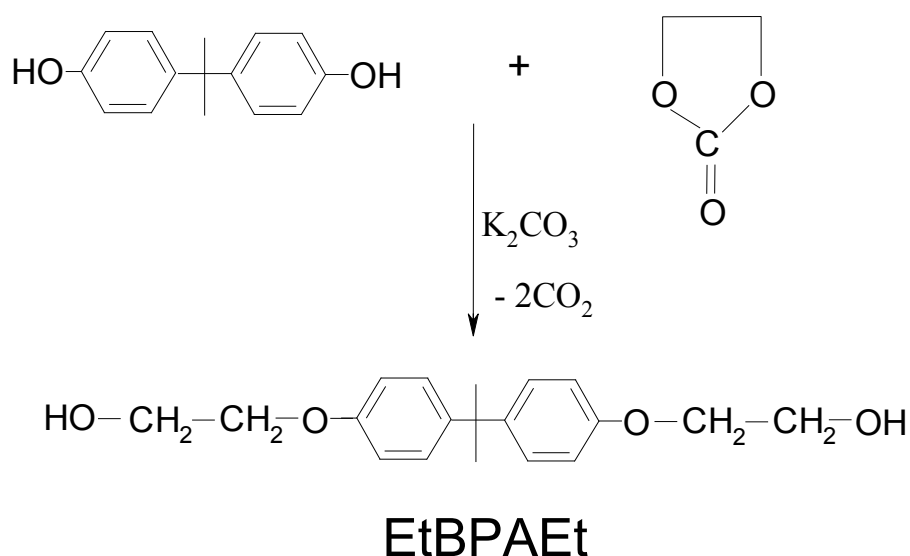


**Scheme 8.** Synthesis reaction of the poly(ethoxy-bisphenolA naphthalate)-co-(diethoxy-bisphenolA naphthalate).

The first stage of polycondensation was conducted to 160°C for 2 hours under N<sub>2</sub> flow. Following three stages of heating at different temperatures: 210 °C for 1 hours under N<sub>2</sub> flow; 250 °C for 2 hours under N<sub>2</sub> flow, and finally 260 °C for 2 hours under vacuum. The reaction product was dissolved in CHCl<sub>3</sub>, precipitated in methanol and dried in vacuum oven at 60 °C for 24 h (5.3 g with a yield of 85%).

## 4.9 – Synthesis of poly(diethoxy-bisphenolA naphthalate)

The monomers used for the synthesis of poly(diethoxy-bisphenolA naphthalate) are dimethylnaphthalate (DMT) and diethoxy-bisphenolA (EtPBAEt). EtPBAEt was synthesized by polycondensation starting BPA and ethylene carbonate (EtC) in molar ratio 1:2 at 160 °C for 12 hours in an oil bath equipped with a thermocouple to monitor temperature. The reaction was conducted in the presence of  $K_2CO_3$  (0.1 mol% of BPA) under  $N_2$  flow and magnetic stirring (Scheme 4.8).

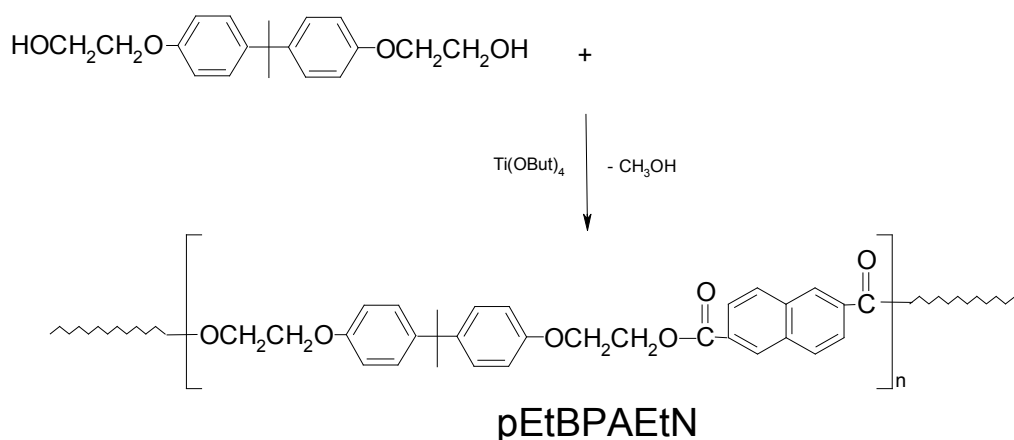


**Scheme 4.8.** Reactions synthesis of the monomers diethoxy-bisphenolA.

The reaction product was dissolved in  $CH_2Cl_2$  and subjected to two washes with 2M NaOH, and two washing with  $H_2O$  in a separating funnel. The organic phase containing the EtPBAEt, was distilled through rotary evaporation; and solid residue was crystallized in acetone and then characterized by DSC ( $T_m = 112$  °C) and  $^1H$ -NMR spectroscopy. Both analysis confirm that the EtPBAEt obtained is pure.

EtPBAEt was reacted with dimetilnaftalato (0.008 mol) in a ratio of moles of 1.2:1 (Scheme 4.9) in the presence  $Ti(OBut)_4$  as catalyst (0.5% w/w compared to EtPBAEt).

The polymerization was conducted in three stages: the first one occurs at 190-200 °C for 3 hours, the second at 230 °C are also under N<sub>2</sub> flow for 2h and finally to 27 °C under vacuum for 2h using the same system used for the synthesis of pPBAN. pEtPBAEtN thus obtained was dissolved in a mixture 80:20 v/v CHCl<sub>3</sub>/TFA and then precipitated in methanol, obtaining 7.65 g of polymer powder of amber colour (yield 87%). The polymer obtained was characterized by NMR spectroscopy, MALDI mass spectrometry, FTIR, DSC, TGA and viscosity.



**Scheme 4.9.** Synthesis reactions of poli(diethoxy-bisphenolA naphtalate).

## 4.10 – Characterization of models polymers

Homopolymers and copolymers models, previous discussed in experimental sections, it has been characterized with the same analysis techniques employed for study the materials produced by reactive melt blending of PC with PEN at 285 °C, with Ti(BuO)<sub>4</sub> (0,2% w) as catalyst, and under nitrogen flow. The reason of these procedure is obtain a complete and reliable understanding of microstructure and composition of produced materials. Following are reported the characterization data performed on PC, PEN, pPBAN, p(BPAC)-alt-(EtC), p(BPAEtN)-co-(EtBPAEtN), and pEtBPAEtN polymer models:

- <sup>1</sup>H-NMR spectroscopy (*Figure 4.1*);
- <sup>13</sup>C-NMR spectroscopy (*Figure 4.2*);
- Fourier Transform Infrared Spectroscopy - FTIR (*Figure 4.3*);
- Viscometry (*Table 4.1*);
- Differential Scanning Calorimetry - DSC (*Figure 4.4*);
- Thermogravimetric Analysis - TGA (*Table 4.1*);
- MALDI-TOF ms (*Figures 4.5a, 4.6a, 4.6b, 4.7, 4.8*).

**Table 4.1.** Thermal and viscosimetric characteristic of polymer models.

Samples	Sy	Structures	Formula repeat unit	Molecular weight repeat unit	$\eta_{inh}$	T <sub>g</sub> <sup>(a)</sup> (°C)	T <sub>c</sub> <sup>(a)</sup> (°C)	T <sub>m</sub> <sup>(a)</sup> (°C)	PDT <sup>(b)</sup> (°C)	Residue% at 800°C <sup>(b)</sup>
PC	A		C <sub>16</sub> H <sub>14</sub> O <sub>3</sub>	254,3	0,53 <sup>(d)</sup>	153	.	.	480	25,0
PEN	B		C <sub>14</sub> H <sub>10</sub> O <sub>4</sub>	242,2	0,67 <sup>(d)</sup>	125	200	267	433	28,0
pPBAN	C		C <sub>27</sub> H <sub>20</sub> O <sub>4</sub>	408,4	0,11 <sup>(c)</sup>	185	.	.	498	28,0
p(BPAC)-alt-(EtC)	D		C <sub>19</sub> H <sub>18</sub> O <sub>6</sub>	342,3	0,32 <sup>(c)</sup>	99	.	.	315 440	12,0
p(PBAEtN)-co-(EtPBAAEtN) <sup>(e)</sup>	E-co-F		C <sub>29</sub> H <sub>24</sub> O <sub>5</sub> C <sub>31</sub> H <sub>28</sub> O <sub>6</sub>	452,5 - 496,6	0,14 <sup>(d)</sup>	103	.	.	453	38,0
PEtPBAAEtN	F		C <sub>31</sub> H <sub>28</sub> O <sub>6</sub>	496,6	0,21 <sup>(d)</sup>	94	.	.	450	30,0

a) by DSC analysis;

b) by TGA analysis;

c) in THF solvent;

d) in phenol/tetrachloroethane 60/40 w/w

e) T<sub>g</sub> = 113,4 °C (calculated by FOX Equation) for homopolymers p(EtPBAAEtN) corresponding to the only sequence E.

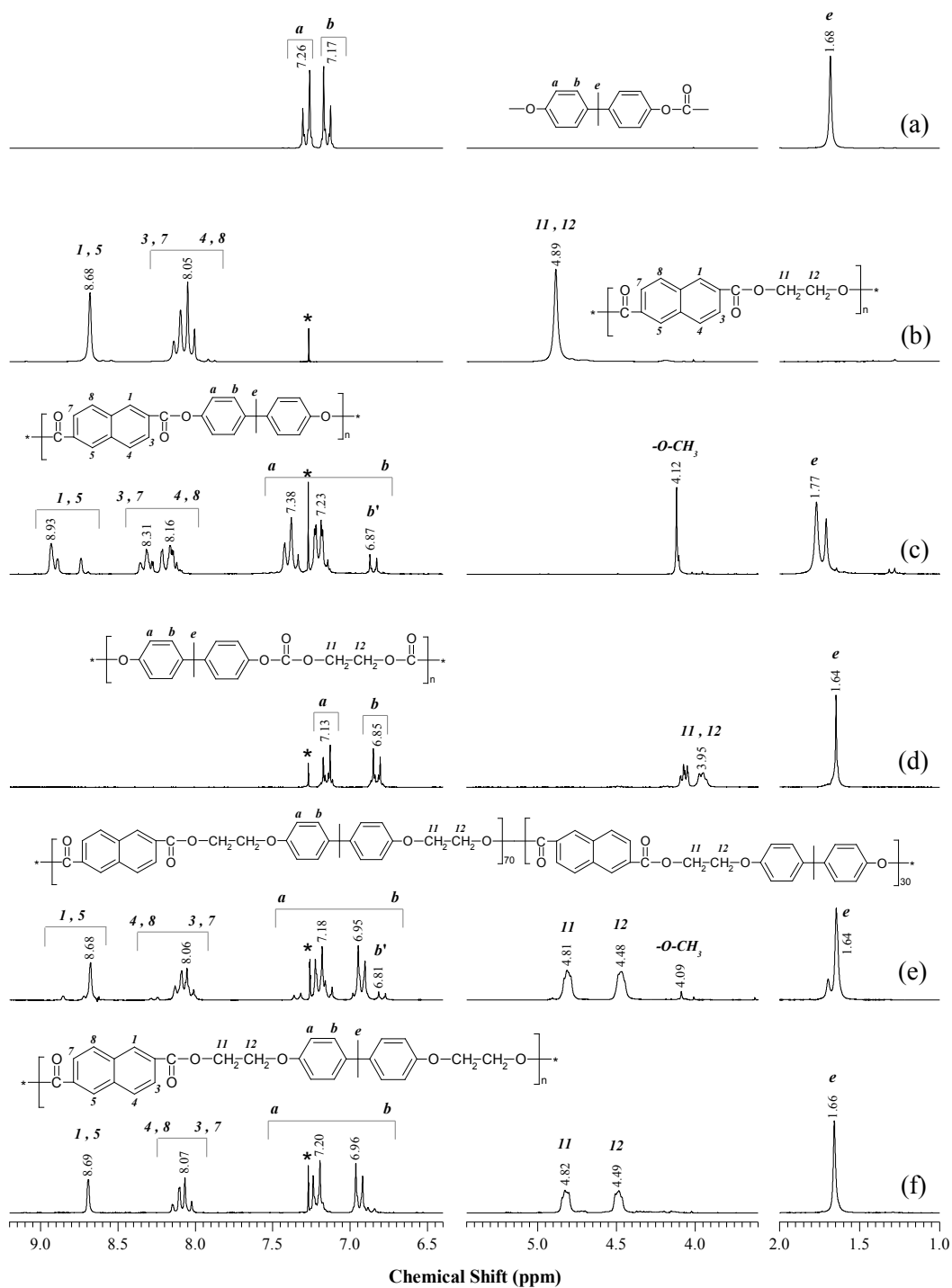


**Figure 4.1.**  $^1\text{H}$  NMR spectra of polymer models: (a) PC, (b) PEN, (c) pBAN, (d) p(BPAC)-alt-(EtC), (e) p(BPAEtN)-co-(EtBPAEtN), and (f) pEtBPAEtN.

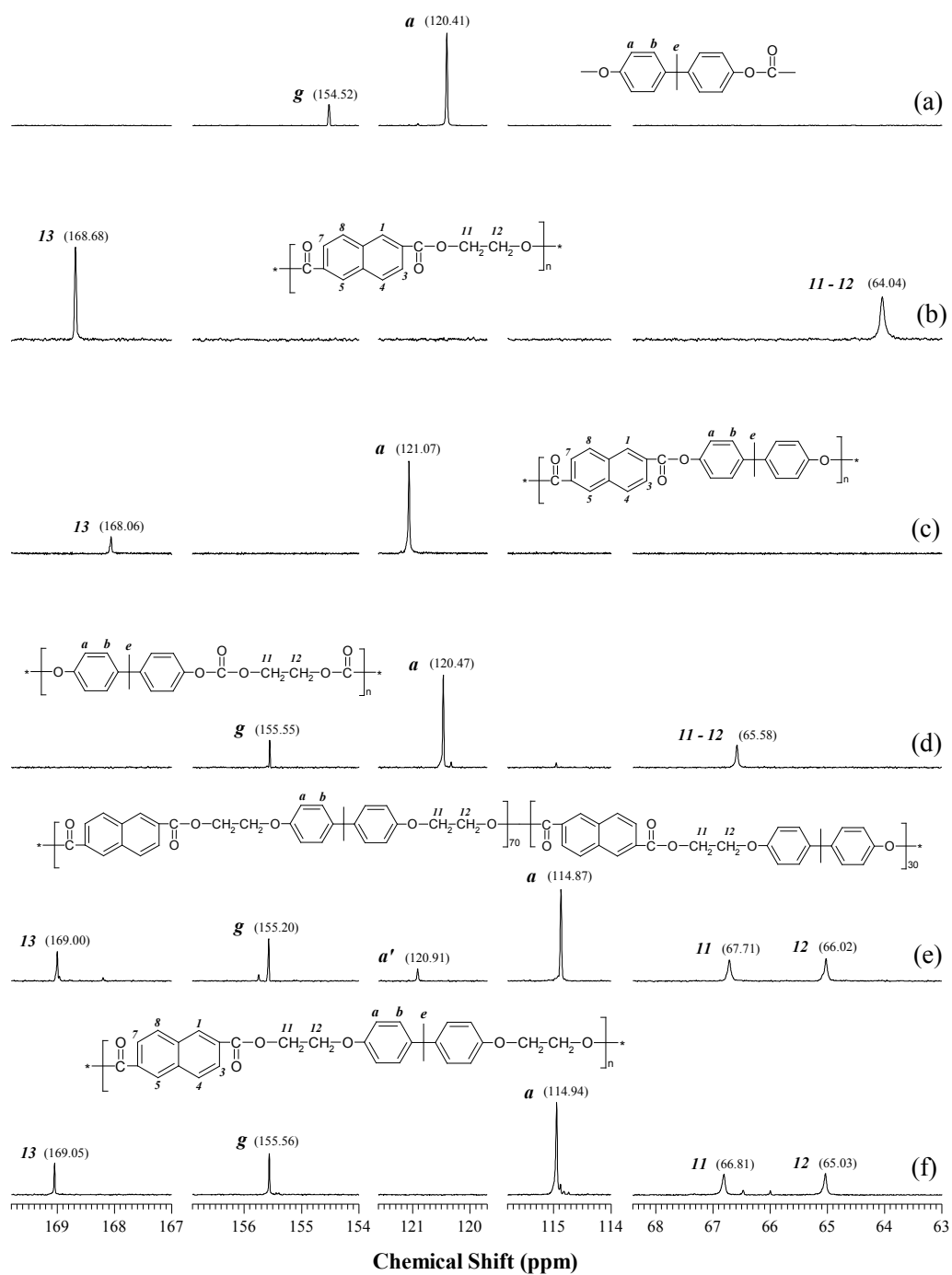


**Figure 4.2.**  $^{13}\text{C}$ -NMR spectra of model polymers: (a) PC, (b) PEN, (c) pBAN, (d) p(BPAC)-alt-(EtC), (e) p(BPAEtN)-co-(EtBPAEtN), and (f) pEtBPAEtN.



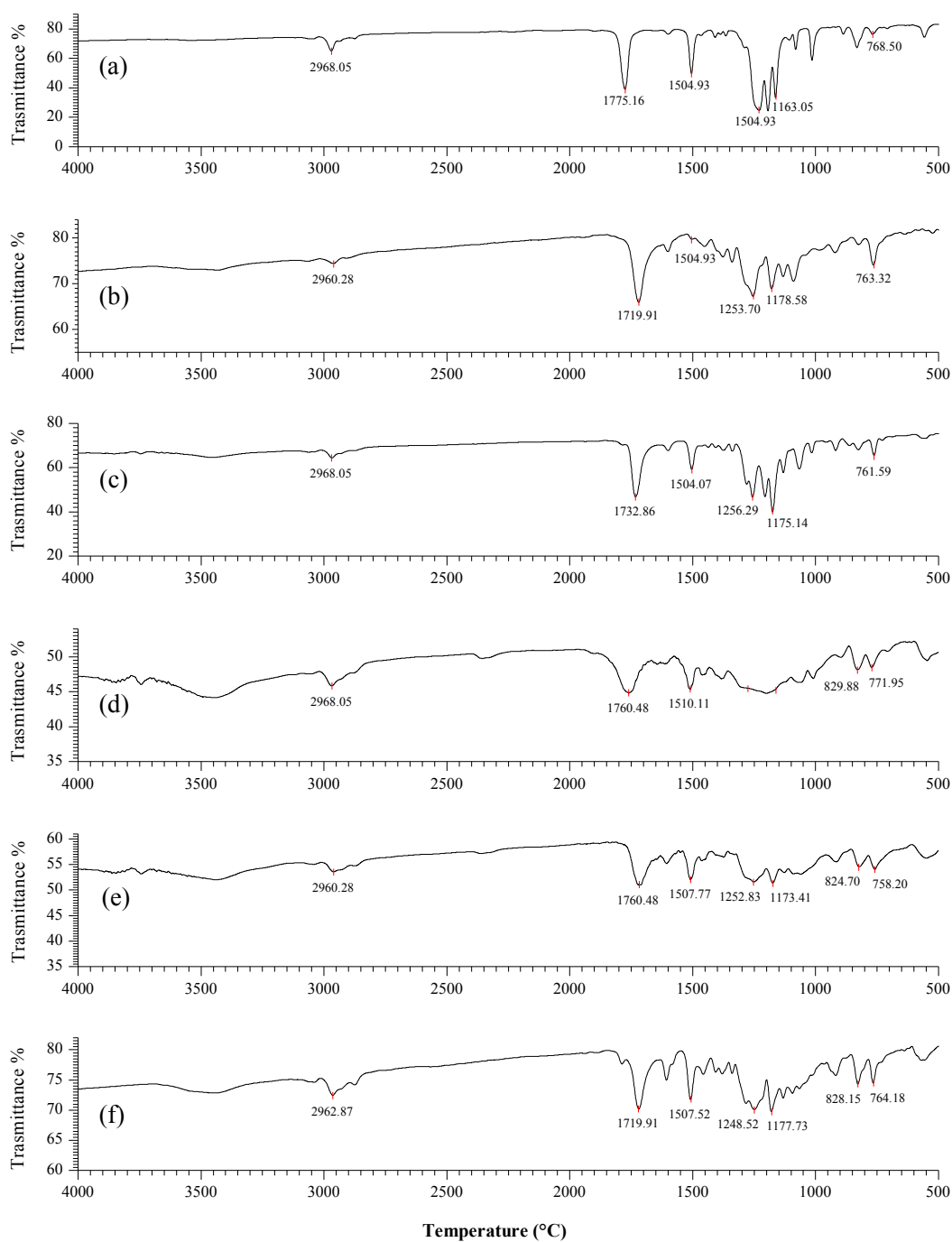


**Figure 4.3.** FTIR Spectra of model polymers (a) PC, (b) PEN, (c) pBAN, (d) p(BPAC)-alt-(EtC), (e) p(BPAEtN)-co-(EtBPAEtN), and (f) pEtBPAEtN.

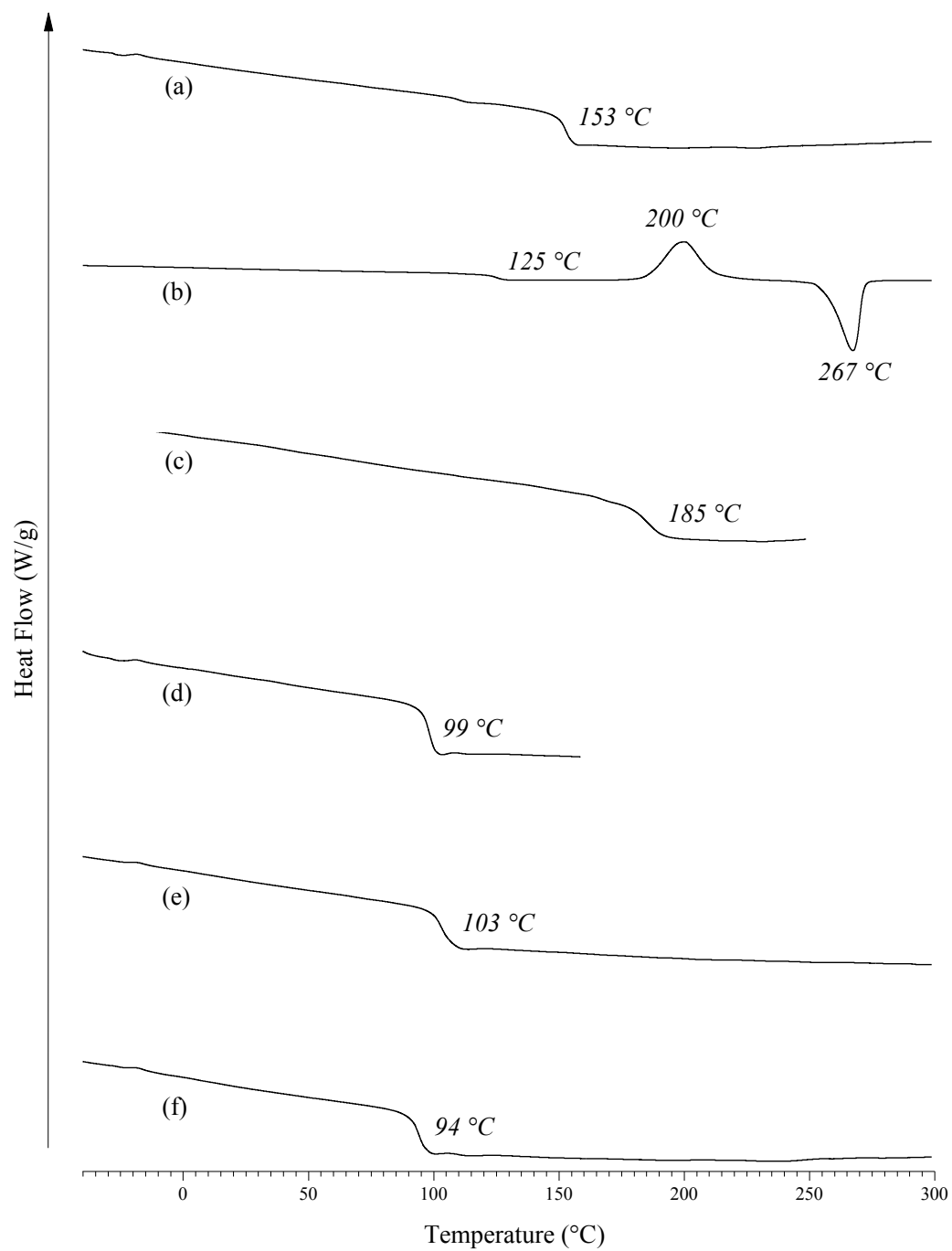
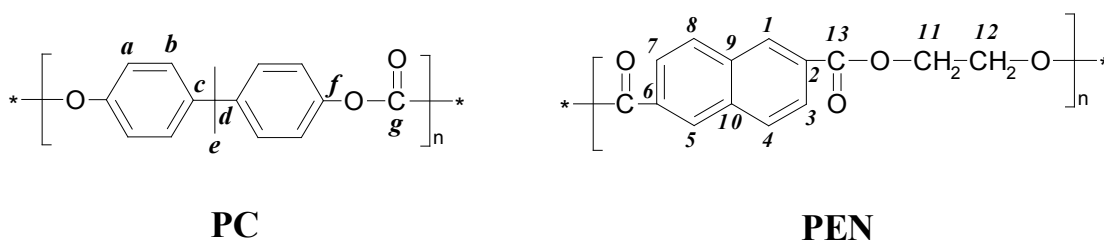


**Figure 4.4.** DSC thermograms of model polymers **(a)** PC, **(b)** PEN, **(c)** pBAN, **(d)** p(BPAC)-alt-(EtC), **(e)** p(BPAEtN)-co-(EtBPAEtN), and **(f)** pEtBPAEtN.

## 4.11 – Characterization of PC and PEN

The initial PC and PEN homopolymers used in reactive blending, have been characterized by MALDI and NMR tools to obtain information on their structure and composition. The calorimetric DSC and TGA data confirm the good thermal stability of PC and PEN (Table 4.1). The PC shows a higher thermal stability than to PEN. In fact it exhibits a T<sub>g</sub> of 146 °C, begin to degrade at 320 °C with a PDT of 480 °C, and at 800 °C leave 25% of carbonaceous residue. Instead, the PEN has a T<sub>g</sub> of 120 °C, a PDT of 433 °C and at 800 °C leave 28% of carbonaceous residue.

The <sup>1</sup>H NMR spectrum (Figure 4.1) of PC, recorded in CDCl<sub>3</sub>/TFA-d (80/20 – v/v), show a typical quartet AB of the aromatic protons centered at 7.17 and 7.26 ppm, and singlet signal at 1.68 ppm due to methylene protons of the isopropylidene unit of the BPA. The proton spectrum of PEN exhibits a broad singlet at 4.89 ppm given by methylene protons of diethylene glycol unit, while aromatic protons given a singlet at 8.68 ppm (protons *1,5*) and one multiplet between 8.00 and 8.15 ppm assigned to the protons *3,4,7* and *8*.

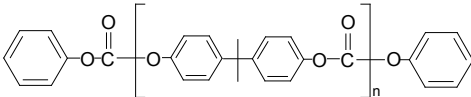
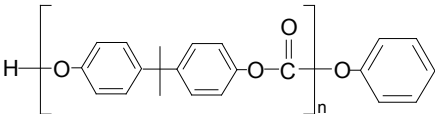
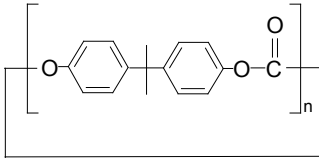


The end groups of the polymer chains PC and PEN were characterized by MALDI-TOF mass spectrometry. The role of terminal groups is important in intermolecular exchange reactions between PC and PEN in the molten state.

The MALDI-TOF mass spectrum of PC (Figure 4.5), recorded in Reflectron mode, reports the mass range from 2500 to 9000 Da and the expanded area from 5100 to 5900 Da (inset). This spectrum shows the

presence of series of mass peaks corresponding to cyclic and linear PC oligomers. In particular, the linear oligomers appear to have different end groups. The high resolution (3000 m/ $\Delta m$ ) and the calibration of the spectra allows to assign each family of peaks to the corresponding oligomers (which are revealed mainly as sodium adducts ions), whose structure is shown in Table 4.2. The most intense peak in 5100-5900 Da are belong to the linear oligomers terminated with phenyl-carbonate units on both sides (PhOCO-/-OPh) and are labeled as A; indeed they are also present in the spectrum as a series of potassium adducts (A'). The other two mass peak families are cyclic oligomers (C) and linear chains terminated with H-/-OPh groups (species B).

**Table 4.2.** m/z values of the chemical species detect on the MALDI-TOF spectrum of the PC.

Species	Structures	n	Adducts (m/z)	
			MNa <sup>+</sup>	MK <sup>+</sup>
A+A'		18	4813	4829
		19	5067	5083
		20	5321	5337
		21	5575	5591
		22	5829	5845
B		18	4693	-
		19	4947	-
		20	5201	-
		21	5455	-
		22	5709	-
C		18	4599	-
		19	4853	-
		20	5107	-
		21	5361	-
		22	5615	-

The MALDI-TOF mass spectrum of PEN is shown in Figures 4.6a and 4.6b. It is possible to observe a series of resolved mass peaks in the mass range 1200-9000 Da, whose structures are reported in Table 4.3.

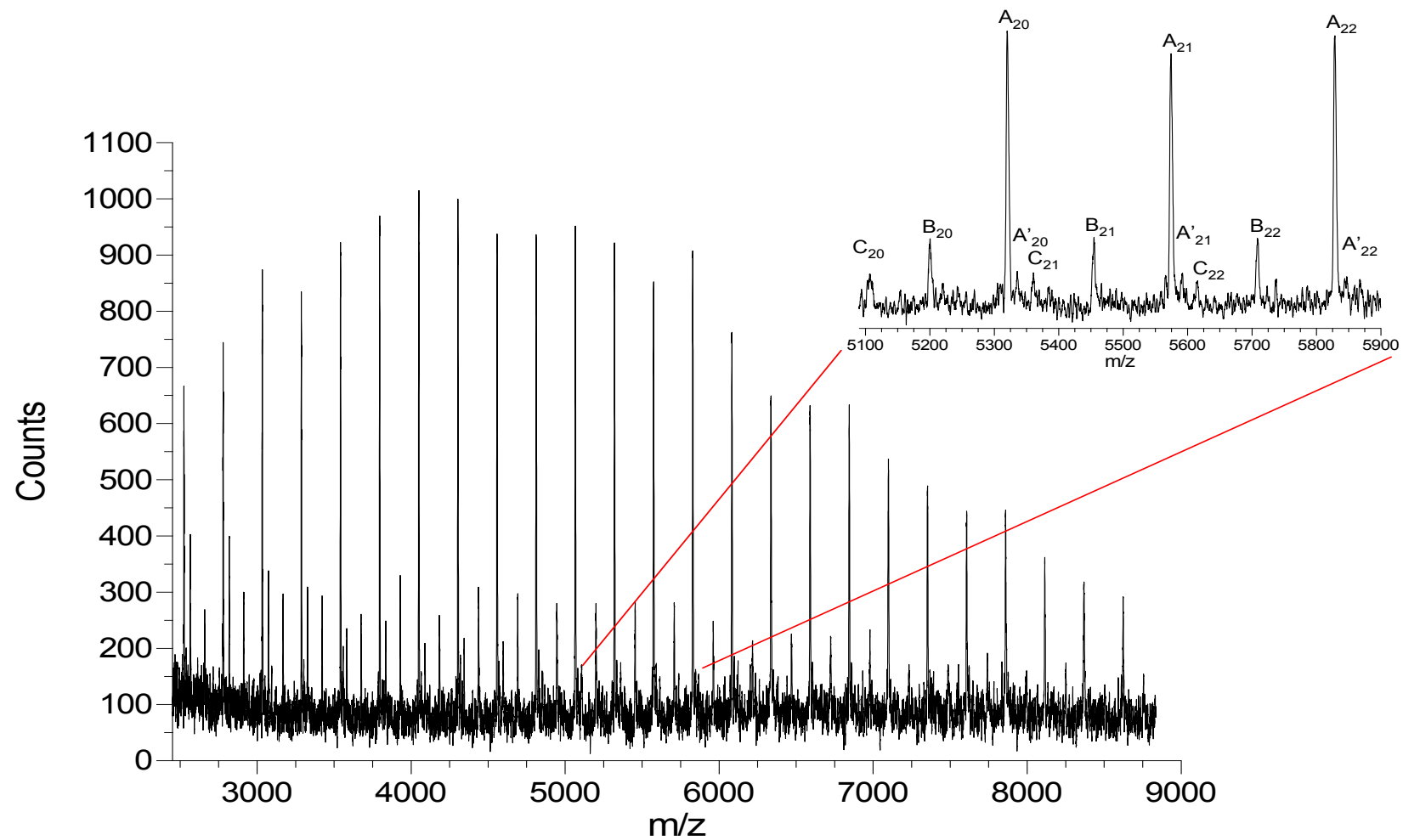


Figure 4.5. MALDI TOF spectrum (in positive mode) of the homopolymer PC.

In the mass range 1200-2200 the more intense mass peaks corresponding to the sodium adducts of oligomers (A see Table 4.3 and Figure 4.6a), while the highest mass in the range 3600-4100 Da (Figure 4.6b), prevail the oligomers terminated with carboxylic and alcohol end groups (series **B**), and those terminated with alcohol groups on both sides (series **C**). The alcohol end-groups might be involved in transesterification reactions, as observed for the systems Polyester/Polyester<sup>4</sup>.

Very intense mass peak data from sodium adducts of PEN chains terminated with carboxylic units on both sides (series **D**) are shown in the spectra in Figure 4.6a and 4.6b.

The two homopolymers PC and PEN were also analyzed by FTIR. In the FTIR spectra in Figure 4.3a and 4.3b particular interesting are the asymmetric vibrational stretching of carbonyl groups (C=O) which gives a broad band at  $1775\text{ cm}^{-1}$  and  $1719\text{ cm}^{-1}$ , respectively in PC and PEN. The other absorption bands give resonance frequencies similar to those observed for the other polymer models, and this suggests that only the spectra range in which absorb the C=O groups could provide information on the structures of copolymers formed by reactive blending of PC with PEN.

**Table 4.3.**  $m/z$  values of the chemical species detected on the MALDI-TOF spectrum of the PEN.

Species	Structures	n	Adducts ( $m/z$ ) $MNa^+$
<b>A</b>		7	1718
		8	1960
		9	2202
		10	2444
		11	2686
<b>A'</b>		7	1762
		8	2004
		9	2246
		10	2488
		11	2730
<b>B</b>		7	1736
		8	1878
		9	2220
		10	2462
		11	2704
<b>C</b>		7	1780
		8	2022
		9	2264
		10	2506
		11	2748
<b>D</b>		7	1934
		8	2176
		9	2418
		10	2660
		11	2902
<b>E</b>		7	1822
		8	2066
		9	2308
		10	2550
		11	2792



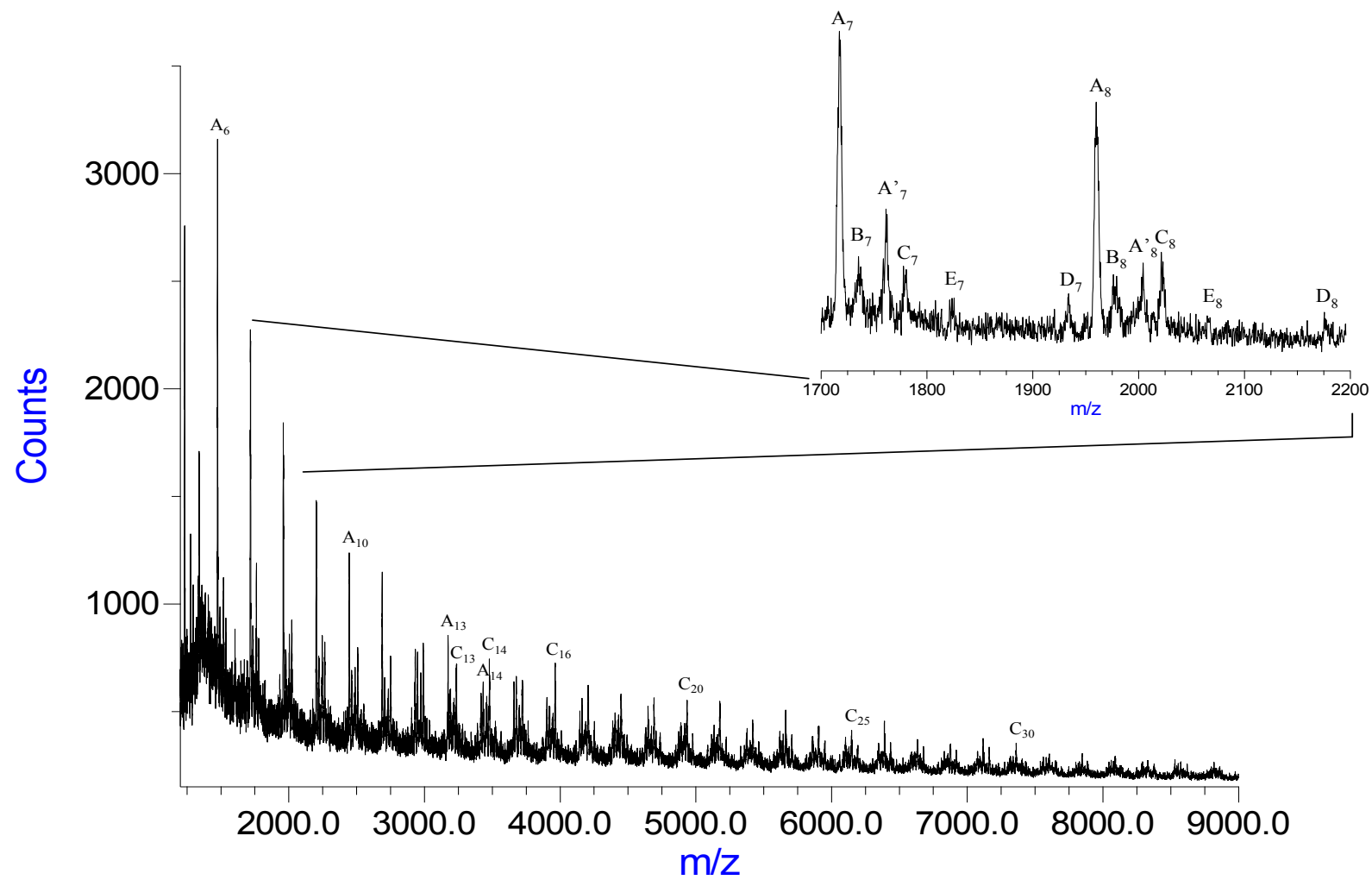


Figure 4.6a. MALDI TOF spectrum (in positive mode) of the homopolymer PEN.

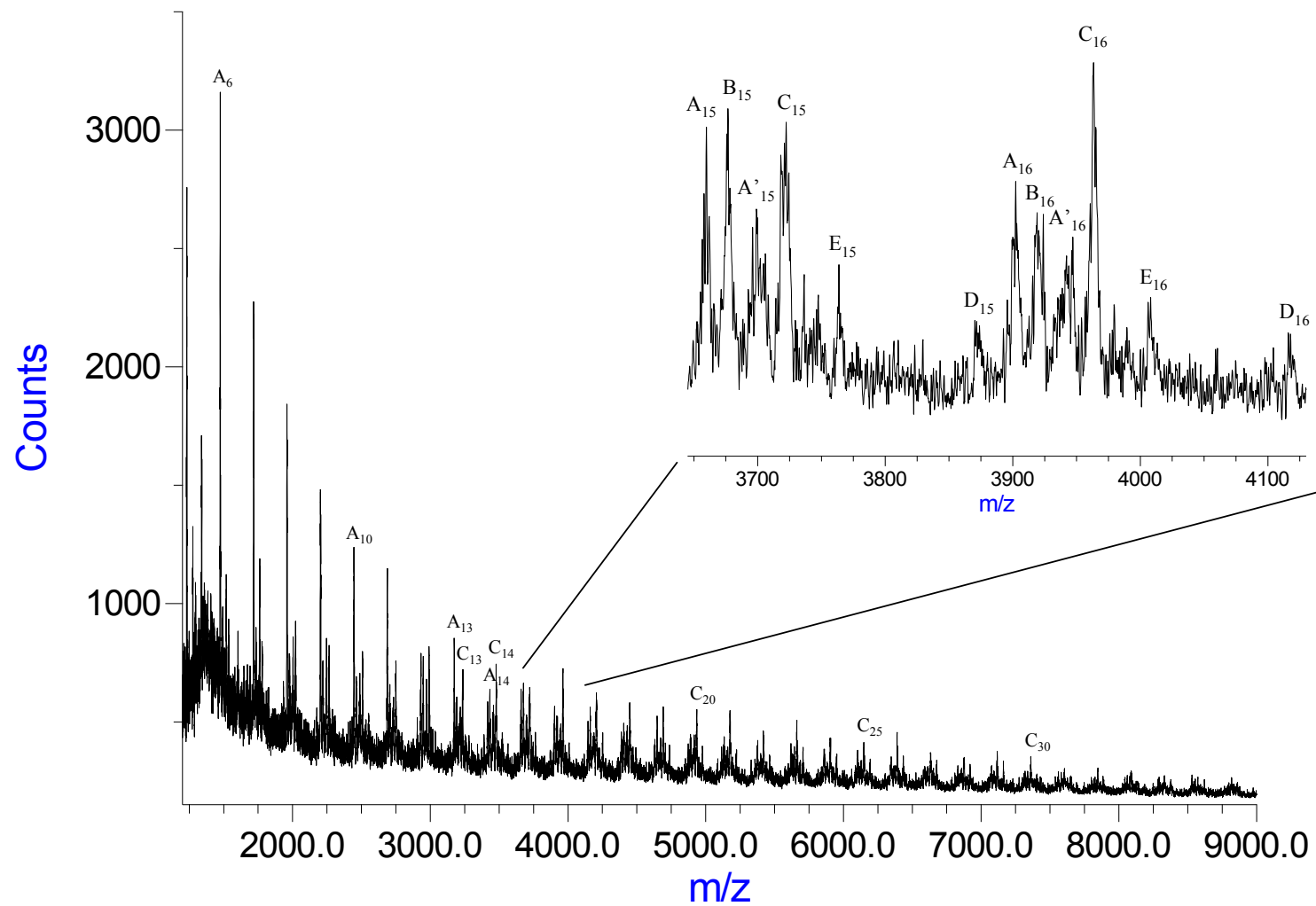
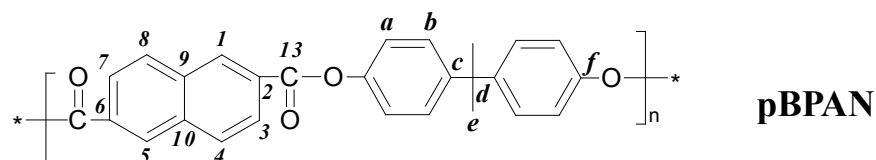


Figure 4.6b. MALDI TOF spectrum (in positive mode) of the homopolymer PEN.

## 4.12 - Characterization of poly(bisphenolA naphthalate)

The aromatic polyester poly(bisphenolA-naphthalate) - pBPAN is an amorphous polymer with high thermal stability. It presents a  $T_g = 185\text{ }^\circ\text{C}$  and a PDT of  $500\text{ }^\circ\text{C}$  (Table 4.1), it begins to degrade at  $320\text{ }^\circ\text{C}$  and at  $800\text{ }^\circ\text{C}$  leaves 28% of carbonaceous residue.



The NMR ( $^1\text{H}$  and  $^{13}\text{C}$ ) spectra show typical signals given by the BPA and naphthalate units (Figure 4.1 and 4.2). The proton spectrum with their assignments is shown in Figure 4.1c. In addition to signals corresponding to protons in the chain, the NMR spectrum reveals the presence of methyl ester terminals (singlet at 4.12 ppm of  $-\text{OCH}_3$ ) and bisphenolA end groups (doublet at 6.87 ppm **b'** of the aromatic protons in meta to the OH).

The nature of end groups was confirmed by MALDI-TOF mass spectrometry analysis. The mass spectrum of pBPAN in the region 1660-2300 Da recorded in linear mode is shown in Figure 4.7. It is possible to observe three different mass peak families (all as adducts of sodium,  $\text{MNa}^+$ ) corresponding to linear oligomers with different end groups as reported in Table 4.4, in agreement to the  $^1\text{H}$ -NMR spectrum (Figure 4.1c). The more intense mass peaks, labeled with **An**, are oligomers terminated with H-/- $\text{OCH}_3$  groups. The mass peak series **Bn**, correspond to linear chains terminated with methyl-naphthalate at both ends ( $\text{CH}_3\text{Onaphthalate-/-OCH}_3$ ). The third mass peak family correspond assigned to the linear chains ended with H-/-EtBPAEtOH groups. Table 4.4 shows the values of  $m/z$  for the families of the tetramers and pentamers as sodium adducts present in mass spectrum of pBPAN.

**Table 4.4.** Assignments of oligomers families observed in the MALDI TOF spectrum of pBPAN in the region 1660-2300 Da.

Olygomer	A Family	B Family	C Family
	H/OCH <sub>3</sub> end groups	Naftoato/OCH <sub>3</sub> end groups	H/OBPA end groups
n = 4	1688	1900	1884
n = 5	2097	2309	2293

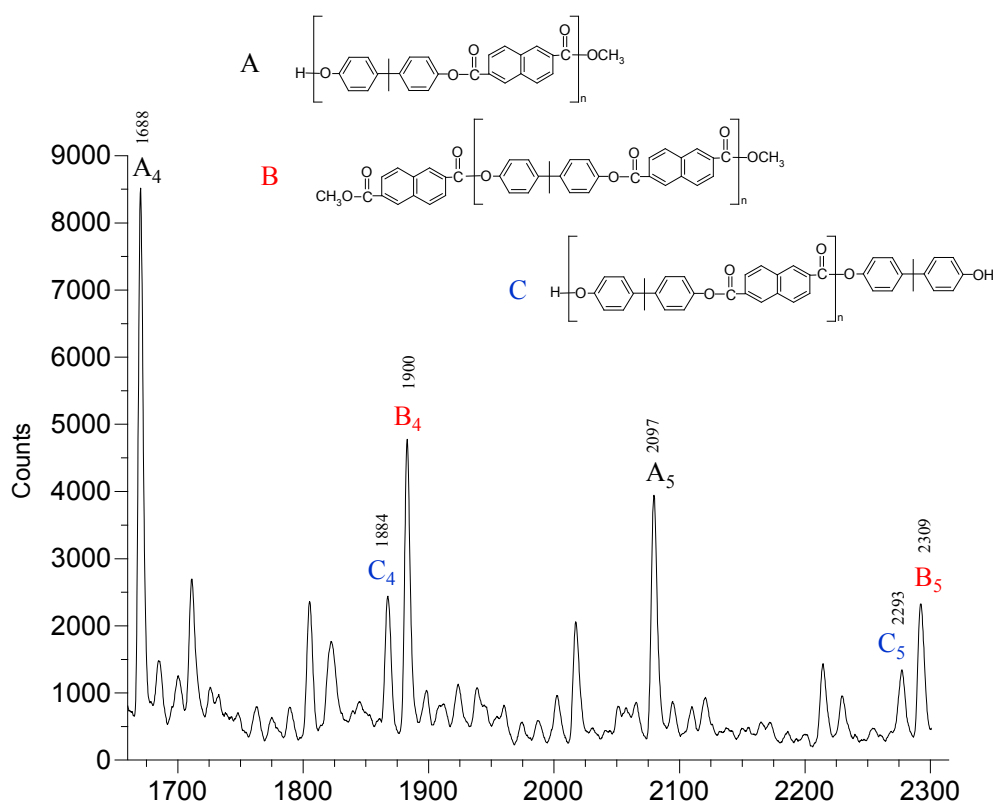


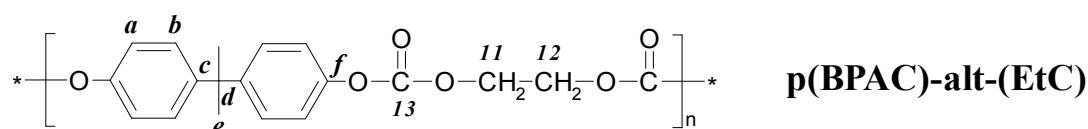
**Figure 4.7.** MALDI TOF spectrum of poly(bisphenolA-naphthalate) - pBPAN.

Further information on structure of pBPAN were obtained by FTIR spectroscopy. The corresponding FTIR spectrum in Figure 4.3c shows an intense absorption band at  $1732\text{ cm}^{-1}$  given by the asymmetric stretching vibrational motions of the carbonyl (C=O) of the BPA-Naphthalate esters units. It also presents characteristics absorption bands corresponding to: the vibrational motion of C=C aromatic stretching to  $1504\text{ cm}^{-1}$ , the COC

stretching at  $1256\text{ cm}^{-1}$  and C-O-C bending at  $761\text{ cm}^{-1}$ . The phenol OH give a broad band between  $3200$  and  $3450\text{ cm}^{-1}$  due to the symmetric stretching, while the motions of aliphatic and aromatic CH stretching give signals between  $2920$  and  $3030\text{ cm}^{-1}$ .

#### 4.13 – Characterization of copoly(bisphenolA carbonate)-alt-(ethylene carbonate)

The copoly(bisphenolA carbonate)-alt-(ethylene carbonate) - p(BPAC)-alt-(EtC) is an amorphous co-polymer with lower thermal stability respect to poly(bisphenolA-carbonate) PC. It present a Tg of 99 °C and two PDT respectively at 315 °C and 440 °C. It begin to degrade at 260 °C and at 800 °C leave 12% of carbonaceous residue (Table 4.1).



The  $^{13}\text{C}$  NMR spectrum with assignments of its characteristic resonance peaks are shown in Figure 4.2d. The  $^1\text{H}$  NMR spectrum exhibits typical quartet AB arises by aromatic protons between 7.00 e 7.40 ppm, one singlet at 1.68 ppm corresponding to the methyl protons, and one broad peak at 4.6 ppm attributed at methyl protons.

The MALDI-TOF mass spectrum of p(BPAC)-alt-(EtC) (Figure 4.8) recorded in Reflectron mode, reports the m/z range from 1200 to 5000 Da. This spectrum show two series of mass peak families: the first one, labeled An, correspond to cyclic oligomers; the second one, labeled with Bn, is assigned to linear chains H-/BPA-OH ended.

The FTIR spectrum in Figure 4.3d shown a strong band at  $1760\text{ cm}^{-1}$  assigned to stretching motions of carbonyl carbonate groups. Moreover, it possible to observe a broad band between  $3200$  and  $3500\text{ cm}^{-1}$  corresponding to stretching motions of OH groups; and a broad band between  $1100$  and  $1350\text{ cm}^{-1}$  of the Ar-C-O stretching. The stretching aliphatic motions of C=O give a broad signal at about  $1050\text{ cm}^{-1}$ ; and two bands respectively at  $772$  and  $830\text{ cm}^{-1}$  assigned to C-O-C bending motions.

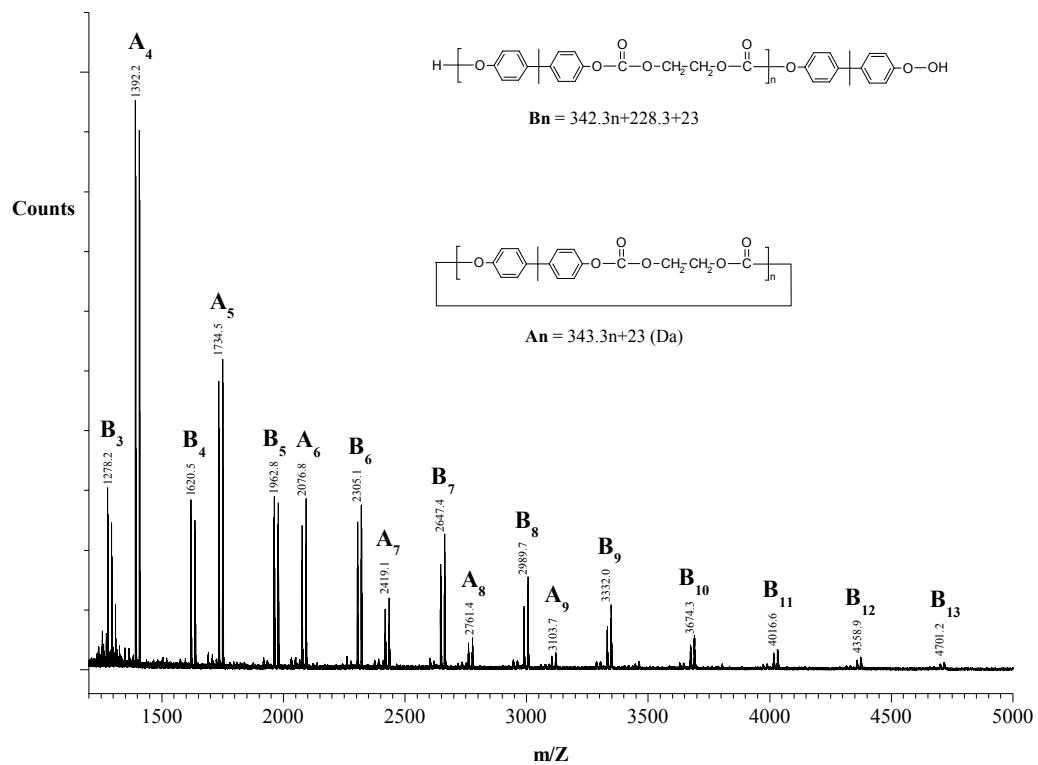


**Figure 4.8.** MALDI-TOF spectrum of copoly(bisphenolA carbonate)-alt-(ethylene carbonate) - p(BPAC)-alt-(EtC).

#### 4.14 – Characterization of poly(ethoxy-bisphenolA naphthalate)-co-(diethoxy-bisphenolA naphthalate)

The copolyester poly(ethoxy-bisphenolA naphthalate)-co-(diethoxy-bisphenolA naphthalate) - p(BPAEtN)-co-(EtBPAEtN) is an amorphous co-polymer with lower thermal stability than pBPAN. It exhibits a Tg of 103 °C and a PDT of 435 °C (Table 4.1). It begins to degrade at 320 °C and at 800 °C leaves 38% of carbonaceous residue.

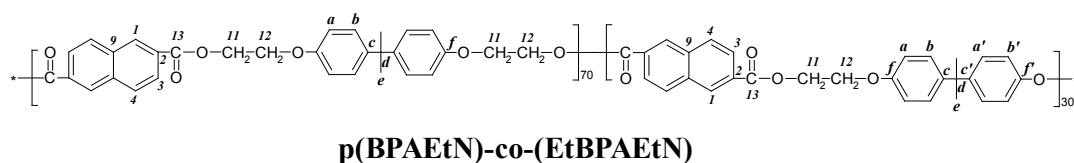


Figure 4.1e shows the <sup>1</sup>H-NMR spectrum of p(BPAEtN)-co-(EtBPAEtN) and the respective assignments. In particular, this spectrum reveals the presence of methyl ester end groups (singlet at 4.09 ppm - **OCH<sub>3</sub>**) and the phenol Bisphenol-A terminals (doublet at 6.81 ppm - **b'**). The absence of signals corresponding to methylene protons in the **α** and **β** to alcoholic OH of the ethylene-glycol units, indicates that the polymer chains do not have these end-groups and suggests a greater reactivity of these groups with respect to phenolic OH, in the step reaction polymerization. From the area ratio between signals of CH<sub>2</sub> at 4.823 ppm and signals of naphthalate protons **1,5** (Figure 4.1e) at 8.67 ppm, the calculated ethoxy-bisphenolA naphthalate / diethoxy-bisphenolA naphthalate molar ratio is 32/68 in the copolymer.

The <sup>13</sup>C NMR spectrum of p(BPAEtN)-co-(EtBPAEtN) together with the assignments of its characteristic resonance peaks are shown in Figure 4.2e.

Figure 4.9 reports the MALDI TOF spectrum of the copolymer p(BPAEtN)-co-(EtBPAEtN) (**E-co-F**) in the mass range 1400 – 9000 Da. The figure shows a series of peaks corresponding to different co-oligomers



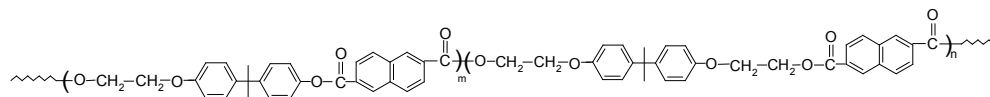
which structure and nature of end groups is consistent with of copolymer synthesis procedure. The enlarged section of the mass spectrum in the range 2300 – 3400 Da (inset in Figure 4.9) show different family peak families corresponding to pentamers and hexamers co-oligomers indicate with  $A_mB_n$ ; **A** correspond to monomer units having one ethoxy group linked to bisphenolA (452.5 amu, repeat mass), while **B** is attributed to monomer units with two ethoxy groups linked to bisphenol A (496.6 amu, repeat mass). The highest intensity peak families observed arises by sodium adducts like  $MNa^+$ , while the lower intensity peak families is attributed to potassium adducts like  $MK^+$ . The sodium adducts families corresponds to series **L** and **M**: the first one is given by polymeric chains H-/-OCH<sub>3</sub> ended, while second one is given by linear chains H-/-EtBPAOH ended. The potassium adducts families corresponds to **C** and **D** series: the first one is given by cycle oligomers while the second one is attributed to linear chains H-/-EtBPAEtOH ended. In Table 4.5 are reported the m/z value of the different chemical species observed in the MALDI TOF spectrum of copolymer *E-co-F* under investigation (Figure 4.9).

The FTIR spectrum of *E-co-F* copolymer not give structural information for distinguish it by **pEtBPAEtN** (Figure 4.3e).

**Table 4.5.** m/z values of the chemical species detected on the MALDI-TOF mass spectrum of the p(BPAEtN)-co-(EtBPAEtN).

<i>Pentamers</i>		<b>Cicle (C)</b>	<b>H/OCH<sub>3</sub> (L)</b>	<b>Mono-Et-BPA</b>	<b>di-Et-BPA (D)</b>
<b>Am</b>	<b>Bn</b>	m/z (K <sup>+</sup> )	m/z (Na <sup>+</sup> )	m/z (Na <sup>+</sup> )	m/z (K <sup>+</sup> )
3	2	2390	2422	2646	2706
4	1	-	2378	2602	2662
2	3	2434	2466	2690	2750
1	4	2478	2510	2734	-
<i>Hexamers</i>		<b>Cicle (C)</b>	<b>H/OCH<sub>3</sub> (L)</b>	<b>Mono-Et-BPA</b>	<b>di-Et-BPA (D)</b>
<b>Am</b>	<b>Bn</b>	m/z (K <sup>+</sup> )	m/z (Na <sup>+</sup> )	m/z (Na <sup>+</sup> )	m/z (K <sup>+</sup> )
3	3	2886	2902	3142	3202
2	4	2930	2946	3186	3246
1	5	2974	2990	3230	-
4	2	-	2858	3098	3158
5	1	-	-	-	-

**Structure of model copolymer *E-co-F***



**A** (452.5 amu)

**B** (496.6 amu)

<b>End groups of the copolymer <i>E-co-F</i></b>	<b>Symbol</b> (utilized on the MALDI TOF mass spectrum)
$\left[ (A)_m (B)_n \right]$	<b>C</b>
$H - (A)_m (B)_n - OCH_3$	<b>L</b>
$H - (A)_m (B)_n - O - CH_2 - CH_2 - O - \text{BPA} - OH$	<b>M</b>
$H - (A)_m (B)_n - O - CH_2 - CH_2 - O - \text{BPA} - O - CH_2 - CH_2 - OH$	<b>D</b>

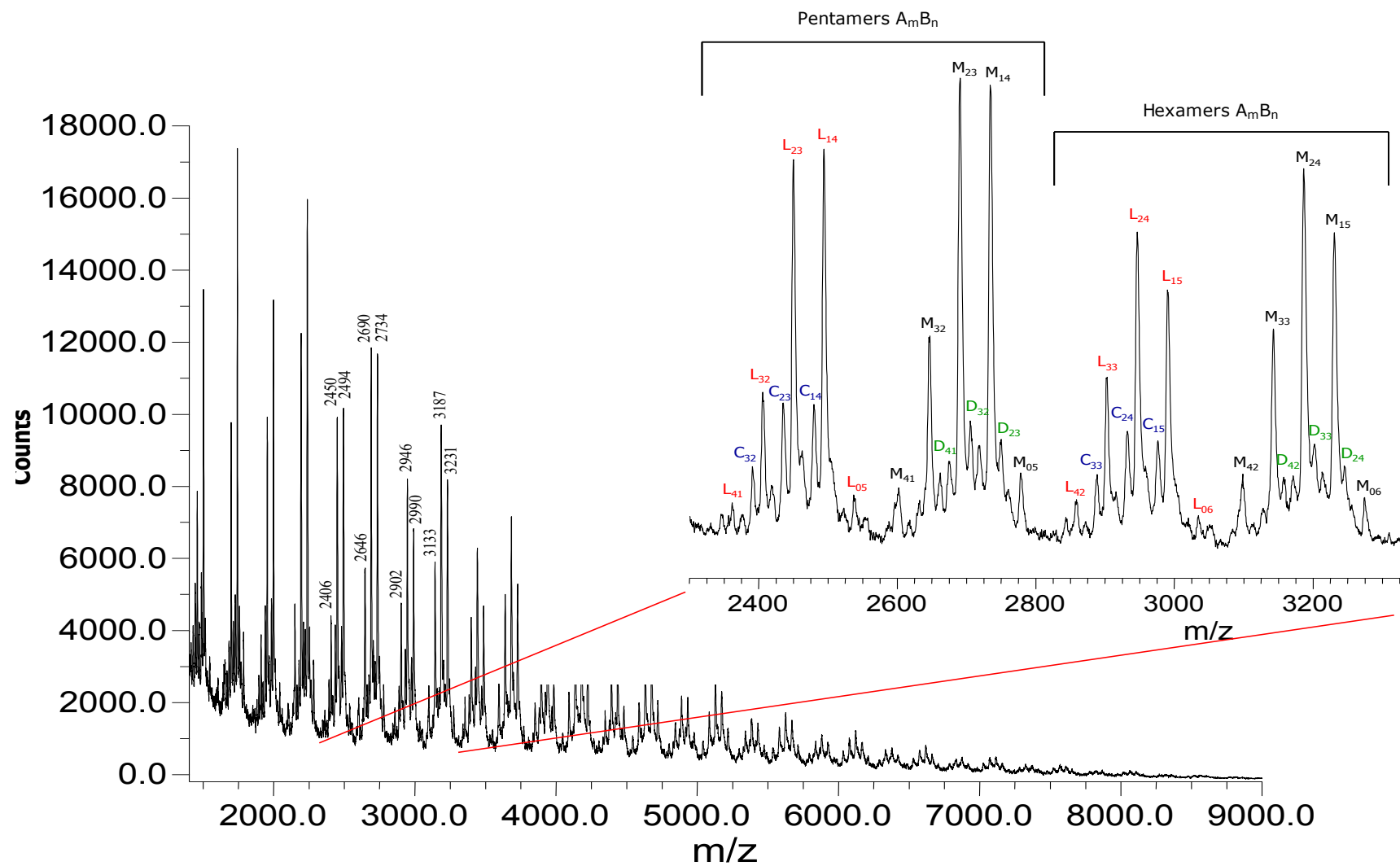
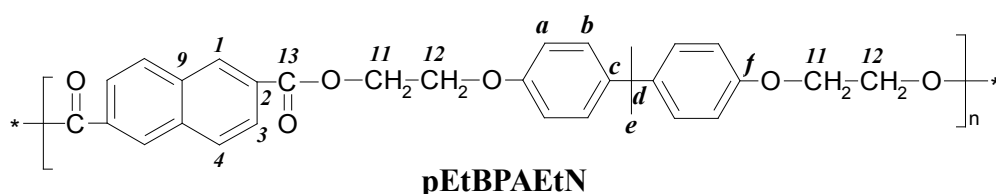


**Figure 4.9.** MALDI TOF mass spectrum (in positive mode) of poly(ethoxy-bisphenolA naphthalate)-co-(diethoxy-bisphenolA naphthalate) - p(BPAEtN)-co-(EtBPAEtN).

## 4.15 – Characterization of poly(diethoxy-bisphenolA naphthalate)

Some thermal and viscosimetric properties of poly(diethoxy-bisphenolA naphthalate) - pEtBPAEtN are shown in Table 4.1. The presence of flexible aliphatic-aromatic ether unit (**E**) give lower thermal stability ( $T_g$  of 94 °C) than pBPAN ( $T_g$  of 185 °C). It begin to degrade at 310 °C, present a PDT at 450 °C and at 800 °C leave 30% of carbonaceous residue.



The  $^1\text{H}$  NMR spectrum (Figure 4.1f), in addition to signals corresponding to protons in the chain, reveals the presence of terminal methyl ester (singlet at 4.092 ppm -  $-\text{OCH}_3$ ). The  $^{13}\text{C}$  NMR spectrum with assignments of its characteristic resonance peaks are shown in Figure 4.2f.

The MALDI-TOF mass spectrum of pEtBPAEtN (Figure 4.10) recorded in Reflectron mode, reports the  $m/z$  range from 1200 to 5000 Da. The principal mass peak families, labeled with  $A_n$ , is assigned to linear chains H-/-EtBPAEt-OH ended.

Further structural characterization by FTIR evidences the presence of absorption bands (Figure 4.3f) similar to those observed in pBPAN (Figure 4.3d); in this case band at  $1718\text{ cm}^{-1}$  correspond to C=O stretching.

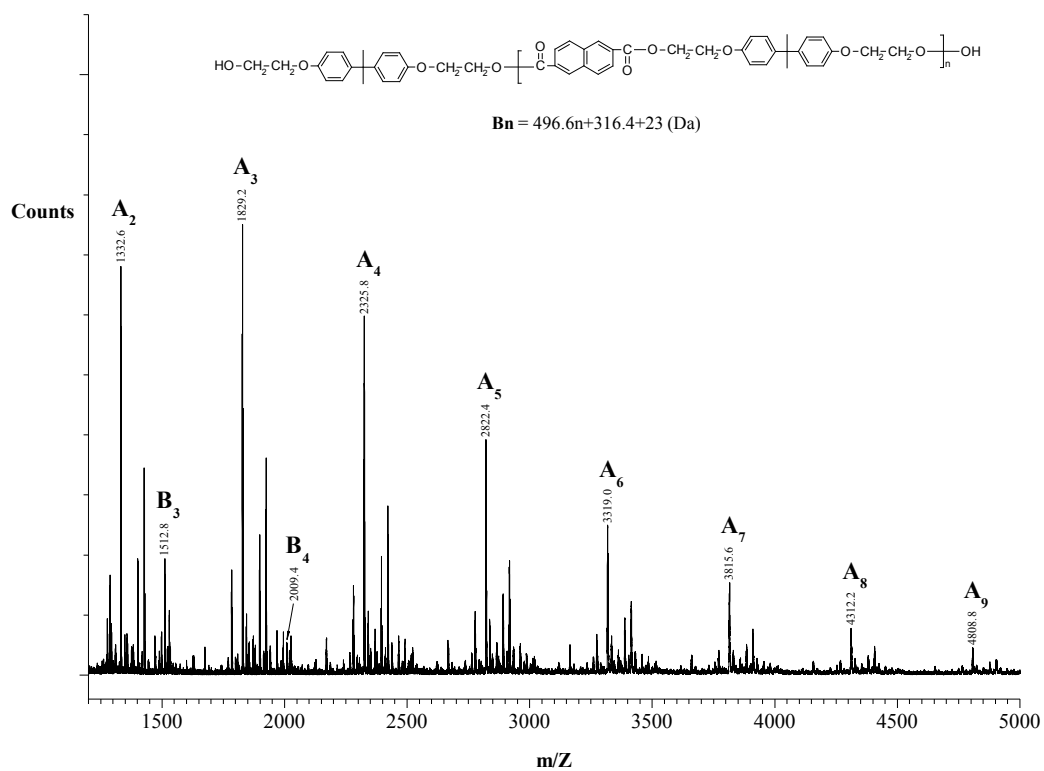


**Figure 4.10.** MALDI TOF mass spectrum (in positive mode) of poly(diethoxy-bisphenolA naphthalate) pEtBPAEtN.

#### 4.16 – Characterizations PC-PEN melt blended materials

New copolymers were prepared by reactive melt blending of equimolar PC-PEN mixtures (with respect to the repeat unit) for different times at 280 °C, in nitrogen flow and in presence of 2% w/w of Ti(OBu)<sub>4</sub> as transesterification catalyst. These materials were characterized by the following analysis techniques:

- Solvent extractions (*Figure 4.11*);
- <sup>1</sup>H-NMR spectroscopy (*Figure 4.12*);
- <sup>13</sup>C –NMR spectroscopy (*Figure 4.13*);
- Thermogravimetric Analysis – TGA (*Figures 4.15, 4.16*);
- Differential Scanning Calorimetry – DSC (*Figure 4.17*);
- Fourier Transform Infra-Red spectroscopy – FTIR (*Figure 4.18*);
- Viscometry (*Table 4.12*);
- Gel Permeation Chromatography – GPC (*Figure 4.19*);
- MALDI-TOF mass spectrometry (*Figures 4.22, 4.23*).

The aim of these studies is a full elucidation of microstructures and composition of new PC-PEN copolymers as well as the kinetic mechanism of the catalyzed exchange reactions ester-carbonate that occurring between PC and PEN homopolymers in the molten state.

#### 4.17 – Solvent extractions

The materials obtained at short mixing times (2, 5, 8, and 10 min) were subjected to selective extraction with solvents to determine the amount of PC-PEN copolymers formed, and to characterize their nature and chemical composition. First one solvent treatment was performed with  $\text{CHCl}_3$  at 25 °C for 6 hours to extract unreacted PC from insoluble components, corresponding to unreacted PEN and PC-PEN block copolymers. The insoluble residue was then treated with  $\text{C}_2\text{H}_2\text{Cl}_4$  (TCE) at 40 °C for 24 hours (second one solvent treatment) to extract PC-PEN copolymers (see block diagram Figure 4.11) from the insoluble PEN. From blends obtained at 2 and 5 min were extracted 25% and 3% of unreacted PC respectively, as confirmed by MALDI and  $^1\text{H-NMR}$  analysis. In addition, from the same blends were obtained 52% and 95% of PC-PEN block copolymers with a equimolar composition of PC and PEN units, as seen by  $^1\text{H NMR}$  analysis. Finally, the mixtures prepared at 2 and 5 min containing respectively 23% and 2% of unreacted PEN, as was confirmed by MALDI-TOF,  $^1\text{H-NMR}$  and FTIR analysis of TCE insoluble fraction. The materials produced at 8 and 10 minutes were completely insoluble in  $\text{CHCl}_3$  but totally soluble in  $\text{C}_2\text{H}_2\text{Cl}_4$ , as a proof that the initial PC and PEN were totally converted in the corresponding copolymers.

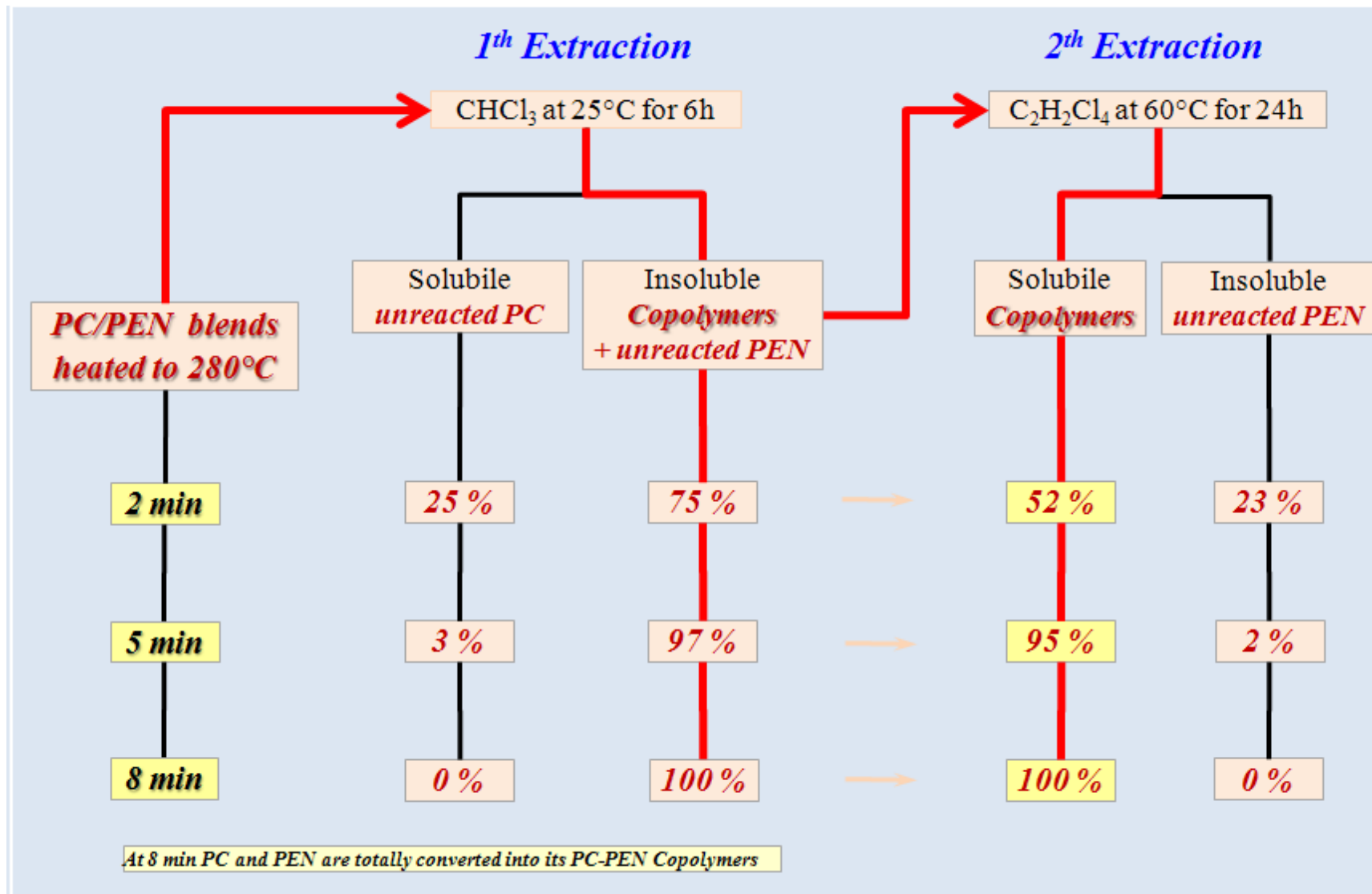


Figure 4.11. block diagram of solvent extractions.



#### 4.18 - $^1\text{H}$ and $^{13}\text{C}$ -NMR analysis of PC-PEN melt blended materials

The reactions at 280 °C between high molar mass PC and PEN should occur analogous mechanisms observed for the PET-PC melt mixed system, previously studied<sup>1, 28-33</sup>. The exchange reactions that can occur in this system are summarized in Scheme 4.1. At first reaction step, a block copoly(ester-carbonate), containing four component like bisphenolA-carbonate (**A**), ethylene-naphthalate (**B**), bisphenolA-naphthalate (**C**), and ethylene-carbonate (**D**), owing catalyzed inner-inner exchange reactions, was formed (see Scheme 4.1 and 4.2). However, at this temperature (280 °C) the new aliphatic carbonate units **D**, undergoes thermal decomposition by elimination of  $\text{CO}_2$  and ethylene carbonate (EtC), simultaneously to the exchange reactions. The elimination of  $\text{CO}_2$  and EtC respectively lead to the formation of ether and di-ether groups along the copolymer chain, therefore introducing a new components such as ethoxy-bisphenolA-naphthalate (**E**) and diethoxy-bisphenolA-naphthalate (**F**) into the copolymer chains (see Scheme 4.2 and 4.3).

The formation of PC-PEN copolymers is indicated by a series of new signals with respect to the initial homopolymers, either in  $^1\text{H}$  NMR and in  $^{13}\text{C}$  NMR spectra (Figure 4.12 and 4.13 - the assignments of the chemical shifts in the figures are summarized in Table 4.6). In particular,  $^1\text{H}$  NMR spectra (Figure 4.12) show also that the intensity of all signals due to Methylene protons ( $-\text{CH}_2-$ ) in the region 4.0 – 5.0 ppm decreases with respect to that of aromatic protons belonging to the naphthalate groups, as increases the reaction time, while the molar ratio bisphenolA/naphthalate units (initial 1:1) unchanged towards the reaction time; it is equal to the feed ratio of the two homopolymers.

The exchange reaction was monitored as a function of time by  $^{13}\text{C}$ -NMR (Figure 4.13) following as change the intensity of signals

corresponding to methylene (63 – 69 ppm) and of bisphenolA (114 – 121 ppm) carbons and also by <sup>1</sup>H-NMR following the intensity ratio of ethylene and naphthalate protons (Figure 4.12 and Table 4.6). Applying the appropriate statistical models by Samperi et al.<sup>34</sup> and using the intensities of these signals, the molar fraction of each copolymer component towards reaction time was calculated.

$$C_i = 100 * \frac{C'_i}{\sum C'_i} \quad (\text{eq. 1})$$

$$\frac{Et}{N} = \frac{\sum I_{H_{11}} + \sum I_{H_{12}}}{\sum I_{H_{1,5}}} \quad (\text{eq. 2})$$

$$C'_A = C_{PC} * \frac{I_{a(120.41)}}{\sum I_a} \quad (\text{eq. 3})$$

$$C'_B = C_{PEN} * \frac{Et}{N} * \frac{I_{12(64.04)}}{\sum I_{11} + \sum I_{12}} \quad (\text{eq. 4})$$

$$C'_C = C_{PC} * \frac{I_{a(121.06)}}{\sum I_a} \quad (\text{eq. 5})$$

$$C'_D = C_{PC} * \frac{I_{a(120.33)}}{\sum I_a} \quad (\text{eq. 6})$$

$$C'_E = C_{PC} * \frac{I_{a(114.91)} + I_{a(120.96)}}{\sum I_a} \quad (\text{eq. 7})$$

$$C'_F = C_{PC} * \frac{I_{a(114.75)}}{\sum I_a} \quad (\text{eq. 8})$$

$$C_{PC} = C_{PEN} = 50 (\%mol) \quad (\text{eq. 9})$$

The calculated material balance is reported in Table 4.8; it shows that after 2 min of reaction was formed an essentially four-components copolymers (**A**, **B**, **C**, **D**), that become a five components after 5 min (**A**, **B**, **C**, **D**, **E**) and six components after 15 min (**A**, **B**, **C**, **D**, **E**, **F**). After 45 min the **A** and **D** carbonate sequences are almost gone by elimination of CO<sub>2</sub> and ethylene carbonate, and an essentially copoly(ester-ether) was produced (Figure 4.14).

To establish the effect of the exchange reactions on the microstructure of the PC-PEN copolymers, their average sequence lengths

( $L_A$ ,  $L_B$ ,  $L_C$ ,  $L_D$ ,  $L_E$  and  $L_F$ ), Degree of Exchange (**DE**) and Degree of Randomness (**DR**) were calculated using the molar fraction of each copolymer sequences ( $n_A$ ,  $n_B$ ,  $n_C$ ,  $n_D$ ,  $n_E$  and  $n_F$  in Table 4.7) previously calculated. For this purpose the following equations were used (statistical model by Samperi et al<sup>5, 34</sup>):

$$L_A = \frac{C_A + C_C + C_D + C_E + C_F}{C_C + C_D + C_E + C_F} \quad (\text{eq. 10})$$

$$L_B = \frac{C_B + C_D + C_E + C_F}{C_D + C_E + C_F} \quad (\text{eq. 11})$$

$$L_C = \frac{C_A + C_C + C_D + C_E + C_F}{C_A + C_D + C_E + C_F} \quad (\text{eq. 12})$$

$$L_D = \frac{C_A + C_C + C_D + C_E + C_F}{C_A + C_C + C_E + C_F} \quad (\text{eq. 13})$$

$$L_E = \frac{C_A + C_C + C_D + C_E + C_F}{C_A + C_C + C_D + C_F} \quad (\text{eq. 14})$$

$$L_F = \frac{C_A + C_C + C_D + C_E + C_F}{C_A + C_C + C_D + C_E} \quad (\text{eq. 15})$$

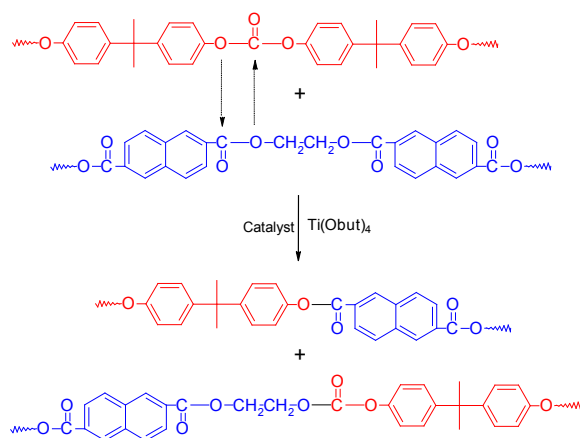
$$DE = C_C + C_D + C_E + C_F \quad (\text{eq. 16})$$

$$DR = \frac{C_C + C_E + C_F}{C_A + C_C + C_E + C_F} + \frac{C_D}{C_B + C_D + C_E + 2 * C_F} \quad (\text{eq. 17})$$

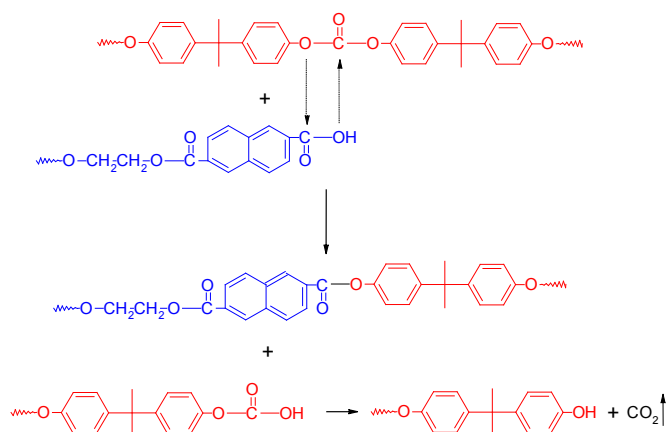
Microstructure data reported in Table 4.10 confirm that PC-PEN block copolymers were formed at shorter reaction time until 8 min. The average sequence lengths of the PC (**A**) and PEN (**B**) blocks decrease as increase the reaction time, and a multi-block copolymers was formed at 20 min mixing with degree of exchange (**DE**) of 45,95%. In presence of only direct ester-carbonate, ester-ester, and carbonate-carbonate exchange reactions the PC-PEN system should reach the thermodynamic equilibrium at about 50% of degree of exchange<sup>1</sup>. However, the consecutive thermal decomposition side reactions, lead to the elimination of **D** units (ethylene-carbonate) with formation of **C** sequences, and in part the conversion of **D** units into two new ether sequences **E** and **F**, with resulting increasing of the degree of exchange that it reaches the almost maximum at 60 min mixing. These indicate that exchange reactions

reaches the completion after 60 min mixing (100% degree of exchange) when the **A**, **B** and **D** sequences are totally disappeared and a pure copoly(ether-ester)s are produced. The degree of randomness values, in Table 4.8, suggest that as the consecutive degradation reactions (Scheme 4.2) progress random copoly(ester-ether)s, were formed.

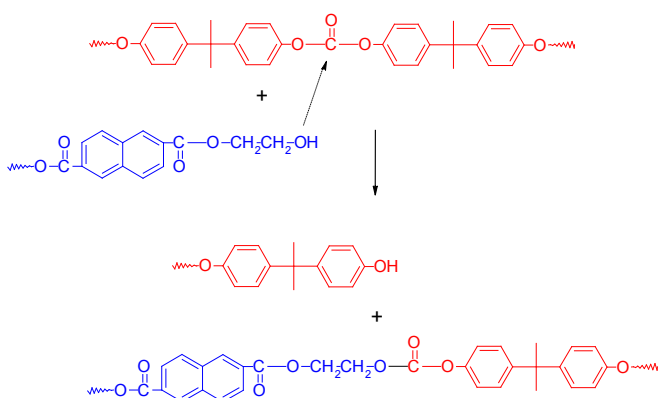
### A) Direct ester-carbonate exchange reactions (inner – inner)



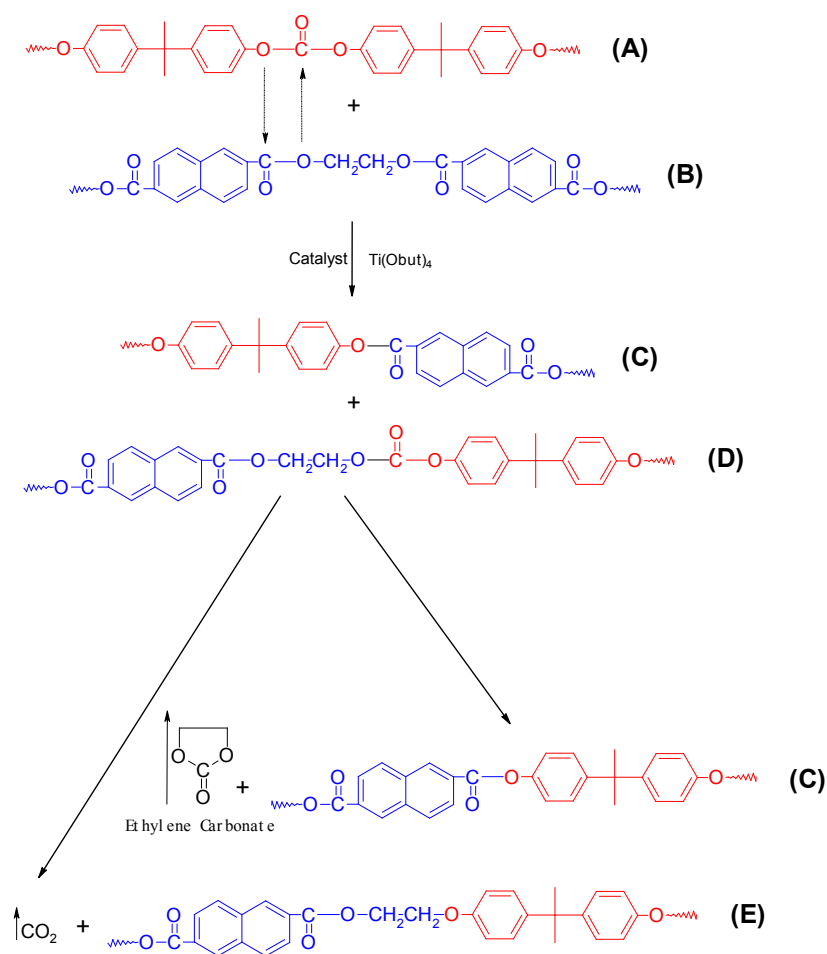
### B) Alcoholysis (outer – inner)



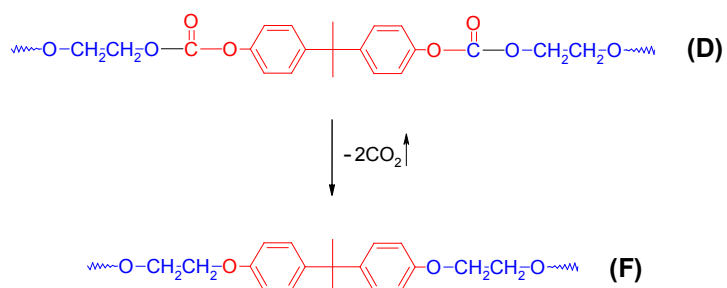
### C) Acidolysis (outer – inner)



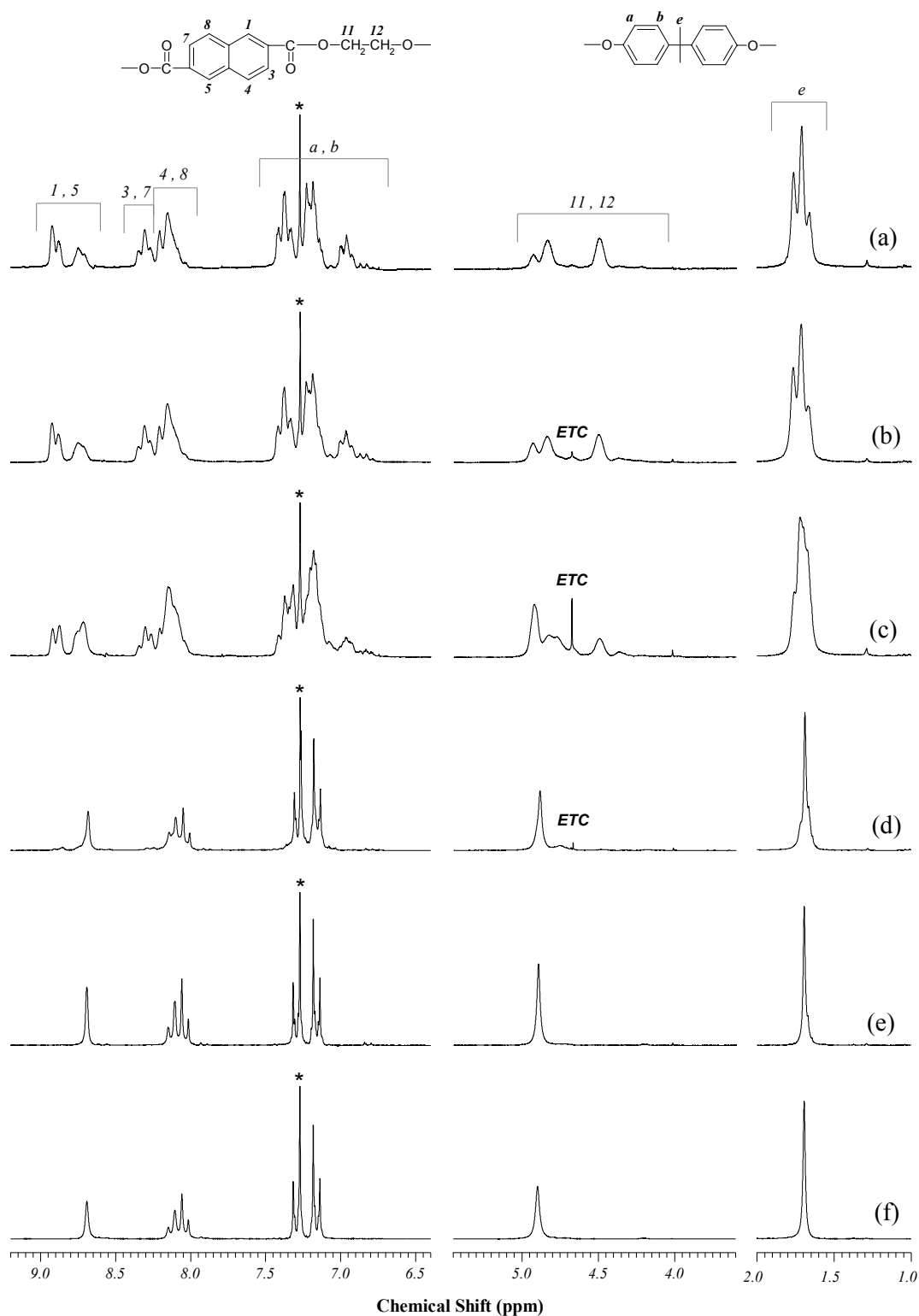
**Scheme 4.1.** Catalyzed Exchange Reactions which that should occur in the Melt Mixing of PC-PEN Blends.



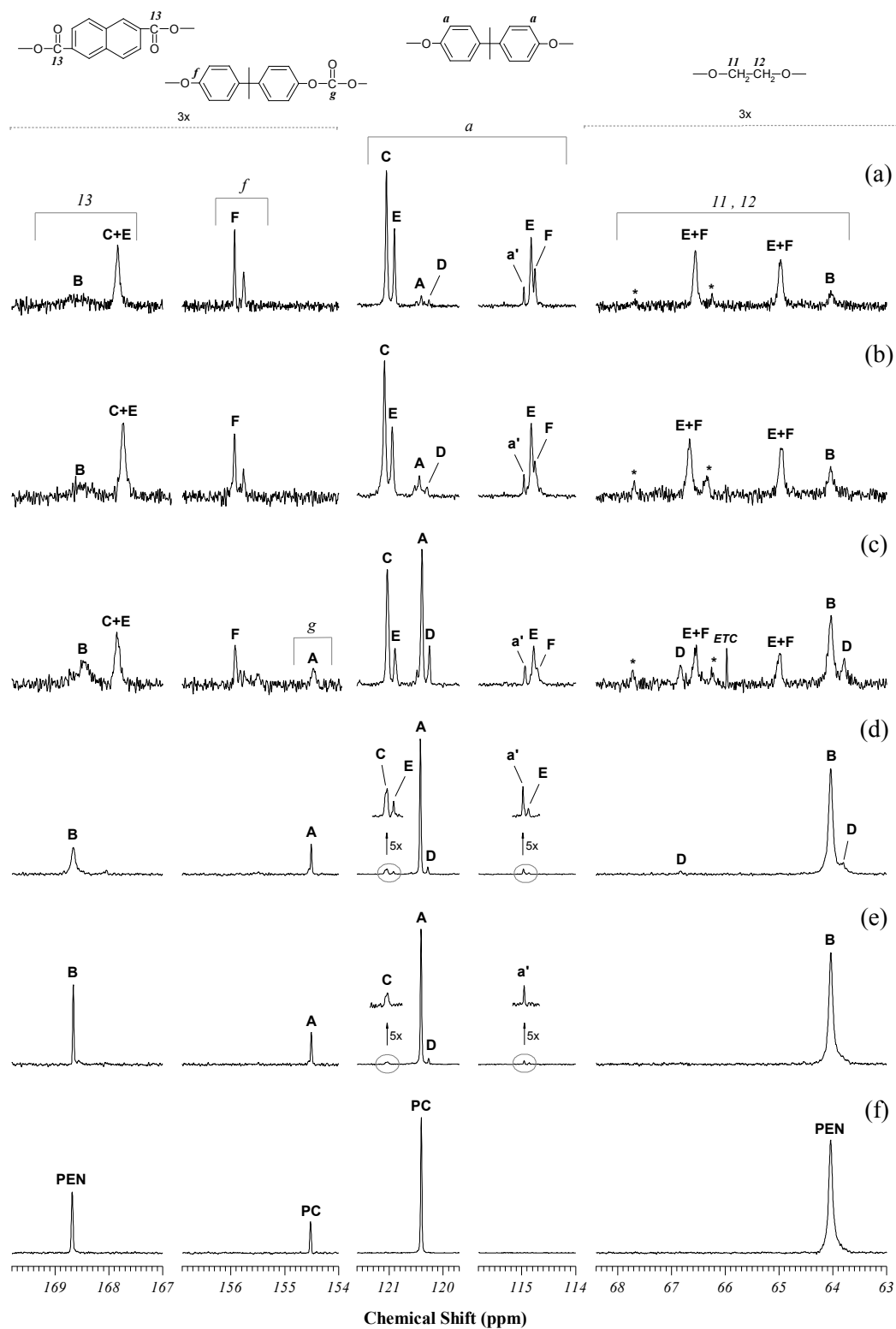
**Scheme 4.2.** Catalyzed Exchange Reactions and consecutive elimination of  $\text{CO}_2$  and ethylene carbonate (EtC) in the Melt Mixing of PC with PEN at  $280^\circ\text{C}$ .



**Scheme 4.3.** Formation of diethoxy-bisphenolA sequences (F).



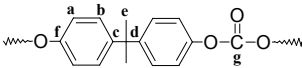
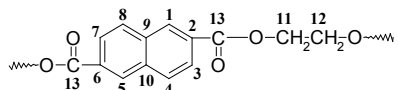
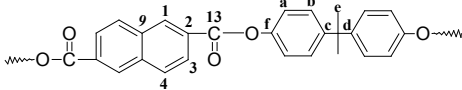
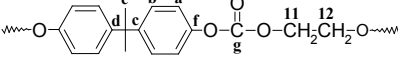
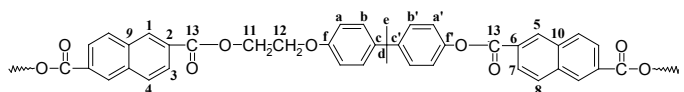
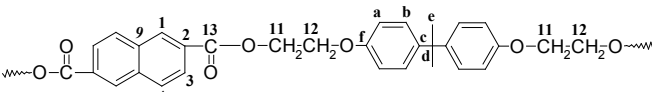
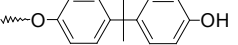
**Figure 4.12.**  $^1\text{H}$  NMR spectra of equimolar PC-PEN mixture melt-mixed at  $280^\circ\text{C}$  for 0, 2, 5, 20, 45, and 60 min in the presence of  $\text{Ti}(\text{O}i\text{Bu})_4$  as catalyst. (EtC = adsorbed molecules of ethylene carbonate; \* = solvent signal –  $\text{CDCl}_3/d\text{-TFA}$  – 80/20 v:v).



**Figure 4.13.**  $^{13}\text{C}$  NMR spectra of equimolar PC-PEN mixture melt-mixed at  $280^\circ\text{C}$  for 0, 2, 5, 20, 45, and 60 min in the presence of  $\text{Ti}(\text{O}i\text{Bu})_4$  as catalyst. The carbon assignments are given in Table 1. (*EtC* = adsorbed molecules of Ethylene Carbonate).



**Table 4.6.** Carbon signal assignments of structural units in the PC-PEN copolymers as observed in their  $^{13}\text{C}$ -NMR spectra.

Units	Structures	C	ppm
<b>A</b> <i>PC</i>		a b c d e f g	120.40 128.27 148.61 42.74 30.67 149.23 154.52
<b>B</b> <i>PEN</i>		1 - 5 2 - 6 3 - 7 4 - 8 9 - 10 11 - 12 13	130.33 131.66 128.59 125.97 135.04 64.04 168.68
<b>C</b>		1 2 3 4 9 10 13 a b c d e f	130.50 132.37 128.69 126.47 135.28 135.28 168.06 121.06 128.44 148.34 42.86 30.75 149.37
<b>D</b>		a b c d e f g 11	120.33 128.33 148.50 42.76 30.62 149.38 155.55 66.58
<b>E</b>		1 - 5 2 - 6 3 - 7 4 - 8 9 - 10 11 - 12 13 - 13' a - a' b - b' c - c' d e f - f'	130.42 - 130.48 131.71 - 132.37 128.53 - 128.83 126.17 - 126.39 135.12 - 135.30 65.06 - 66.52 169.00 - 168.23 114.91 - 120.96 128.26 - 128.44 144.44 - 148.22 42.45 30.87 155.79 - 149.92
<b>F</b>		1 2 3 4 9 11 - 12 13 a b c d e f	130.11 131.50 128.51 125.83 134.89 64.83 - 66.61 168.85 114.75 128.02 144.82 41.81 30.63 155.36
<b>a'</b>		a'	114.95

**Table 4.7.** Molar ratio of ethylenic to naphthalate units (Et/N) and normalized molar composition (%mol) of the sequences **A**, **B**, **C**, **D**, **E** and **F** in the PC-PEN copolymers calculated by  $^1\text{H}$  and  $^{13}\text{C}$  NMR analysis.

Reaction Time (min)	Et/N	C <sub>A</sub>	C <sub>B</sub>	C <sub>C</sub>	C <sub>D</sub>	C <sub>E</sub>	C <sub>F</sub>
0	1,000	50,00	50,00	0,00	0,00	0,00	0,00
2	1,000	48,45	49,00	1,00	1,00	0,00	0,00
5	0,981	47,87	48,37	1,70	1,65	0,40	0,00
8	0,954	44,43	46,20	4,42	2,90	2,05	0,00
10	0,893	41,20	41,83	10,00	4,70	2,60	0,00
15	0,841	36,80	34,20	16,00	5,90	6,00	1,10
20	0,795	28,44	25,63	23,85	6,40	14,20	1,50
30	0,724	14,35	17,50	33,50	3,46	29,40	1,90
45	0,666	3,42	12,30	46,20	2,60	31,90	3,50
60	0,660	1,40	4,20	56,60	0,60	31,90	6,30

**Table 4.8.** Average sequence lengths (**L<sub>A</sub>**, **L<sub>B</sub>**, **L<sub>C</sub>**, **L<sub>D</sub>**, **L<sub>E</sub>** and **L<sub>F</sub>**), Degree of Exchange (**DE**), and Degree of Randomness (**DR**) in the PC-PEN copolymers calculated by  $^1\text{H}$  and  $^{13}\text{C}$  NMR analysis.

Reaction Time (min)	L <sub>A</sub>	L <sub>B</sub>	L <sub>C</sub>	L <sub>D</sub>	L <sub>E</sub>	L <sub>F</sub>	DE	DR
0	n.d.	n.d.	0,00	0,00	0,00	0,00	0,00	0,00
2	25,23	50,00	1,02	1,02	1,00	1,00	2,00	0,04
5	13,77	24,60	1,03	1,03	1,01	1,00	3,75	0,07
8	5,74	10,33	1,09	1,06	1,04	1,00	9,37	0,18
10	3,38	6,73	1,21	1,09	1,05	1,00	17,30	0,33
15	2,27	3,63	1,32	1,10	1,10	1,02	29,00	0,51
20	1,62	2,16	1,47	1,09	1,24	1,02	45,95	0,71
30	1,21	1,50	1,68	1,04	1,55	1,02	68,26	0,88
45	1,04	1,32	2,12	1,03	1,57	1,04	84,20	1,01
60	1,01	1,11	2,41	1,01	1,49	1,07	95,80	1,00

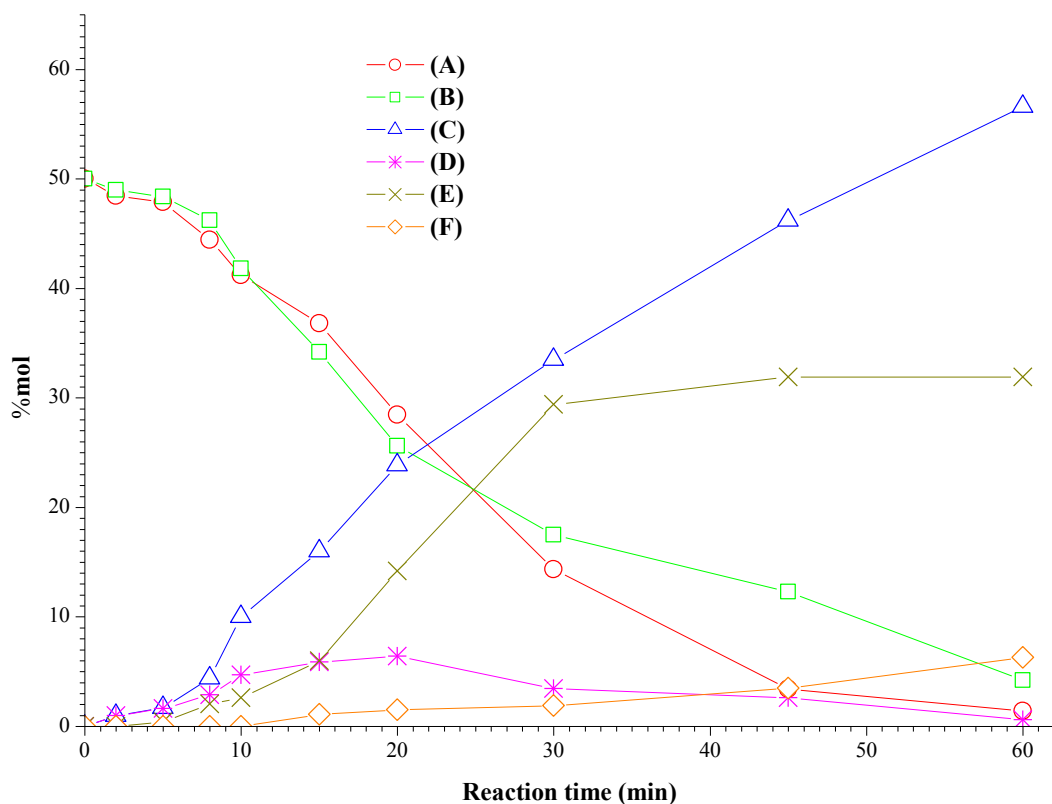


**Figure 4.14.** Evolution of the molar composition of the sequences A, B, C, D, E and F into PC-PEN copolymers as a functions of reactions time: (A) bisphenolA-carbonate, (B) ethylene-naphthalate, (C) bisphenolA-naphthalate, (D) ethylene-carbonate, (E) ethoxy-bisphenolA-naphthalate, (F) diethoxy-bisphenolA-naphthalate.

## 4.19 – Thermogravimetric analysis of PC-PEN melt blended materials

The thermal stability of copolymers was studied by thermogravimetric analysis (TGA) and weight loss curves as a function of temperature are shown in Figure 4.15. Figure 4.16 shows the derivative curves of weight loss (DTGA) as a function of temperature. The study of the two Figures shows that the copolymers obtained from 2 at 30 min by mixing of PC-PEN blends at 280 °C in the presence of  $\text{Ti}(\text{OBut})_4$ , degrade in the range 200-650 °C with three maximum of speed of weight loss (PDT) at: 310 °C, 445 °C, and 530 °C. The copolymers obtained at 45 and 60 min of mixing are thermally more stable and degrade in the range 280-650 °C, with two maxima (PDT) at 445 °C and 530 °C. The lower thermal stability of copolymers obtained below than 45 min is due to the presence of bisphenolA-ethylene-carbonate units (**D**), which are the least thermally stable as can be seen from the characteristics of the homopolymers model in Table 4.1. Therefore at temperatures around of first PDT should be eliminated  $\text{CO}_2$  and EtC.

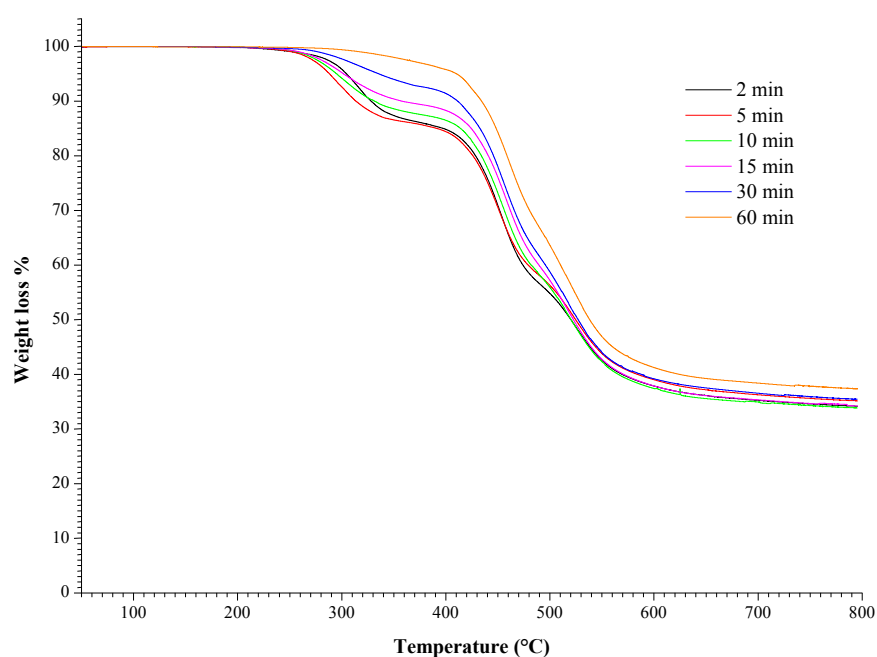


**Figure 4.15.** Thermogravimetric curves obtained by TGA of the PC-PEN copolymers produced by reactive blending of PC and PEN in the molten state.

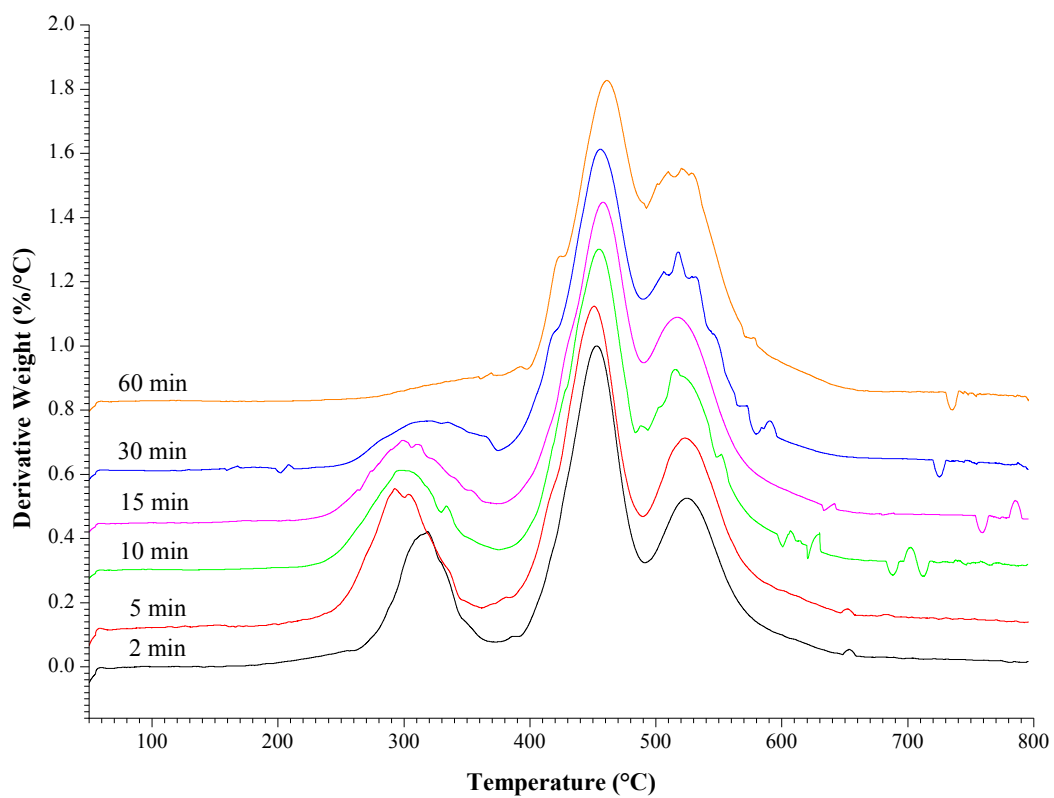


**Figure 4.16.** Loss weight derivative curves (DTGA) obtained by TGA of the PC-PEN copolymers produced by reactive blending of PC and PEN in the molten state.

The weight loss of EtC and CO<sub>2</sub>, calculated by NMR (<sup>1</sup>H and <sup>13</sup>C), is in agreement with the weight loss values found by isothermal thermogravimetric analysis at 280 °C, and in N<sub>2</sub> flow, of a equimolar PC-PEN mixture in the presence of 0,2%w of Ti(OBut)<sub>4</sub> as catalyst (Table 4.9).

**Table 4.9.** % Mol and % weight of eliminated ethylene carbonate (EtC) and CO<sub>2</sub>, as a function of reaction time, during reactive melt blending at 280 °C of equimolar PC-PEN blends in the presence of Ti(OBut)<sub>4</sub> (0,2% w) as catalyst. The following data are calculated by (<sup>1</sup>H and <sup>13</sup>C) NMR and compared to %loss weight by Themogravimetric analysis (TGA) of the same initial mixture at 280 °C and in N<sub>2</sub> flow.

Reaction time (min)	Et/N	% mol ETC	% mol CO <sub>2</sub>	% weight ETC	% weight CO <sub>2</sub>	%weight loss of ETC+CO <sub>2</sub>	%weight loss by TGA
0	0,00	0,00	0,00	0,00	0,00	0,00	0,00
2	0,00	0,00	0,00	0,00	0,00	0,00	0,00
5	0,95	0,95	0,40	0,34	0,07	0,41	0,60
8	2,30	2,30	2,05	0,82	0,36	1,18	1,50
10	5,35	5,35	2,59	1,90	0,46	2,36	2,80
15	7,95	7,95	8,11	2,82	1,44	4,26	3,50
20	10,25	10,25	16,94	3,64	3,00	6,64	7,20
30	13,80	13,80	32,55	4,90	5,77	10,67	9,20
45	16,70	16,70	37,61	5,93	6,67	12,59	12,50
60	17,00	17,00	41,47	6,03	7,35	13,38	13,10

$$\%mol_{ETC} = \%mol_{Et_0} - \%mol_{Et_t} = 50 * \left(1 - \frac{Et}{N}\right) \quad (\text{eq. 10})$$

$$\%mol_{CO_2} = C_E + 2C_F \quad (\text{eq. 11})$$

$$\%weight_{ETC} = 100 * \frac{\%mol_{ETC} * MW_{ETC}}{C_{PC} * MW_{PC} + C_{PEN} * MW_{PEN}} \quad (\text{eq. 12})$$

$$\%weight_{CO_2} = 100 * \frac{\%mol_{CO_2} * MW_{CO_2}}{C_{PC} * MW_{PC} + C_{PEN} * MW_{PEN}} \quad (\text{eq. 13})$$

$$C_{PC} = C_{PEN} = 50 \%mol \quad (\text{eq. 14})$$

## 4.20 – DSC analysis of melt mixed PC-PEN materials

The thermal properties of PC-PEN copolymers formed at different reaction times were determined by Differential Scanning Calorimetry (DSC). Figure 4.17 shows thermograms recorded by heating from 50 °C up to 280 °C with a heating rate of 10 °C/min of the crude samples quenched from the molten state. The corresponding thermal glass transition ( $T_g$ ), peak crystallization temperatures ( $T_c$ ), peak melting temperatures ( $T_m$ ), and their corresponding enthalpies are given in Table 4.11.

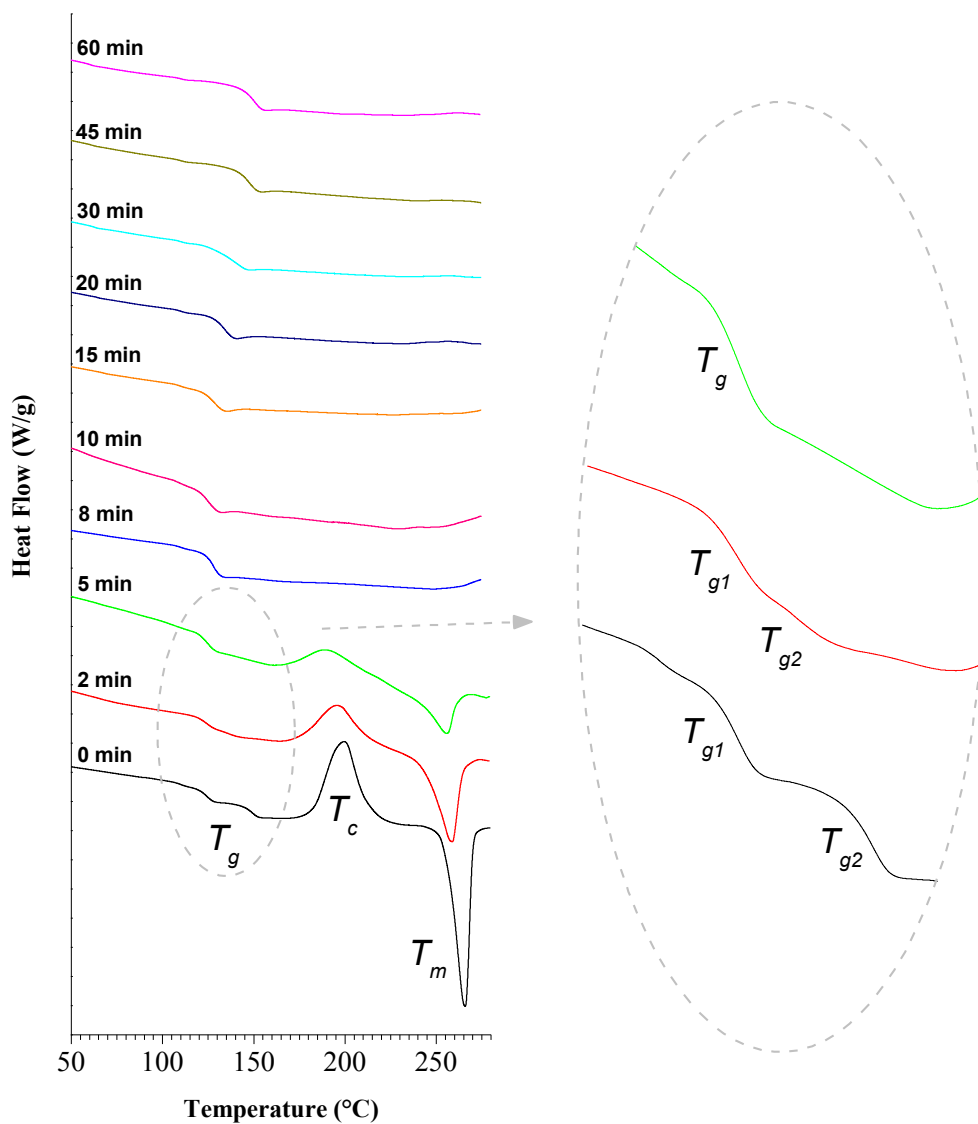


**Figure 4.17.** DSC thermograms of PC-PEN equimolar mixtures (50/50 in mole) melt blended at 280 °C in nitrogen flow at different mixing times.

**Table 4.10.** Thermal Properties of PC-PEN copolymer by DSC analysis.

<b>Reaction time (min)</b>	<b>T<sub>g</sub> (°C)</b>	<b>T<sub>c</sub> (°C)</b>	<b>ΔH<sub>c</sub> (J/g)</b>	<b>T<sub>m</sub> (°C)</b>	<b>ΔH<sub>m</sub> (J/g)</b>
<i>0</i>	125/149	200	17.4	266	17.8
<i>2</i>	125/135	196	6.13	258	14.6
<i>5</i>	127	190	2.20	255	6.47
<i>8</i>	128	---	---	---	---
<i>10</i>	128	---	---	---	---
<i>15</i>	131	---	---	---	---
<i>20</i>	135	---	---	---	---
<i>30</i>	139	---	---	---	---
<i>45</i>	148	---	---	---	---
<i>60</i>	152	---	---	---	---

The presence of two characteristic glass transitions at 125 °C and 149 °C in the physical blend (0 min), almost identical to the values obtained for neat PC and PEN homopolymers respectively, confirms that these polymers are incompatible in the molten state (biphasic physical blend). It also exhibits semicrystalline behavior due an exothermic crystallization process (T<sub>c</sub>) at 200 °C and an endothermic process of melting (T<sub>m</sub>) at 266 °C due to the PEN homopolymer. As the exchange reaction progress semicrystalline samples were produced until 5 of mixing, which T<sub>c</sub> and T<sub>m</sub> progressively decrease to 190 °C and 255 °C, respectively. Decreasing in T<sub>c</sub> and T<sub>m</sub> are due to shortening of PEN blocks in PC-PEN copolymers formed. Formation of block copolymers is also indicated by the presence of two T<sub>g</sub> respectively at 125 °C and 135 °C in the sample at 2 min. The appearance of a single T<sub>g</sub> in the sample produced at 5 min is a clear proof that average of block lengths in produced copolymers decrease allowing to obtain monophasic system. Subsequent mixing times to 5 min produce amorphous and homogeneous



materials with a single  $T_g$  that shift from 127 °C to 152 °C (raising of the thermal stability) as the reaction progress.

DSC data are in agreement with those obtained by solvent extraction. The solvent extraction reveals the formation of samples composed of 100% of PC-PEN copolymers for mixing time higher than 5 min. The samples at 2 and 5 min correspond to blends containing, 52%w and 95%w of PC-PEN copolymers respectively.

These results suggest changes in microstructure and composition in the formed copolymers, as increase the reaction time, that are in agreement with the molar composition data obtained by NMR analysis.

Applying the classical Fox equation (eq. 18) to our case is possible calculate the theoretical value of thermal glass transition for a two component PC-PEN random copolymers.

$$\frac{1}{T_g} = \frac{W_{PC}}{T_{gPC}} + \frac{W_{PEN}}{T_{gPEN}} \quad (\text{eq. 18})$$

where  $W_{PC}$  (0,512) and  $W_{PEN}$  (0,488) are the weight fractions of PC and PEN composing the initial blend, while  $T_{g1}$  (419,15 °K) and  $T_{g2}$  (398,15 °K) are the respective glass transitions. By this equation, generally used to calculate the  $T_g$  value of two component random copolymers formed by melt-mixing of binary A/B blends,<sup>2,35-37</sup> it was the calculated value of 132 °C that is lower than experimental  $T_g$  (152 °C) for the copolymer produced at 60 min of mixing (random copolymers on the base of molar composition obtained by NMR data). This result can be explained considering the different stiffness of new sequences **C**, **D**, **E** and **F** (see Scheme 4.2 and 4.3) formed during reactive melt blending. This hypothesis is supported by calorimetric data of the corresponding polymer models pBPAN, p(BPAC)-alt-(ETC), pBPAEtN, pEtBPAEtN for the sequences **C**, **D**, **E**, and **F**. In particular the aromatic pBPAN exhibits a thermal glass transition (185,0 °C) more high than other polymer models

that have Tg value below 105 °C ( $T_{g_{p(BPAC)\text{-alt-(EtC)}}} = 99,0 \text{ °C} - T_{g_{pBPAEtN}} = 103,0 \text{ °C} - T_{g_{pEtBPAEtN}} = 94,0 \text{ °C}$ ). On the other hand, the significant increasing of the molar fraction of the BPAN units respect to the other new sequences p(BPAC)-alt-(EtC), pBPAEtN, pEtBPAEtN with the extent of reaction time, is in accordance with raising of dimensional stability of the produced samples. In light of these consideration, the two-component Fox equation was expanded in new six-component equation (eq 19) that take into account the composition of the copolymer determined by NMR analysis, as well as in the PET-MXD6 melt mixed materials<sup>5</sup>, in agreement to equation of Johnston<sup>38</sup>.

$$\frac{1}{T_g} = \frac{W_{PC}}{T_{g_{PC}}} + \frac{W_{PEN}}{T_{g_{PEN}}} + \frac{W_{BPAN}}{T_{g_{BPAN}}} + \frac{W_{BPAETC}}{T_{g_{BPAETC}}} + \frac{W_{BPAEtN}}{T_{g_{BPAEtN}}} + \frac{W_{BPAdEt}}{T_{g_{BPAdEtN}}} \quad (\text{eq. 19})$$

$W_{PC}$ ,  $W_{PEN}$ ,  $W_{BPAN}$ ,  $W_{p(BPAC)\text{-alt-(EtC)}}$ ,  $W_{pBPAEtN}$ , and  $W_{pEtBPAEtN}$  are the weight fractions of the sequences **A**, **B**, **C**, **D**, **E** and **F**, respectively;  $T_{g_{PC}}$ ,  $T_{g_{PEN}}$ ,  $T_{g_{BPAN}}$ ,  $T_{g_{p(BPAC)\text{-alt-(EtC)}}$ ,  $T_{g_{pBPAEtN}}$ , and  $T_{g_{pEtBPAEtN}}$  are the glass transition value in °K of the corresponding polymers PC, PEN, pBPAN, p(BPA)-co-(EtC), pBPAEtN, and pEtBPAEtN, respectively. The weight fraction of each sequences was calculated by the following eq. 20.

$$W_i = \frac{C_i * m_i}{\sum_{i=1}^6 C_i * m_i} \quad (\text{eq. 20})$$

$C_i$  is the molar fractions of the corresponding sequences and  $m_i$  is the molecular mass of each copolymer component (254,3 g/mol for PC sequences; 242,2 g/mol for PEN sequences; 498,5 g/mol for pBPAN sequences; 342,3 g/mol for p(BPAC)-alt-(EtC) sequences; 452,1 g/mol for pBPAEtN sequences; 496,6 g/mol for pEtBPAEtN sequences). Using the molar fraction values calculated determined by NMR analysis (see Table 4.7), the Tg of all copolymers were calculated, and values are summarized in Table 4.11. The good agreement of calculated and experimental values for the samples produced at 60 and 45 min, indicates that structural and

molar composition of each sequence influence the glass transition of the PC-PEN copolymers, and confirm that at 45 and 60 min mixing random copolymers were formed. The PC-PEN copolymers formed at reaction time between 0 min and 45 min exhibits Tg values about 10 °C lower with respect to theoretical values calculated by eq. 18. Such behavior can be due to the increasing of disorder in the sequences of the chain copolymers due to the significant concentration of the **A**, **B** and **D** units, as well as to effect of the triads. Increasing of disorder by formation of six component copolymer and the effect of the triads can give lowering in interchange interactions and consequently increasing in the segmental mobility (Tg) of the formed chain copolymers.

**Table 4.11.** % weight of the component sequences ( $W_A$ ,  $W_B$ ,  $W_C$ ,  $W_D$ ,  $W_E$  and  $W_F$ ), calculated Tg by eq. 19, and experimental Tg, of the equimolar PC-PEN blends.

Reaction Time (min)	$W_A^{(a)}$	$W_B^{(a)}$	$W_C^{(a)}$	$W_D^{(a)}$	$W_E^{(a)}$	$W_F^{(a)}$	Tg Calc <sup>(b)</sup> (°C)	Tg exp (°C)
0	0,51	0,49	0,00	0,00	0,00	0,00	135	125_149
2	0,49	0,47	0,02	0,01	0,00	0,00	136	125_135
5	0,48	0,46	0,03	0,02	0,01	0,00	136	127
8	0,42	0,42	0,08	0,04	0,03	0,00	136	128
10	0,37	0,36	0,18	0,06	0,04	0,00	139	128
15	0,30	0,27	0,26	0,07	0,09	0,02	141	131
20	0,21	0,18	0,34	0,06	0,19	0,02	142	135
30	0,09	0,11	0,42	0,03	0,33	0,02	143	139
45	0,02	0,07	0,52	0,02	0,33	0,04	148	148
60	0,01	0,02	0,60	0,00	0,30	0,07	152	153

(a) Calculated by eq. 20;

(b) Calculated by eq. 19.

## 4.21 – FTIR analysis of PC-PEN Blends

Figure 4.18 shows the FTIR spectra between 1630 and 1870  $\text{cm}^{-1}$  of PC-PEN copolymers obtained at 10, 20, 30, 45 and 60 min. The same section also shows the spectrum on the original PC-PEN blend, in which it is possible to distinguish two absorption bands related to asymmetric stretching motions of the C=O in PC ( $1775 \text{ cm}^{-1}$ ) and in PEN ( $1730 \text{ cm}^{-1}$ ). The other spectra sections are not reported here because they don't show variations due to different structural units in copolymers. The spectra obtained at 2, 5 and 8 min are very similar to that obtained at 10 min. The maximum absorption of carbonyl carbonate units moves around  $1750 \text{ cm}^{-1}$  with the progress of mixing time, confirming the formation of BisphenolA-Ethylene-Carbonate sequences (**D**). In addition, its absorption intensity decreases compared to that of carbonyl ester units of PEN up to almost disappearance in the copolymers obtained at 45 and 60 min of reaction, in agreement with  $^{13}\text{C}$ -NMR analysis.

Unlike the  $^{13}\text{C}$ -NMR, the FTIR analysis does not allow to obtain unique information on the copolymer sequences.

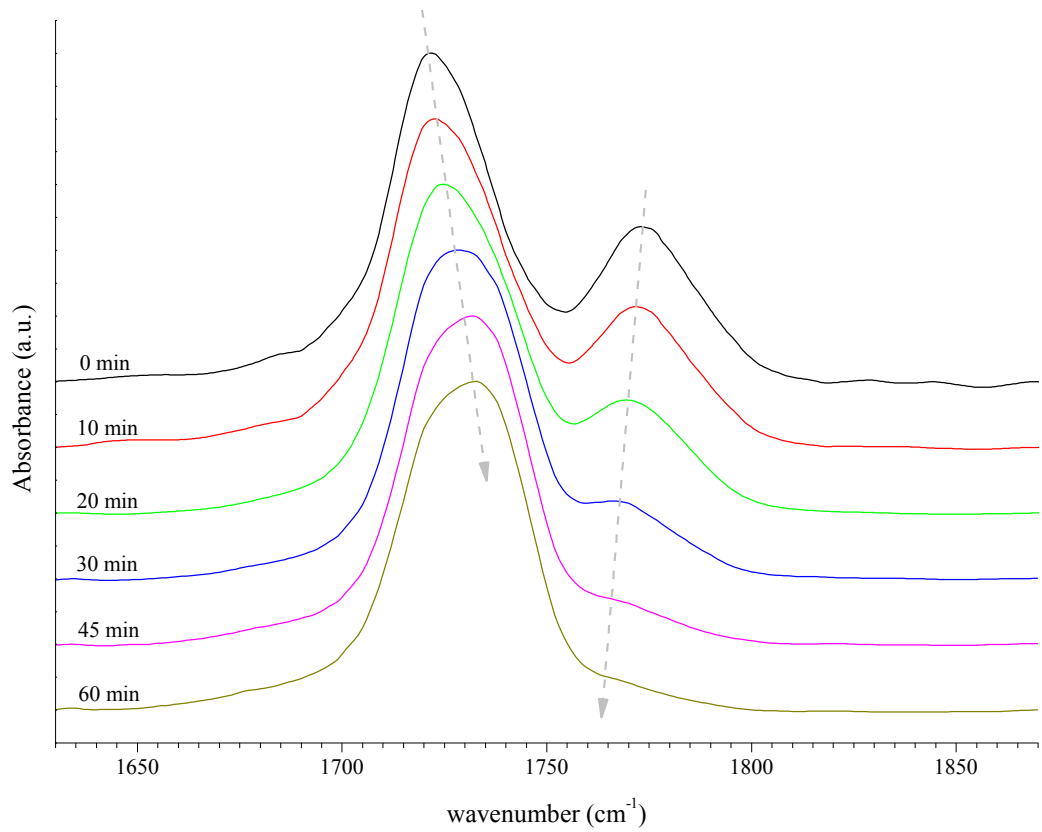


**Figure 4.18.** FTIR spectra in the range 1630 – 1870 cm<sup>-1</sup> of the material obtained by reactive melt mixing of PC and PEN to 0, 10, 20, 30, 45 and 60 min.

## 4.22 – Viscosimetric analysis of PC-PEN Blends

Viscosimetric measurements in solution were performed either for all materials produced by reactive melt blending of PC and PEN. The values of measured inherent viscosity ( $\eta_{inh}$ ) have been summarized in Table 4.12. All materials melt blended exhibit viscosity values lower than initial mixture (0,5360). In particular, it is evident a progressive decreasing of viscosity up to the minimum value of 0,28 at 8 min, while for more high mixing times the viscosity raise up to the maximum value of 0,41 at the end of blending. This behavior can be due to the different hydrodynamic volume of copolymers with different composition and structure that are produced at various mixing times by transesterification reactions (Schemes 4.1a) and, mostly by elimination reaction of Ethylene Carbonate (EtC) and CO<sub>2</sub> (Schemes 4.2 and 4.3). Other factors can be affect the above-mentioned viscosity trend. For example, the formation of cyclic compounds for short reaction times involves lowering of the viscosity. Moreover, the self-assembled block-copolymers obtained by melt mixing reactions always at short reactions times, give compatibilization of initial biphasic system PC-PEN, which implies further lowering of viscosity. On the other hand, the same cyclic compounds initially produced can give ring opening reactions catalyzed by Ti(OBut)<sub>4</sub>, with formation of linear copolymer that contribute at increase the viscosity.

## 4.23 – GPC analysis of melt mixed PC-PEN materials

The average molar mass ( $M_w$  and  $M_n$ ) values of the PC-PEN copolymers soluble in THF (20, 30, 45 and 60 min mixing) were calculated by GPC analysis using relative calibration curve by linear polystyrene (PS) narrow standards. In a typical analysis, 100  $\mu\text{L}$  of a polymer solution in THF (2–3 mg/mL) was injected and eluted at a flow rate of 1 mL/min, using THF as eluent and *o*-dichlorobenzene (1  $\mu\text{L}$ ) as flow marker. The corresponding GPC curves compared with that of initial PC homopolymer are shown in Figure 4.19, while the calculated  $M_w$ ,  $M_n$  and polydispersity ( $D = M_w/M_n$ ) values are listed in Table 4.12.

The increasing in relative average  $M_w$  of PC-PEN copolymers is in agreement with the increment on its inherent viscosity discussed above. However only relative molecular weight is measured with this SEC method because the calibration is related to mono-disperse standard of polystyrene (PS) that have different hydrodynamic volume with respect to that of PC-PEN copolymers. Indeed, is possible that the hydrodynamic volume of PC-PEN copolymers change with the progress of reaction time because change its molar composition as well as the type of co-monomers sequences in the chain. The determination of absolute molecular weight with GPC analysis require auto-self-calibration derived from combination of MALDI-TOF analysis with GPC measurements. In other words the absolute calibration GPC curve calculated by MALDI-TOF analysis of selected mono-disperse fractions of PC-PEN copolymers. The absolute molecular weight determined in this manner for each fraction of PC-PEN copolymers and its corresponding elution time is used for obtained the its auto-calibration GPC curve. Reliable absolute molar mass can be calculated using the MALLS (Multi Angle Laser Light Scattering) as detector. At the moment the SEC-MALDI-TOF methods are in progress for further studies on this PC-PEN blends.

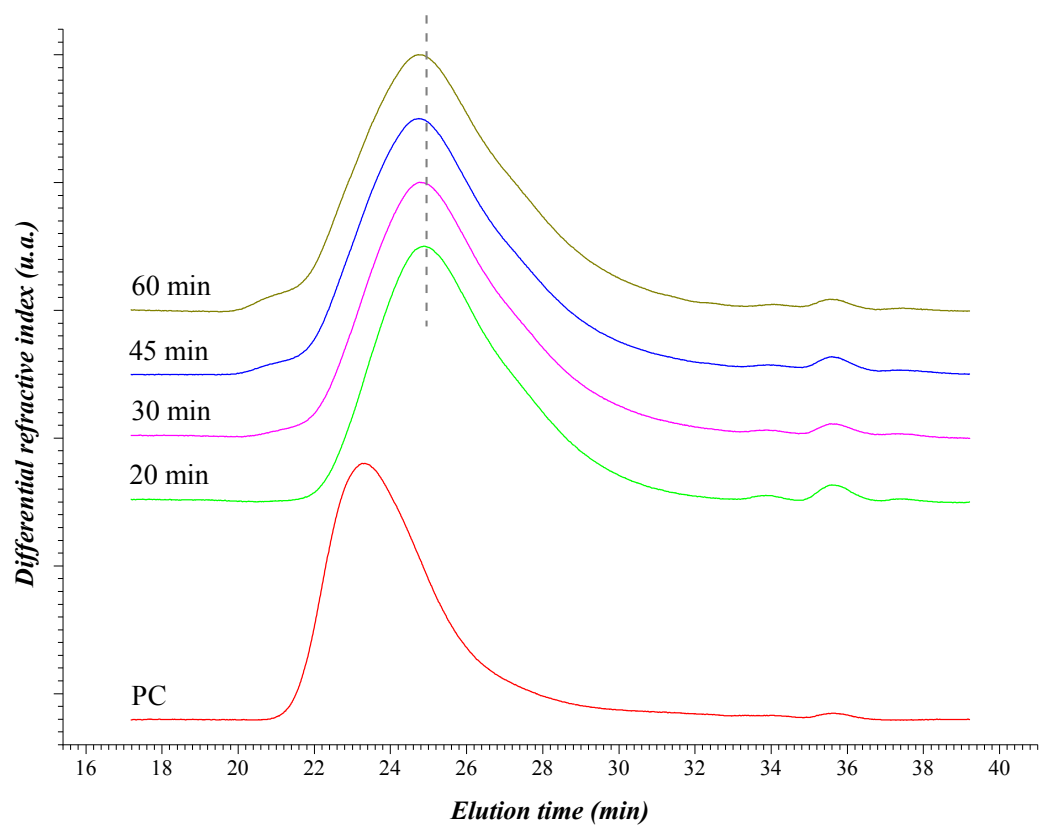


**Figure 4.19.** Comparison of GPC curves of the initial PC homopolymer with that of THF soluble PC-PEN copolymers (20, 30, 45 and 60 min).



**Table 4.12.** Viscosity data ( $\eta_{inh}$ ) and GPC data (Mw, Mn and PD) of the material obtained by reactive melt blending of equimolar PC-PEN blends.

<b>Reaction Time (min)</b>	<b><math>\eta_{inh}^{(a)}</math></b>	<b>Mw<sup>(b)</sup></b>	<b>Mn<sup>(b)</sup></b>	<b>D<sup>(b)</sup></b>
<b>0</b>	0,54	n.d	n.d	n.d
<b>2</b>	0,30	n.d	n.d	n.d
<b>5</b>	0,28	n.d	n.d	n.d
<b>8</b>	0,28	n.d	n.d	n.d
<b>10</b>	0,25	n.d	n.d	n.d
<b>15</b>	0,30	n.d	n.d	n.d
<b>20</b>	0,35	26300	11400	2,30
<b>30</b>	0,34	29800	11000	2,70
<b>45</b>	0,35	33500	11200	2,99
<b>60</b>	0,41	35500	11400	3,11

(a) Measured at 30°C ( $\pm 0,2^\circ\text{C}$ ) in phenol/tetrachloroethane (60/40 - w/w) mix solvent;

(b) Calculated by SEC analysis using relative calibration curve derived by linear narrow standards of polystyrene (PS). The SEC data for initial PC homopolymer are the following: Mw = 30200, Mn = 63400, D = 2,10.

#### 4.24 – MALDI-TOF measurements of PC-PEN Blends

All PC-PEN copolymers soluble in THF solvent obtained after respectively 20, 30, 45 and 60 min of reactive melt blending at 280 °C of equimolar PC-PEN blends in the presence of Ti(OBut)<sub>4</sub> (0,2% w) as catalyst, were analyzed by MALDI-TOF mass spectrometry in reflectron mode.

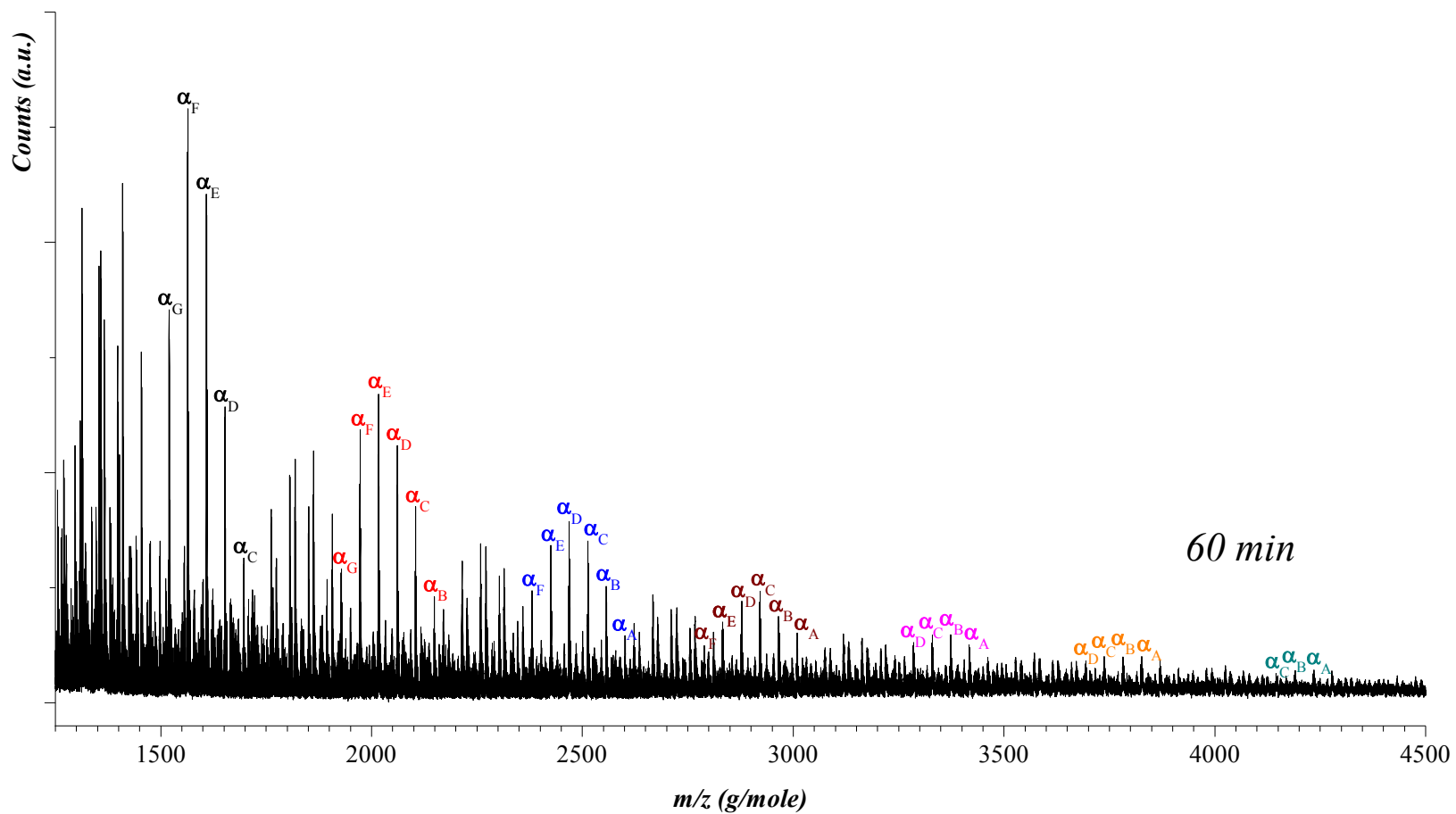
The MALDI-TOF mass spectrum of PC-PEN copolymers obtained after 60 min mixing show a series of mass peaks in the range 1250 – 4500 Da (Figure 4.20) assigned to the different co-oligomer families (Table 4.13). The most intense peaks labeled with  $\alpha_n$  correspond to linear co-oligomers terminated with hydroxyl groups at both of ends; one terminal always correspond to hydroxyl group belonging to bisphenolA terminals (-BPA-OH terminals). These assignments are in agreement with that found by <sup>13</sup>C NMR, since these BPA-OH mainly gives a signal at 114,10 ppm due the tertiary carbon in ortho to the phenol OH (see Figure 4.14).

Each mass family includes a series of mass peaks that differ 44 Da each of the other. Indeed each mass family  $\alpha_n$  differs 408,4 Da by the subsequent high mass family: This value correspond of the molecular weight of the C sequences (bisphenolA-naphthalate).

The proposed assignments of the mass families  $\alpha_n$ , listed in Table 7, correspond to a series of co-oligomers with different distribution of the sequences A, B, C, D, E and F, already observed by NMR, along the chains. The different relative intensity of  $\alpha_n$  peaks towards the reaction time, reflect the different molar composition as can be observe in Figure 4.21, which reports the enlarged section, from m/z 1700 Da up to m/z 2200 Da, of MALDI spectra of the melt mixed materials taken at 20, 30, 45, and 60 min. The same mass range show other two mass peak series with high intensity belonging to  $\gamma_n$ , and  $\lambda_n$  families respectively (see Table 4.14 for the assignments). In the  $\gamma_n$  family, respect to the  $\alpha_n$ , series lack

one sequence **B** - ethylene-naphthalate (less 242.2 Da). By replacing of one sequence **A** - bisphenolA-carbonate with one sequence **B** - ethylene-naphthalate in  $\gamma_n$  series,  $\lambda_n$  family are obtained (less 12.1 Da).

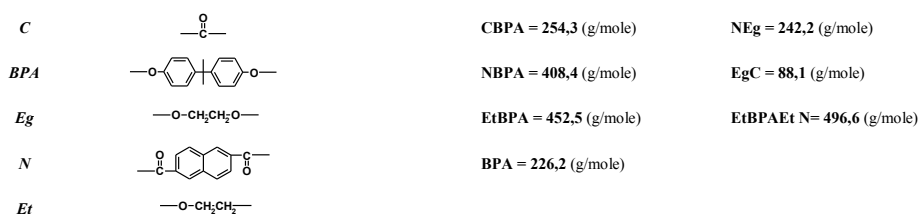
However, at the moment, only qualitative information can be achieved by MALDI-TOF mass spectra; because the possibility of most isobar co-oligomers for each mass peak does not allow unambiguous assignments. Further studies on the fragmentation by Post Source Decay techniques in MALDI-TOF/TOF tandem are in progress to overcome the problem of isobar co-oligomers and to obtain more information on the distribution of the sequences along the copolymer chains.



**Figure 4.20.** MALDI-TOF spectra of PC-PEN copolymers obtained after 60 min of reactive melt blending at 280°C of equimolar PC-PEN blend.

**Table 4.13.** Assignments of the mass peaks observed in the MALDI-TOF spectra of PC-PEN copolymers obtained after 60 min of reactive melt blending at 280 °C of equimolar PC-PEN blends in the presence of Ti(OBut)<sub>4</sub> (0,2% w) as catalyst.

Sy	Structure	n	[M + Na <sup>+</sup> ]
$\alpha_A$	H-BPA-[CBPA] <sub>1</sub> -[NEg] <sub>1</sub> -[NBPA] <sub>1+n</sub> -[CEg] <sub>1</sub> -[NEtBPA] <sub>1</sub> -[NEtBPAEt] <sub>1</sub> -H	0	
		1	
		2	2601,9
		3	3010,3
		4	3418,7
		5	3827,1
$\alpha_B$	H-BPA-[CBPA] <sub>1</sub> -[NEg] <sub>1</sub> -[NBPA] <sub>1+n</sub> -[CEg] <sub>1</sub> -[NEtBPA] <sub>2</sub> -H	0	
		1	2149,4
		2	2557,8
		3	2966,2
		4	3374,6
		5	3783,0
$\alpha_C$	H-BPA-[CBPA] <sub>1</sub> -[NEg] <sub>1</sub> -[NBPA] <sub>2+n</sub> -[CEg] <sub>1</sub> -[NEtBPA] <sub>1</sub> -H	0	1696,9
		1	2105,3
		2	2513,7
		3	2922,1
		4	3330,5
		5	3738,9
$\alpha_D$	H-BPA-[CEg] <sub>1</sub> -[NBPA] <sub>3+n</sub> -[NEtBPAEt] <sub>1</sub> -H	0	1652,8
		1	2061,2
		2	2469,6
		3	2878,0
		4	3286,4
		5	3694,8
$\alpha_E$	H-BPA-[CEg] <sub>1</sub> -[NBPA] <sub>3+n</sub> -[NEtBPA] <sub>1</sub> -H	0	1608,7
		1	2017,1
		2	2425,5
		3	2833,9
		4	3242,3
		5	
$\alpha_F$	H-BPA-[NBPA] <sub>3+n</sub> -[NEtBPAEt] <sub>1</sub> -H	0	1564,6
		1	1973,0
		2	2381,4
		3	2789,8
		4	
		5	
$\alpha_G$	H-BPA-[NBPA] <sub>3</sub> -[NEtBPA] <sub>1</sub> -H	0	1520,5
		1	1928,9
		2	
		3	
		4	
		5	



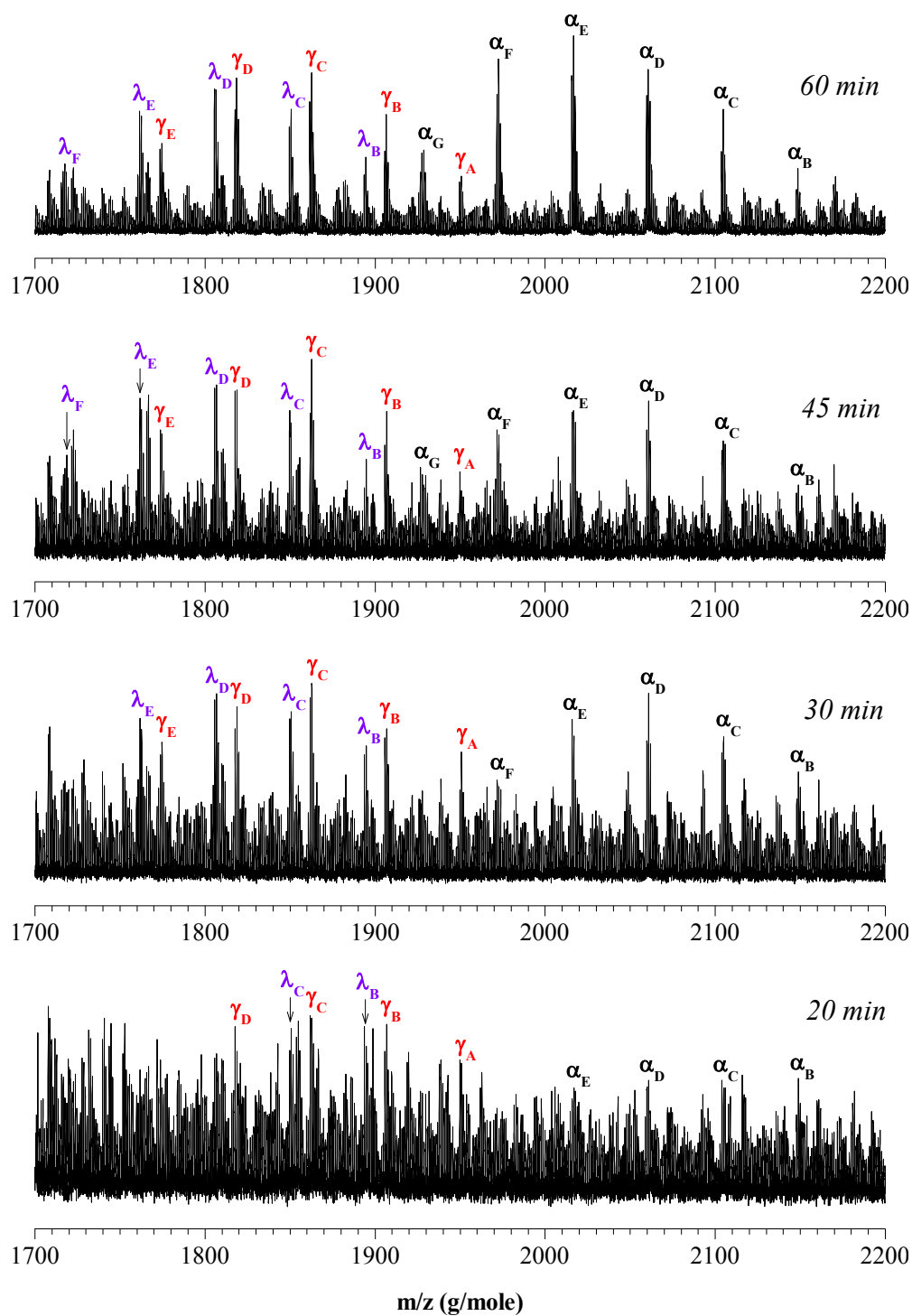
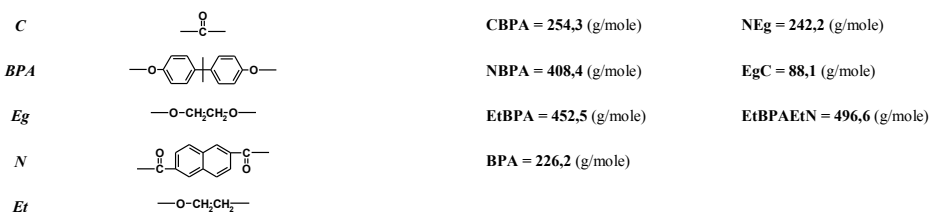


**Figure 4.21.** MALDI-TOF spectra of THF soluble PC-PEN copolymers (20, 30, 45 and 60 min) obtained by reactive melt blending at 280 °C of equimolar mixture PC-PEN (respect to the repeat unit) in the presence of  $\text{Ti}(\text{O}i\text{Bu})_4$  (0,2% w) as catalyst.

**Table 4.14.** Assignments of the mass peaks observed in the MALDI-TOF spectra of THF soluble PC-PEN copolymers (20, 30, 45 and 60 min) obtained by reactive melt blending at 280 °C of equimolar PC-PEN blends in the presence of Ti(OBut)<sub>4</sub> (0,2% w) as catalyst.

Sy	Structures	m/z (g/mole)
$\alpha_B$	H-BPA-[CBPA] <sub>1</sub> -[NEg] <sub>1</sub> -[NBPA] <sub>1</sub> -[CEg] <sub>1</sub> -[NEtBPA] <sub>2</sub> -H H-BPA-[CBPA] <sub>1</sub> -[NEg] <sub>1</sub> -[NEtBPAEt] <sub>1</sub> -[NEtBPA] <sub>2</sub> -H	2149,3
$\alpha_C$	H-BPA-[CBPA] <sub>1</sub> -[NEg] <sub>1</sub> -[NBPA] <sub>2</sub> -[CEg] <sub>1</sub> -[NEtBPA] <sub>1</sub> -H	2105,3
$\alpha_D$	H-BPA-[CBPA] <sub>1</sub> -[NEg] <sub>1</sub> -[NBPA] <sub>3</sub> -[CE] <sub>1</sub> -H H-BPA-[NBPA] <sub>3</sub> -[CEg] <sub>1</sub> -[NEtBPAEt] <sub>1</sub> -H	2061,1
$\alpha_E$	H-BPA-[NBPA] <sub>3</sub> -[CEg] <sub>1</sub> -[NEtBPA] <sub>1</sub> -H	2017,2
$\alpha_F$	H-BPA-[NBPA] <sub>4</sub> -[CEg] <sub>1</sub> -H H-BPA-[NBPA] <sub>3</sub> -[NEtBPAEt] <sub>1</sub> -H	1973,1
$\alpha_G$	H-BPA-[NBPA] <sub>3</sub> -[NEtBPA] <sub>1</sub> -H	1929,1
$\gamma_A$	H-BPA-[CBPA] <sub>1</sub> -[NBPA] <sub>1</sub> -[CEg] <sub>1</sub> -[NEtBPA] <sub>1</sub> -[NEtBPAEt] <sub>1</sub> -H	1955,1
$\gamma_B$	H-BPA-[CBPA] <sub>1</sub> -[NBPA] <sub>1</sub> -[CEg] <sub>1</sub> -[NEtBPA] <sub>2</sub> -H	1907,1
$\gamma_C$	H-BPA-[CBPA] <sub>1</sub> -[NBPA] <sub>2</sub> -[CEg] <sub>1</sub> -[NEtBPA] <sub>1</sub> -H	1863,0
$\gamma_D$	H-BPA-[CBPA] <sub>1</sub> -[NBPA] <sub>3</sub> -[CEg] <sub>1</sub> -H H-BPA-[CBPA] <sub>1</sub> -[NBPA] <sub>2</sub> -[NEtBPAEt] <sub>1</sub> -H	1818,9
$\gamma_E$	H-BPA-[CBPA] <sub>1</sub> -[NBPA] <sub>2</sub> -[NEtBPA] <sub>1</sub> -H	1775,0
$\lambda_B$	H-BPA-[NEg] <sub>1</sub> -[NBPA] <sub>1</sub> -[CEg] <sub>1</sub> -[NEtBPA] <sub>2</sub> -H	1895,0
$\lambda_C$	H-BPA-[NEg] <sub>1</sub> -[NBPA] <sub>2</sub> -[CEg] <sub>1</sub> -[NEtBPA] <sub>1</sub> -H	1851,1
$\lambda_D$	H-BPA-[NEg] <sub>1</sub> -[NBPA] <sub>3</sub> -[CEg] <sub>1</sub> -H H-BPA-[CBPA] <sub>1</sub> -[NBPA] <sub>2</sub> -[NEtBPAEt] <sub>1</sub> -H	1806,8
$\lambda_E$	H-BPA-[NEg] <sub>1</sub> -[NBPA] <sub>2</sub> -[NEtBPA] <sub>1</sub> -H	1762,9
$\lambda_F$	H-BPA-[NEg] <sub>1</sub> -[NBPA] <sub>3</sub> -H	1718,9



## 4.24 – Conclusions

Our studies have allowed the characterization of the reactions that occurring during the reactive melt mixing of PC-PEN blends and also the characterization of the chemical structures and chemical compositions of the formed copolymers.

At first step of the exchange reaction (2min) a block copoly(ester-carbonate) was formed. multicomponent copolymers containing new units, like ether-bisphenolA and diether-bisphenolA, have been produced, owing of the consecutive reactions that involve the elimination of CO<sub>2</sub> and ethylene carbonate (EtC). At longer reaction time (> 30 min), owing of the almost gone of carbonate and di-ethylene oxide units, a new copoly(ester-ether) with a higher dimensional stability were obtained.

The reactive blending of PC-PEN could be a synthetic procedure for the preparation of new copolymers with structure and composition known that could be synthesized with much serious difficulty from its commoners.



## 4.26 – References

1. G. Montaudo, C. Puglisi, and S. Samperi, *Transreactions in Condensation Polymers* – Fakirov S, Ed. Wiley-VCH: New York, Chapt.4;
2. AIM “Macromolecole, Scienza e Tecnologia” Vol.1;
3. G. Montaudo, C. Puglisi, F. Samperi, and F. La Mantia, *J Polym Sci, Part A; Polym Chem Ed* - **1996**, 34, 1283;
4. G. Montaudo, C. Puglisi, and F. Samperi, *Macromolecules* – **1998**, 31, 650;
5. B. Plage, H.R. Schulten, *J Anal Appl Pyrolysis* - **1989**, 15, 197;
6. C. C.Huang, F.C. Chang, *Polymer* - **1997**, 38 (9, 179), 2135;
7. F. Pilati, E. Marianucci, C. Berti *J Appl Polym Sci* - **1985**, 30, 1267;
8. Z. Denchev, A. Duchesne, M. Stamm, S. Fakirov *J Appl Polym Sci* - **1998**, 68, 429;
9. J.M.R.C.A. Santos, J. Guthrie *J Mater Chem* - **2006**, 16, 237;
10. F. Samperi, M.S. Montaudo, C. Puglisi, S. Battiato, D. Carbone, *J Polym Sci. part A: Polym Chem* – **2010**, 48, 5135-5155;
11. S.C. Lee, K.H. Yoon, I. H. Park, H.C. Kim, T.W. Son *Polymer* - **1997**, 38, 4831;
12. M.Guo, H.G. Zachmann *Polymer* - **1993**, 34, 2503;
13. M.E. Stewart, A.J. Cox, D.M. Naylor *Polymer* - **1993**, 34, 4060;
14. M. Okamoto, T. Kotaka, *Polymer* - **1997**, 38, 1357;
15. K.H. Yoon, S.C. Lee, I.H. Park, H.M. Lee, O.O. Park, T.W. Son *Polymer* - **1997**, 38, 6079;
16. D.W. Ihm, S.Y. Park, C.G. Chang, Y.S. Kim, H.K. Lee *J Polym Sc. Polym Chem* - **1996**, 34, 2841;
17. C.F. Ou *J. Appl. Polym. Sci.* **1998**, 68, 1591;
18. Y. Aoki, T. Amari, K. Nishimura, Y. Arashiro *Macromolecules* - **1999**, 32, 1923;

19. A.M. Kenwright, S.K. Peace, R.W. Richards, A. Bunn, W.A. MacDonald *Polymer* - **1999**, 40, 5851;
20. H.J. Bang, J.K. Lee, K.H. Lee, *J Polym Sci Polym Phys* - **2000**, 38, 2625;
21. M.J.F. Berridi, J.J. Iruin, I. Maiza *Macromol Rapid Commun* - **1995**, 16, 483;
22. V.K. Karavia, E.G. Koulouri, and J.K. Kallitis *J Macromol Sci–Pure Appl Chem* - **2002**, A39, 527;
23. G. Montaudo, C. Puglisi, F. Samperi, in: “*Transreaction in Condensation Polymers*” – S. Fakirov, Ed – Wiley-VCH: Weinheim, **1998** – New York, Chapter four;
24. K.K.L. Eersels, A.M. Aerdt, G. Groeninckx, in: “*Transreaction in Condensation Polymers*” – S. Fakirov, Ed – Wiley-VCH: Weinheim, **1998** – New York, Chapter seven;
25. Montaudo G.; Montaudo M. S.; Scamporrino E.; Vitalini, D. - *Macromolecules* 1992, 25, 5099–5107;
26. Samperi F.; Puglisi C.; Alicata R.; Montaudo G. *J Polym Sci Part A: Polym Chem* 2003, 41, 2778–2793;
27. Samperi, F.; Montaudo, M.; Puglisi, C.; Alicata, R.; Montaudo, G. *Macromolecules* 2003, 36, 7143–7154;
28. Samperi, F.; Montaudo, M.; Puglisi, C.; Di Giorgi, S.; Montando, G. *Macromolecules* 2004, 37, 6449–6459;
29. Fakirov, S.; Evstatiev, M.; Petrovich, S. *Macromolecules* 1993, 26, 5219–5226;
30. Evstatiev, M.; Schultz, J. M.; Petrovich, S.; Georgiev, G.; Fakirov, S.; Friedrich, K. *J Appl Polym Sci* 1998, 67, 723–737;
31. Johnston, N.W., *J. Macromol. Sci., Rev. Mcromol. Chem.* 1976, 14B, 215.